Feynman rules for fermions using two-component spinor notation

DRAFT version 0.71 December 7, 2004

Herbi K. Dreiner[1], Howard E. Haber[2] and Stephen P. Martin[3]

[1]*Physikalisches Institut der Universität Bonn, Nußallee 12, 53115 Bonn, Germany*

[2]*Santa Cruz Institute for Particle Physics, University of California, Santa Cruz CA 95064*

[3]*Department of Physics, Northern Illinois University, DeKalb IL 60115* and

Fermi National Accelerator Laboratory, P.O. Box 500, Batavia IL 60510

Abstract

We provide a complete set of Feynman rules for fermions using two-component spinor notation. These rules are suitable for practical calculations of cross-sections, decay rates, and radiative corrections in the Standard Model and its extensions, including supersymmetry. A unified treatment applies for massless Weyl fermions and massive Dirac and Majorana fermions. Numerous examples are given.

Contents

1 Introduction

A crucial feature of the Standard Model of particle physics is the chiral nature of fermion quantum numbers and interactions. According to the modern understanding of the electroweak symmetry, the fundamental degrees of freedom for quarks and leptons are two-component Weyl fermions that transform as irreducible representations under $SU(2)_L \times U(1)_Y$. Despite this, most pedagogical treatments and practical calculations in high-energy physics continue to use the old-fashioned four-component Dirac notation, which combines distinct irreducible representations of the symmetry groups. In some cases, this inertia is understandable; for example in pure QED and QCD calculations, parity violation is not relevant. There is also a certain perceived advantage to familiarity. However, as we progress to phenomena at and above the scale of electroweak symmetry breaking, it seems increasingly natural to employ two-component fermion notation, in harmony with the irreducible transformation properties dictated by the physics.

One occasionally encounters the misconception that two-component fermion notations are somehow inherently ill-suited or unwieldy for practical use. Perhaps this is due in part to a lack of examples of calculations using two-component language in the pedagogical literature. In this paper, we seek to dispel this idea by presenting Feynman rules for fermions using two-component spinor notation, intended for practical calculations of cross-sections, decays, and radiative corrections. It uses a unified framework that applies equally well to Dirac fermions like the Standard Model quarks and leptons, to Majorana fermions like the MSSM neutralinos, to Weyl fermions appropriate for the massless limit of Standard Model neutrinos, or to any combination thereof.

2 Essential conventions and notations

We begin with a discussion of necessary conventions. The metric is taken[1] to be:

$$g^{\mu\nu} = \mathrm{diag}(+,-,-,-)\,, \tag{2.1}$$

[1]The published version of this paper uses the $(+,-,-,-)$ metric. An otherwise identical version, using the $(-,+,+,+)$ metric favored by one of the authors, may be found at `http://zippy.physics.niu.edu/rules.html`. It can also be constructed by changing a single macro within the LaTeX source file, in an obvious way. You can tell which version you are presently reading from equation (2.1).

where $\mu, \nu, \rho \ldots = 0, 1, 2, 3$ are spacetime vector indices. Contravariant four-vectors (e.g. positions and momenta) are defined with indices raised, and covariant four-vectors (e.g. derivatives) with lowered indices:

$$x^\mu = (t\,;\,\vec{\boldsymbol{x}}), \tag{2.2}$$

$$p^\mu = (E\,;\,\vec{\boldsymbol{p}}), \tag{2.3}$$

$$\partial_\mu = (\partial/\partial t\,;\,\vec{\boldsymbol{\nabla}})\,, \tag{2.4}$$

in units of $c = 1$. The totally antisymmetric pseudo-tensor $\epsilon^{\mu\nu\rho\sigma}$ is defined such that

$$\epsilon^{0123} = -\epsilon_{0123} = +1\,. \tag{2.5}$$

The irreducible building blocks for fermions are fields that transform either under the left-handed $(\frac{1}{2}, 0)$ or the right-handed $(0, \frac{1}{2})$ representation of the Lorentz group. Hermitian conjugation interchanges these two representations. A massive Majorana fermion field can be constructed from either representation; this is the spin-1/2 analog of a real scalar field. The Dirac field combines two equal mass two-component fields into a reducible representation of the form $(\frac{1}{2}, 0) \oplus (0, \frac{1}{2})$; this is the spin-1/2 analog of a complex scalar field. It is also possible to use four-component notation to describe Majorana fermions by imposing a reality condition on the spinor in order to reduce the number of degrees of freedom in half. However, in this paper, we shall focus primarily on two-component spinor notation for all fermions. In the following, $(\frac{1}{2}, 0)$ spinors carry undotted indices $\alpha, \beta, \ldots = 1, 2$, and $(0, \frac{1}{2})$ spinors carry dotted indices $\dot{\alpha}, \dot{\beta}, \ldots = 1, 2$.

To be more specific, let [1]

$$M = \exp(-\tfrac{1}{2} i \theta_{\mu\nu} s^{\mu\nu}) \simeq I - i\vec{\boldsymbol{\theta}}\cdot\vec{\boldsymbol{J}} - i\vec{\boldsymbol{\zeta}}\cdot\vec{\boldsymbol{K}} \tag{2.6}$$

be the spin-1/2 representation of the Lorentz group, where $\vec{\boldsymbol{J}}$ and $\vec{\boldsymbol{K}}$ are the generators of rotations and boosts, respectively. In the $(\frac{1}{2}, 0)$ representation $\vec{\boldsymbol{J}} = \vec{\boldsymbol{\sigma}}/2$ and $\vec{\boldsymbol{K}} = -i\vec{\boldsymbol{\sigma}}/2$, while in the $(0, \frac{1}{2})$ representation, $\vec{\boldsymbol{J}} = \vec{\boldsymbol{\sigma}}/2$ and $\vec{\boldsymbol{K}} = i\vec{\boldsymbol{\sigma}}/2$. M is a matrix labeled by spinor indices as $M_\alpha{}^\beta$. A generic two-component $(\frac{1}{2}, 0)$ spinor is denoted by ψ_α, and transforms as $\psi_\alpha \to M_\alpha{}^\beta \psi_\beta$. The Lorentz group transformation matrix in the $(0, \frac{1}{2})$ representation is given by M^*; this is a matrix labeled as $(M^*)_{\dot{\alpha}}{}^{\dot{\beta}}$. A two-component $(0, \frac{1}{2})$ spinor is denoted by $\bar{\psi}_{\dot{\alpha}}$, and transforms as $\bar{\psi}_{\dot{\alpha}} \to (M^*)_{\dot{\alpha}}{}^{\dot{\beta}} \bar{\psi}_{\dot{\beta}}$.

¿From the definition of the dotted indices, we see that the $(0, \frac{1}{2})$ and $(\frac{1}{2}, 0)$ representations can be related by complex conjugation. That is, if $\bar{\psi}_{\dot{\alpha}}$ is a $(0, \frac{1}{2})$ fermion, then $(\bar{\psi}_{\dot{\alpha}})^*$ transforms as a $(\frac{1}{2}, 0)$ fermion. This means that we can describe all fermion degrees of freedom using only

fields defined as left-handed $(\frac{1}{2},0)$ fermions ψ_α, and their conjugates. We will usually combine spinors to make Lorentz tensors, so it is useful to regard $\bar{\psi}_{\dot{\alpha}}$ as a row vector, and ψ_α as a column vector, with:

$$\bar{\psi}_{\dot{\alpha}} \equiv (\psi_\alpha)^\dagger. \tag{2.7}$$

The Lorentz transformation property of $\bar{\psi}_{\dot{\alpha}}$ can then be obtained as $(\psi_\alpha)^\dagger \to (\psi_\beta)^\dagger (M^\dagger)^\beta{}_\alpha$, where $(M^\dagger)^\beta{}_\alpha = (M^*)_\alpha{}^\beta$ is simply a statement of the well known definition of the hermitian adjoint matrix as the complex conjugate transpose of the matrix. We will continue to use the dotted-index notation in association with the bar over the symbol (instead of a hermitian conjugation symbol).

There are two additional spin-1/2 irreducible representations of the Lorentz group, represented by the matrices $(M^{-1})^T$ and $(M^{-1})^\dagger$. But these are equivalent representations to the $(\frac{1}{2},0)$ and the $(0,\frac{1}{2})$ representations, respectively. The spinors that transform under these representations have raised spinor indices. The spinor indices are raised and lowered with the two-index antisymmetric tensor with components $\epsilon^{12} = -\epsilon^{21} = \epsilon_{21} = -\epsilon_{12} = 1$, and the same set of sign conventions for the corresponding dotted spinor indices. Thus

$$\psi_\alpha = \epsilon_{\alpha\beta}\psi^\beta\,, \qquad \psi^\alpha = \epsilon^{\alpha\beta}\psi_\beta\,, \qquad \bar{\psi}_{\dot{\alpha}} = \epsilon_{\dot{\alpha}\dot{\beta}}\bar{\psi}^{\dot{\beta}}\,, \qquad \bar{\psi}^{\dot{\alpha}} = \epsilon^{\dot{\alpha}\dot{\beta}}\bar{\psi}_{\dot{\beta}}\,. \tag{2.8}$$

The ϵ-tensor satisfies:

$$\epsilon_{\alpha\beta}\epsilon^{\gamma\delta} = -\delta^\gamma_\alpha\delta^\delta_\beta + \delta^\delta_\alpha\delta^\gamma_\beta, \qquad\qquad \epsilon_{\dot{\alpha}\dot{\beta}}\epsilon^{\dot{\gamma}\dot{\delta}} = -\delta^{\dot{\gamma}}_{\dot{\alpha}}\delta^{\dot{\delta}}_{\dot{\beta}} + \delta^{\dot{\delta}}_{\dot{\alpha}}\delta^{\dot{\gamma}}_{\dot{\beta}}, \tag{2.9}$$

from which it follows that:

$$\epsilon_{\alpha\beta}\epsilon^{\beta\gamma} = \epsilon^{\gamma\beta}\epsilon_{\beta\alpha} = \delta^\gamma_\alpha, \qquad\qquad \epsilon_{\dot{\alpha}\dot{\beta}}\epsilon^{\dot{\beta}\dot{\gamma}} = \epsilon^{\dot{\gamma}\dot{\beta}}\epsilon_{\dot{\beta}\dot{\alpha}} = \delta^{\dot{\gamma}}_{\dot{\alpha}}\,. \tag{2.10}$$

To construct Lorentz invariant Lagrangians and observables, one needs to first combine products of spinors to make objects that transform as Lorentz tensors. In particular, Lorentz vectors are obtained by introducing the sigma matrices $\sigma_{\mu\,\alpha\dot{\beta}}$ and $\overline{\sigma}^{\dot{\alpha}\beta}_\mu$ defined by

$$\begin{aligned}
&\overline{\sigma}_0 = \sigma_0 = \begin{pmatrix} 1 & 0 \\ 0 & 1 \end{pmatrix}, \qquad && \overline{\sigma}_1 = -\sigma_1 = \begin{pmatrix} 0 & 1 \\ 1 & 0 \end{pmatrix}, \\
&\overline{\sigma}_2 = -\sigma_2 = \begin{pmatrix} 0 & -i \\ i & 0 \end{pmatrix}, \qquad && \overline{\sigma}_3 = -\sigma_3 = \begin{pmatrix} 1 & 0 \\ 0 & -1 \end{pmatrix}.
\end{aligned} \tag{2.11}$$

The σ-matrices above have been defined with a lower (covariant) index. We also define the corresponding quantities with upper (contravariant) indices:

$$\sigma^\mu = g^{\mu\nu}\sigma_\nu = (I_2\,;\,\vec{\boldsymbol{\sigma}})\,, \qquad\qquad \overline{\sigma}^\mu = g^{\mu\nu}\sigma_\nu = (I_2\,;\,-\vec{\boldsymbol{\sigma}})\,, \tag{2.12}$$

where I_2 is the 2×2 identity matrix. The relations between σ^μ and $\overline{\sigma}^\mu$ are

$$\sigma^\mu_{\alpha\dot\alpha} = \epsilon_{\alpha\beta}\epsilon_{\dot\alpha\dot\beta}\overline{\sigma}^{\mu\,\dot\beta\beta}\,, \qquad\qquad \overline{\sigma}^{\mu\,\dot\alpha\alpha} = \epsilon^{\alpha\beta}\epsilon^{\dot\alpha\dot\beta}\sigma^\mu_{\beta\dot\beta}\,, \tag{2.13}$$

$$\epsilon^{\alpha\beta}\sigma^\mu_{\beta\dot\alpha} = \epsilon_{\dot\alpha\dot\beta}\overline{\sigma}^{\mu\dot\beta\alpha}\,, \qquad\qquad \epsilon^{\dot\alpha\dot\beta}\sigma^\mu_{\alpha\dot\beta} = \epsilon_{\alpha\beta}\overline{\sigma}^{\mu\dot\alpha\beta}\,. \tag{2.14}$$

When constructing Lorentz tensors from fermion fields, the heights of spinor indices must be consistent in the sense that lowered indices must only be contracted with raised indices. As a convention, indices contracted like

$$\psi^{\alpha}\psi_{\alpha} \qquad \text{and} \qquad \bar\psi_{\dot\alpha}\bar\psi^{\dot\alpha}\,, \tag{2.15}$$

can be suppressed. In all spinor products given in this paper, contracted indices are always to have heights that conform to eq. (2.15). For example,

$$\xi\eta \equiv \xi^\alpha\eta_\alpha, \tag{2.16}$$

$$\bar\xi\bar\eta \equiv \bar\xi_{\dot\alpha}\bar\eta^{\dot\alpha}, \tag{2.17}$$

$$\bar\xi\overline{\sigma}^\mu\eta \equiv \bar\xi_{\dot\alpha}\overline{\sigma}^{\mu\dot\alpha\beta}\eta_\beta, \tag{2.18}$$

$$\xi\sigma^\mu\bar\eta \equiv \xi^\alpha\sigma^\mu_{\alpha\dot\beta}\bar\eta^{\dot\beta}. \tag{2.19}$$

The behavior of the spinor products under hermitian conjugation (for quantum field operators) or complex conjugation (for classical fields) is as follows:

$$(\xi\eta)^\dagger = \bar\eta\bar\xi, \tag{2.20}$$

$$(\xi\sigma^\mu\bar\eta)^\dagger = \eta\sigma^\mu\bar\xi, \tag{2.21}$$

$$(\xi\sigma^\mu\overline{\sigma}^\nu\eta)^\dagger = \bar\eta\overline{\sigma}^\nu\sigma^\mu\bar\xi\,. \tag{2.22}$$

Note that these relations are applicable both to anti-commuting and to commuting spinors.

The following identities[2] can be used to systematically simplify expressions involving products of σ and $\overline{\sigma}$ matrices:

$$\sigma^\mu_{\alpha\dot\alpha}\overline{\sigma}^{\dot\beta\beta}_\mu = 2\delta^\beta_\alpha\delta^{\dot\beta}_{\dot\alpha}\,, \tag{2.23}$$

$$[\sigma^\mu\overline{\sigma}^\nu + \sigma^\nu\overline{\sigma}^\mu]_\alpha{}^\beta = 2g^{\mu\nu}\delta^\beta_\alpha\,, \tag{2.24}$$

$$[\overline{\sigma}^\mu\sigma^\nu + \overline{\sigma}^\nu\sigma^\mu]^{\dot\alpha}{}_{\dot\beta} = 2g^{\mu\nu}\delta^{\dot\alpha}_{\dot\beta}\,, \tag{2.25}$$

$$\sigma^\mu\overline{\sigma}^\nu\sigma^\rho = g^{\mu\nu}\overline{\sigma}^\rho - g^{\mu\rho}\overline{\sigma}^\nu + g^{\nu\rho}\overline{\sigma}^\mu + i\epsilon^{\mu\nu\rho\kappa}\overline{\sigma}_\kappa\,, \tag{2.26}$$

$$\overline{\sigma}^\mu\sigma^\nu\overline{\sigma}^\rho = g^{\mu\nu}\sigma^\rho - g^{\mu\rho}\sigma^\nu + g^{\nu\rho}\sigma^\mu - i\epsilon^{\mu\nu\rho\kappa}\sigma_\kappa\,. \tag{2.27}$$

[2]The Fierz identities of eqs. (2.23) and (2.38)–(2.40) and the identities (2.26), (2.27), (2.29), (2.30) involving the 4-dimensional ϵ tensor are not valid unless μ is a Lorentz vector index in exactly 4 dimensions. In $d \neq 4$ dimensions, as used for loop amplitudes in dimensional regularization and dimensional reduction schemes, the necessary modifications are given in Appendix A.

Computations of cross sections and decay rates generally require traces of alternating products of σ and $\overline{\sigma}$ matrices:

$$\mathrm{Tr}[\sigma^\mu\overline{\sigma}^\nu] = \mathrm{Tr}[\overline{\sigma}^\mu\sigma^\nu] = 2g^{\mu\nu}\,, \tag{2.28}$$

$$\mathrm{Tr}[\sigma^\mu\overline{\sigma}^\nu\sigma^\rho\overline{\sigma}^\kappa] = 2\left(g^{\mu\nu}g^{\rho\kappa} - g^{\mu\rho}g^{\nu\kappa} + g^{\mu\kappa}g^{\nu\rho} + i\epsilon^{\mu\nu\rho\kappa}\right)\,, \tag{2.29}$$

$$\mathrm{Tr}[\overline{\sigma}^\mu\sigma^\nu\overline{\sigma}^\rho\sigma^\kappa] = 2\left(g^{\mu\nu}g^{\rho\kappa} - g^{\mu\rho}g^{\nu\kappa} + g^{\mu\kappa}g^{\nu\rho} - i\epsilon^{\mu\nu\rho\kappa}\right)\,. \tag{2.30}$$

Traces involving a larger even number of σ and $\overline{\sigma}$ matrices can be systematically obtained from eqs. (2.28)–(2.30) by repeated use of eqs. (2.24)–(2.25) and the cyclic property of the trace. Traces involving an odd number of σ and $\overline{\sigma}$ matrices cannot arise, since there is no way to connect the spinor indices consistently.

In addition to manipulating expressions containing anticommuting fermion fields, we often must deal with products of *commuting* spinor wave functions that arise when evaluating the Feynman rules. In the following expressions we denote the generic spinor by z_i. In the various identities listed below, an extra minus sign arises when manipulating a product of anti-commuting fermion fields. Thus, we employ the notation:

$$(-1)^A \equiv \begin{cases} +1\,, & \text{commuting spinors,} \\ -1\,, & \text{anticommuting spinors.} \end{cases} \tag{2.31}$$

The following identities hold for the z_i:

$$z_1 z_2 = -(-1)^A z_2 z_1 \tag{2.32}$$

$$\bar{z}_1\bar{z}_2 = -(-1)^A \bar{z}_2\bar{z}_1 \tag{2.33}$$

$$z_1\sigma^\mu\bar{z}_2 = (-1)^A \bar{z}_2\overline{\sigma}^\mu z_1 \tag{2.34}$$

$$z_1\sigma^\mu\overline{\sigma}^\nu z_2 = -(-1)^A z_2\sigma^\nu\overline{\sigma}^\mu z_1 \tag{2.35}$$

$$\bar{z}_1\overline{\sigma}^\mu\sigma^\nu\bar{z}_2 = -(-1)^A \bar{z}_2\overline{\sigma}^\nu\sigma^\mu\bar{z}_1 \tag{2.36}$$

$$\bar{z}_1\overline{\sigma}^\mu\sigma^\rho\overline{\sigma}^\nu z_2 = (-1)^A z_2\sigma^\nu\overline{\sigma}^\rho\sigma^\mu\bar{z}_1\,, \tag{2.37}$$

and so on.

Finally, we note that eq. (2.23) can be used to derive a series of Fierz identities for two-component spinor products. For example,

$$\tfrac{1}{2}(z_1\sigma^\mu\bar{z}_2)(\bar{z}_3\overline{\sigma}_\mu z_4) = (-1)^A(z_1 z_4)(\bar{z}_3\bar{z}_2) \tag{2.38}$$

$$\tfrac{1}{2}(\bar{z}_1\overline{\sigma}^\mu z_2)(\bar{z}_3\overline{\sigma}_\mu z_4) = (-1)^A(\bar{z}_1\bar{z}_3)(z_4 z_2) \tag{2.39}$$

$$\tfrac{1}{2}(z_1\sigma^\mu\bar{z}_2)(z_3\sigma_\mu\bar{z}_4) = (-1)^A(z_1 z_3)(\bar{z}_4\bar{z}_2) \tag{2.40}$$

Additional Fierz identities can be found in Appendix A of ref. [6].

Many further identities are listed in Appendix A. We also direct the reader's attention to Appendix B, which gives a detailed correspondence between two-component spinor and four-component spinor notations.

3 Properties of fermion fields and external-state wave functions

3.1 A single two-component fermion field

We begin by describing the properties of a free neutral massive anti-commuting spin-1/2 field, denoted $\xi_\alpha(x)$, which transforms as $(\frac{1}{2},0)$ under the Lorentz group. The field ξ_α therefore corresponds to a Majorana fermion. The Lagrangian density is:

$$\mathcal{L} = i\bar{\xi}\overline{\sigma}^\mu\partial_\mu\xi - \tfrac{1}{2}m(\xi\xi + \bar{\xi}\bar{\xi})\,. \tag{3.1}$$

On-shell, ξ satisfies the free-field Dirac equation,

$$i\overline{\sigma}^{\mu\dot{\alpha}\beta}\partial_\mu\xi_\beta = m\bar{\xi}^{\dot{\alpha}}\,. \tag{3.2}$$

Consequently, ξ_α can be expanded in a Fourier series:

$$\xi_\alpha(x) = \sum_s \int \frac{d^3\mathbf{p}}{(2\pi)^{3/2}(2E_{\boldsymbol{p}})^{1/2}}\left[x_\alpha(\vec{\boldsymbol{p}},s)a(\vec{\boldsymbol{p}},s)e^{-ip\cdot x} + y_\alpha(\vec{\boldsymbol{p}},s)a^\dagger(\vec{\boldsymbol{p}},s)e^{ip\cdot x}\right], \tag{3.3}$$

where $E_{\boldsymbol{p}} \equiv (|\vec{\boldsymbol{p}}|^2 + m^2)^{1/2}$, and the creation and annihilation operators $a^\dagger$ and a satisfy anti-commutation relations:

$$\{a(\vec{\boldsymbol{p}},s), a^\dagger(\vec{\boldsymbol{p}}',s')\} = \delta^3(\vec{\boldsymbol{p}}-\vec{\boldsymbol{p}}')\delta_{ss'}\,, \tag{3.4}$$

and all other anticommutators vanish. It follows that

$$\bar{\xi}_{\dot{\alpha}}(x) \equiv (\xi_\alpha)^\dagger = \sum_s \int \frac{d^3\mathbf{p}}{(2\pi)^{3/2}(2E_{\boldsymbol{p}})^{1/2}}\left[\bar{x}_{\dot{\alpha}}(\vec{\boldsymbol{p}},s)a^\dagger(\vec{\boldsymbol{p}},s)e^{ip\cdot x} + \bar{y}_{\dot{\alpha}}(\vec{\boldsymbol{p}},s)a(\vec{\boldsymbol{p}},s)e^{-ip\cdot x}\right]. \tag{3.5}$$

We employ covariant normalization of the one particle states, *i.e.*, we act with one creation operator on the vacuum with the following convention

$$|\vec{\boldsymbol{p}},s\rangle \equiv (2\pi)^{3/2}(2E_{\boldsymbol{p}})^{1/2}a^\dagger(\vec{\boldsymbol{p}},s)\,|0\rangle\,, \tag{3.6}$$

so that $\langle\vec{\boldsymbol{p}},s|\vec{\boldsymbol{p}}',s'\rangle = (2\pi)^3(2E_{\boldsymbol{p}})\delta^3(\vec{\boldsymbol{p}}-\vec{\boldsymbol{p}}')\delta_{ss'}$. Therefore,

$$\langle 0|\,\xi_\alpha(x)\,|\vec{\boldsymbol{p}},s\rangle = x_\alpha(\vec{\boldsymbol{p}},s)e^{-ip\cdot x}\,, \qquad \langle 0|\,\bar{\xi}_{\dot{\alpha}}(x)\,|\vec{\boldsymbol{p}},s\rangle = \bar{y}_{\dot{\alpha}}(\vec{\boldsymbol{p}},s)e^{-ip\cdot x}\,, \tag{3.7}$$

$$\langle\vec{\boldsymbol{p}},s|\,\xi_\alpha(x)\,|0\rangle = y_\alpha(\vec{\boldsymbol{p}},s)e^{ip\cdot x}\,, \qquad \langle\vec{\boldsymbol{p}},s|\,\bar{\xi}_{\dot{\alpha}}(x)\,|0\rangle = \bar{x}_{\dot{\alpha}}(\vec{\boldsymbol{p}},s)e^{ip\cdot x}\,. \tag{3.8}$$

It should be emphasized that $\xi_\alpha(x)$ is an anticommuting spinor field, whereas x_α and y_α are *commuting* two-component spinor wave functions. The anticommuting properties of the fields are carried by the creation and annihilation operators.

Applying eq. (3.2) to eq. (3.3), we find that the x_α and y_α satisfy momentum space Dirac equations. These conditions can be written down in a number of equivalent ways:

$$(p\cdot\overline{\sigma})^{\dot\alpha\beta}x_\beta = m\bar y^{\dot\alpha}\,, \qquad (p\cdot\sigma)_{\alpha\dot\beta}\bar y^{\dot\beta} = mx_\alpha\,, \tag{3.9}$$

$$(p\cdot\sigma)_{\alpha\dot\beta}\bar x^{\dot\beta} = -my_\alpha\,, \qquad (p\cdot\overline{\sigma})^{\dot\alpha\beta}y_\beta = -m\bar x^{\dot\alpha}\,, \tag{3.10}$$

$$x^\alpha(p\cdot\sigma)_{\alpha\dot\beta} = -m\bar y_{\dot\beta}\,, \qquad \bar y_{\dot\alpha}(p\cdot\overline{\sigma})^{\dot\alpha\beta} = -mx^\beta\,, \tag{3.11}$$

$$\bar x_{\dot\alpha}(p\cdot\overline{\sigma})^{\dot\alpha\beta} = my^\beta\,, \qquad y^\alpha(p\cdot\sigma)_{\alpha\dot\beta} = m\bar x_{\dot\beta}\,. \tag{3.12}$$

Using the identity $(p\cdot\overline{\sigma})(p\cdot\sigma) = (p\cdot\sigma)(p\cdot\overline{\sigma}) = p^2$, one can quickly check that both x_α and y_α must satisfy the mass-shell condition, $p^2 = m^2$ (or equivalently, $p^0 = E_{\boldsymbol{p}}$). We will later see that eqs. (3.9)–(3.12) are often useful for simplifying matrix elements.

The quantum number s labels the spin or helicity of the spin-1/2 fermion. In order to construct the spin-1/2 helicity states, consider a basis of two-component spinors χ_λ that are eigenstates of $\frac{1}{2}\vec{\boldsymbol{\sigma}}\cdot\hat{\boldsymbol{p}}$, *i.e.*,

$$\tfrac{1}{2}\vec{\boldsymbol{\sigma}}\cdot\hat{\boldsymbol{p}}\,\chi_\lambda = \lambda\chi_\lambda, \qquad \lambda = \pm\tfrac{1}{2}\,. \tag{3.13}$$

If $\hat{\boldsymbol{p}}$ is a unit vector with polar angle θ and azimuthal angle ϕ with respect to a fixed z-axis, then the two-component spinors are[3]

$$\chi_{1/2}(\hat{\boldsymbol{p}}) = \begin{pmatrix} \cos\frac{\theta}{2} \\ e^{i\phi}\sin\frac{\theta}{2} \end{pmatrix}, \qquad \chi_{-1/2}(\hat{\boldsymbol{p}}) = \begin{pmatrix} -e^{-i\phi}\sin\frac{\theta}{2} \\ \cos\frac{\theta}{2} \end{pmatrix}. \tag{3.14}$$

The two-component helicity spinors satisfy:[4]

$$\chi_{-\lambda}(\hat{\boldsymbol{p}}) = \;\; 2\lambda\epsilon\chi^*_\lambda(\hat{\boldsymbol{p}})\,, \tag{3.15}$$

$$\chi_\lambda(-\hat{\boldsymbol{p}}) = -2\lambda e^{2i\lambda\phi}\chi_{-\lambda}(\hat{\boldsymbol{p}})\,, \tag{3.16}$$

where ϵ is the 2×2 matrix whose matrix elements are $\epsilon_{\alpha\beta}$. Alternatively, we could construct spin states where the spin is quantized in the particle's rest frame along a fixed axis, pointing along the unit three-vector $\hat{\boldsymbol{s}}$. If we denote χ_s to be an eigenstate of $\frac{1}{2}\vec{\boldsymbol{\sigma}}\cdot\hat{\boldsymbol{s}}$, then we may use the above formulas, where the angles θ and ϕ are now the polar and azimuthal angles of $\hat{\boldsymbol{s}}$. In

[3]One can construct $\chi_\lambda(\hat{\boldsymbol{p}})$ from $\chi_\lambda(\hat{\boldsymbol{z}})$ by employing the spin-1/2 rotation operator corresponding to a rotation from the $\hat{\boldsymbol{z}}$-direction to the direction of $\hat{\boldsymbol{p}}$ (characterized by polar angle θ and azimuthal angle ϕ). More explicitly, $\chi_\lambda(\hat{\boldsymbol{p}}) = \exp\left(-i\theta\hat{\boldsymbol{n}}\cdot\vec{\boldsymbol{\sigma}}/2\right)\,\chi_\lambda(\hat{\boldsymbol{z}})$, where $\hat{\boldsymbol{n}} = (-\sin\phi, \cos\phi, 0)$.

[4]Note that $-\hat{\boldsymbol{p}}$ is a unit vector with polar angle $\pi-\theta$ and azimuthal angle $\phi+\pi$ with respect to the fixed z-axis.

relativistic scattering processes, it is usually more convenient to employ helicity states. Note that for massless particles, there is no rest frame and one must use helicity states.

For fermions of mass $m \neq 0$, it is possible to define the spin four-vector s^μ, which satisfies $s\cdot p = 0$ and $s\cdot s = -1$. In the rest frame of the particle, $s^\mu = 2\lambda(0;\hat{\boldsymbol{s}})$, where $\lambda = +1/2$ $[-1/2]$ corresponds to spin-up [spin-down] with respect to the spin quantization axis that points in the direction of the unit three-vector $\hat{\boldsymbol{s}}$. For helicity states, the spin four-vector is defined as

$$s^\mu = (2\lambda)\frac{1}{m}\,(|\vec{\boldsymbol{p}}|\,;\,E\hat{\boldsymbol{p}})\ , \tag{3.17}$$

where $2\lambda = \pm 1$ is twice the spin-1/2 particle helicity. Note that in the rest frame, $s^\mu = 2\lambda\,(0\,;\,\hat{\boldsymbol{p}})$, whereas in the high energy limit (where $E \gg m$), $s^\mu = 2\lambda p^\mu/m + \mathcal{O}(m/E)$. For a massless fermion, the spin four-vector does not exist (there is no rest frame). Nevertheless, one can obtain consistent results by working with massive helicity states and taking the $m \to 0$ limit at the end of the computation. In this case, we can simply use $s^\mu = 2\lambda p^\mu/m + \mathcal{O}(m/E)$; in practical computations the final result will be well-defined in the zero mass limit.

The two-component spinors x and y can now be given explicitly in terms of the χ_λ defined in eq. (3.14):

$$x_\alpha(\vec{\boldsymbol{p}},\lambda) = \sqrt{p\cdot\sigma}\,\chi_\lambda\,, \qquad x^\alpha(\vec{\boldsymbol{p}},\lambda) = -2\lambda\chi^\dagger_{-\lambda}\sqrt{p\cdot\overline{\sigma}}\,, \tag{3.18}$$

$$y_\alpha(\vec{\boldsymbol{p}},\lambda) = 2\lambda\sqrt{p\cdot\sigma}\,\chi_{-\lambda}\,, \qquad y^\alpha(\vec{\boldsymbol{p}},\lambda) = \chi^\dagger_\lambda\sqrt{p\cdot\overline{\sigma}}\,, \tag{3.19}$$

or equivalently

$$\bar{x}^{\dot\alpha}(\vec{\boldsymbol{p}},\lambda) = -2\lambda\sqrt{p\cdot\overline{\sigma}}\,\chi_{-\lambda}\,, \qquad \bar{x}_{\dot\alpha}(\vec{\boldsymbol{p}},\lambda) = \chi^\dagger_\lambda\sqrt{p\cdot\sigma}\,, \tag{3.20}$$

$$\bar{y}^{\dot\alpha}(\vec{\boldsymbol{p}},\lambda) = \sqrt{p\cdot\overline{\sigma}}\,\chi_\lambda\,, \qquad \bar{y}_{\dot\alpha}(\vec{\boldsymbol{p}},\lambda) = 2\lambda\chi^\dagger_{-\lambda}\sqrt{p\cdot\sigma}\,. \tag{3.21}$$

In the above equations, $p^0 = E_{\boldsymbol{p}}$ is satisfied and[5]

$$\sqrt{p\cdot\sigma} \equiv \frac{E_{\boldsymbol{p}} + m - \vec{\boldsymbol{\sigma}}\cdot\vec{\boldsymbol{p}}}{\sqrt{2(E_{\boldsymbol{p}}+m)}}\,, \tag{3.22}$$

$$\sqrt{p\cdot\overline{\sigma}} \equiv \frac{E_{\boldsymbol{p}} + m + \vec{\boldsymbol{\sigma}}\cdot\vec{\boldsymbol{p}}}{\sqrt{2(E_{\boldsymbol{p}}+m)}}\,. \tag{3.23}$$

The phase choices employed in eqs. (3.18)–(3.21) are conventional and consistent with the phase choices for four-component spinor wave functions [see Appendix B]. We again emphasize that in eqs. (3.18)–(3.21), one may either choose χ_λ to be an eigenstate of $\vec{\boldsymbol{\sigma}}\cdot\hat{\boldsymbol{p}}$ (which yields

[5]The matrix square root of $p\cdot\sigma$ [or $p\cdot\overline{\sigma}$] as defined here is the unique hermitian matrix with non-negative eigenvalues whose square is equal to $p\cdot\sigma$ [or $p\cdot\overline{\sigma}$]. One can check the validity of eqs. (3.22) and (3.23) by squaring both sides.

the helicity spinor wave functions), or choose χ_λ to be an eigenstate of $\vec{\boldsymbol{\sigma}}\cdot\hat{\boldsymbol{s}}$, where the spin is measured in the rest frame along the quantization axis $\hat{\boldsymbol{s}}$.

The following equations can now be verified by explicit computation:

$$(s\cdot\overline{\sigma})^{\dot\alpha\beta}x_\beta = \bar y^{\dot\alpha}\,, \qquad (s\cdot\sigma)_{\alpha\dot\beta}\bar y^{\dot\beta} = -x_\alpha\,, \tag{3.24}$$

$$(s\cdot\sigma)_{\alpha\dot\beta}\bar x^{\dot\beta} = -y_\alpha\,, \qquad (s\cdot\overline{\sigma})^{\dot\alpha\beta}y_\beta = \bar x^{\dot\alpha}\,, \tag{3.25}$$

$$x^\alpha(s\cdot\sigma)_{\alpha\dot\beta} = -\bar y_{\dot\beta}\,, \qquad \bar y_{\dot\alpha}(s\cdot\overline{\sigma})^{\dot\alpha\beta} = x^\beta\,, \tag{3.26}$$

$$\bar x_{\dot\alpha}(s\cdot\overline{\sigma})^{\dot\alpha\beta} = y^\beta\,, \qquad y^\alpha(s\cdot\sigma)_{\alpha\dot\beta} = -\bar x_{\dot\beta}\,. \tag{3.27}$$

The consistency of these results can be checked as follows. First, from each of eqs. (3.24)–(3.27) one finds that

$$(s\cdot\sigma)_{\alpha\dot\alpha}(s\cdot\overline{\sigma})^{\dot\alpha\beta} = -\delta^\beta_\alpha\,, \qquad (s\cdot\overline{\sigma})^{\dot\alpha\alpha}(s\cdot\sigma)_{\alpha\dot\beta} = -\delta^{\dot\alpha}_{\dot\beta}\,. \tag{3.28}$$

¿From eqs. (A.1) and (A.2) it follows that $s\cdot s = -1$, as required. Second, if one applies

$$p\cdot\sigma\, s\cdot\overline{\sigma} + s\cdot\sigma\, p\cdot\overline{\sigma} = 2p\cdot s\,, \qquad p\cdot\overline{\sigma}\, s\cdot\sigma + s\cdot\overline{\sigma}\, p\cdot\sigma = 2p\cdot s\,, \tag{3.29}$$

to eqs. (3.9)–(3.12) and eqs. (3.24)–(3.27), it follows that $p\cdot s = 0$.

It is useful to combine the results of eqs. (3.9)–(3.12) and eqs. (3.24)–(3.27) as follows:

$$(p^\mu - ms^\mu)\overline{\sigma}^{\dot\alpha\beta}_\mu x_\beta = 0\,, \qquad (p_\mu - ms_\mu)\sigma^\mu_{\alpha\dot\beta}\bar x^{\dot\beta} = 0\,, \tag{3.30}$$

$$(p^\mu + ms^\mu)\overline{\sigma}^{\dot\alpha\beta}_\mu y_\beta = 0\,, \qquad (p_\mu + ms_\mu)\sigma^\mu_{\alpha\dot\beta}\bar y^{\dot\beta} = 0\,, \tag{3.31}$$

$$x^\alpha\sigma^\mu_{\alpha\dot\beta}(p_\mu - ms_\mu) = 0\,, \qquad \bar x_{\dot\alpha}\overline{\sigma}^{\dot\alpha\beta}_\mu(p^\mu - ms^\mu) = 0\,, \tag{3.32}$$

$$y^\alpha\sigma^\mu_{\alpha\dot\beta}(p_\mu + ms_\mu) = 0\,, \qquad \bar y_{\dot\alpha}\overline{\sigma}^{\dot\alpha\beta}_\mu(p^\mu + ms^\mu) = 0\,. \tag{3.33}$$

The above results are applicable only for massive fermions (where the spin four-vector s^μ exists). However, in the case of a massless fermion we can obtain valid results for helicity spinors simply by setting $s^\mu = 2\lambda p^\mu/m$ and then taking the $m\to 0$ limit. In particular, replacing $ms^\mu = 2\lambda p^\mu$ in eqs. (3.30)–(3.33), and using the results of eqs. (3.9)–(3.12) [before taking the $m\to 0$ limit] yields

$$(1+2\lambda)x(\vec{\boldsymbol{p}},\lambda) = 0\,, \qquad (1-2\lambda)y(\vec{\boldsymbol{p}},\lambda) = 0\,, \tag{3.34}$$

where λ is the helicity. Finally, we take the $m\to 0$ limit. The meaning of the end result is clear; for massless fermions, only one helicity component of x and y is non-zero. Applying this result to neutrinos, we find that massless neutrinos are left-handed ($\lambda = -1/2$), while anti-neutrinos are right-handed ($\lambda = +1/2$).

As a further check on the consistency of the explicit forms of eqs. (3.18)–(3.21), one may apply the results of eq. (3.24) to obtain

$$s\cdot\overline{\sigma}\sqrt{p\cdot\sigma}\,\chi_\lambda = \sqrt{p\cdot\overline{\sigma}}\,\chi_\lambda\,. \tag{3.35}$$

Using $\sqrt{p\cdot\sigma}\sqrt{p\cdot\overline{\sigma}} = m$, one finds:

$$\sqrt{p\cdot\sigma}(s\cdot\overline{\sigma})\sqrt{p\cdot\sigma}\;\chi_\lambda = m\chi_\lambda\,. \tag{3.36}$$

Now eq. (3.36) can be independently verified by using using eqs. (3.13) and (3.22) and the explicit form for s^μ [eq. (3.17)]. (Keep in mind that s^μ implicitly includes a factor of 2λ.) That is, in eq. (3.36), the *same* λ occurs implicitly in s^μ and explicitly in χ_λ. Since s^μ changes sign when λ changes sign, we can generalize eq. (3.36) to obtain the relation:

$$\tfrac{1}{2}\left[1 + \frac{1}{m}\sqrt{p\cdot\sigma}(s\cdot\overline{\sigma})\sqrt{p\cdot\sigma}\right]\chi_{\lambda'} = \delta_{\lambda\lambda'}\chi_\lambda\,, \tag{3.37}$$

which will be useful shortly. In eq. (3.37), the λ implicit in the definition of s is *fixed*.

Having defined explicit forms for the two-component spinor wave functions, we can now write down the spin projection operators. For massive fermions, they are:

$$x_\alpha(\vec{\boldsymbol{p}},\lambda)\bar{x}_{\dot\beta}(\vec{\boldsymbol{p}},\lambda) = \tfrac{1}{2}(p_\mu - ms_\mu)\sigma^\mu_{\alpha\dot\beta}\,, \tag{3.38}$$

$$\bar{y}^{\dot\alpha}(\vec{\boldsymbol{p}},\lambda)y^\beta(\vec{\boldsymbol{p}},\lambda) = \tfrac{1}{2}(p^\mu + ms^\mu)\overline{\sigma}_\mu^{\dot\alpha\beta}\,, \tag{3.39}$$

$$x_\alpha(\vec{\boldsymbol{p}},\lambda)y^\beta(\vec{\boldsymbol{p}},\lambda) = \tfrac{1}{2}\left(m\delta_\alpha{}^\beta - [s\cdot\sigma\, p\cdot\overline{\sigma}]_\alpha{}^\beta\right)\,, \tag{3.40}$$

$$\bar{y}^{\dot\alpha}(\vec{\boldsymbol{p}},\lambda)\bar{x}_{\dot\beta}(\vec{\boldsymbol{p}},\lambda) = \tfrac{1}{2}\left(m\delta^{\dot\alpha}{}_{\dot\beta} + [s\cdot\overline{\sigma}\, p\cdot\sigma]^{\dot\alpha}{}_{\dot\beta}\right)\,, \tag{3.41}$$

or equivalently,

$$\bar{x}^{\dot\alpha}(\vec{\boldsymbol{p}},\lambda)x^\beta(\vec{\boldsymbol{p}},\lambda) = \tfrac{1}{2}(p^\mu - ms^\mu)\overline{\sigma}_\mu^{\dot\alpha\beta}\,, \tag{3.42}$$

$$y_\alpha(\vec{\boldsymbol{p}},\lambda)\bar{y}_{\dot\beta}(\vec{\boldsymbol{p}},\lambda) = \tfrac{1}{2}(p_\mu + ms_\mu)\sigma^\mu_{\alpha\dot\beta}\,, \tag{3.43}$$

$$y_\alpha(\vec{\boldsymbol{p}},s)x^\beta(\vec{\boldsymbol{p}},s) = -\tfrac{1}{2}\left(m\delta_\alpha{}^\beta + [s\cdot\sigma\, p\cdot\overline{\sigma}]_\alpha{}^\beta\right)\,, \tag{3.44}$$

$$\bar{x}^{\dot\alpha}(\vec{\boldsymbol{p}},\lambda)\bar{y}_{\dot\beta}(\vec{\boldsymbol{p}},\lambda) = -\tfrac{1}{2}\left(m\delta^{\dot\alpha}{}_{\dot\beta} - [s\cdot\overline{\sigma}\, p\cdot\sigma]^{\dot\alpha}{}_{\dot\beta}\right)\,. \tag{3.45}$$

The derivation of these results is straightforward. For example, with both spinor indices in the lowered position,

$$\begin{aligned} x(\vec{\boldsymbol{p}},\lambda)\bar{x}(\vec{\boldsymbol{p}},\lambda) &= \sqrt{p\cdot\sigma}\chi_\lambda\chi_\lambda^\dagger\sqrt{p\cdot\sigma} \\ &= \tfrac{1}{2}\sqrt{p\cdot\sigma}\left[1 + \frac{1}{m}\sqrt{p\cdot\sigma}s\cdot\overline{\sigma}\sqrt{p\cdot\sigma}\right]\sum_{\lambda'}\chi_{\lambda'}\chi_{\lambda'}^\dagger\sqrt{p\cdot\sigma} \\ &= \tfrac{1}{2}\left[p\cdot\sigma + \frac{1}{m}p\cdot\sigma s\cdot\overline{\sigma}p\cdot\sigma\right] \\ &= \tfrac{1}{2}\left[p\cdot\sigma - ms\cdot\sigma\right]\,. \end{aligned} \tag{3.46}$$

In this derivation, we made use of eq. (3.37) and the completeness of the χ_λ, and simplified the product of three dot-products by noting that $p\cdot s = 0$ implies that $s\cdot\overline{\sigma}\; p\cdot\sigma = -p\cdot\overline{\sigma}\; s\cdot\sigma$. The other spin projection formulas can be similarly derived.

For the case of massless spin-1/2 fermions, we must use helicity spinor wave functions. Setting $s = 2\lambda p/m$ in the above formulas and letting $m \to 0$ yields

$$x_\alpha(\vec{\boldsymbol{p}},\lambda)\bar{x}_{\dot\beta}(\vec{\boldsymbol{p}},\lambda) = (\tfrac{1}{2}-\lambda)p\cdot\sigma_{\alpha\dot\beta}\,, \qquad \bar{x}^{\dot\alpha}(\vec{\boldsymbol{p}},\lambda)x^\beta(\vec{\boldsymbol{p}},\lambda) = (\tfrac{1}{2}-\lambda)p\cdot\overline{\sigma}^{\dot\alpha\beta}\,, \tag{3.47}$$

$$\bar{y}^{\dot\alpha}(\vec{\boldsymbol{p}},\lambda)y^\beta(\vec{\boldsymbol{p}},\lambda) = (\tfrac{1}{2}+\lambda)p\cdot\overline{\sigma}^{\dot\alpha\beta}\,, \qquad y_\alpha(\vec{\boldsymbol{p}},\lambda)\bar{y}_{\dot\beta}(\vec{\boldsymbol{p}},\lambda) = (\tfrac{1}{2}+\lambda)p\cdot\sigma_{\alpha\dot\beta}\,, \tag{3.48}$$

$$x_\alpha(\vec{\boldsymbol{p}},\lambda)y^\beta(\vec{\boldsymbol{p}},\lambda) = 0\,, \qquad y_\alpha(\vec{\boldsymbol{p}},\lambda)x^\beta(\vec{\boldsymbol{p}},\lambda) = 0\,, \tag{3.49}$$

$$\bar{y}^{\dot\alpha}(\vec{\boldsymbol{p}},\lambda)\bar{x}_{\dot\beta}(\vec{\boldsymbol{p}},\lambda) = 0\,, \qquad \bar{x}^{\dot\alpha}(\vec{\boldsymbol{p}},\lambda)\bar{y}_{\dot\beta}(\vec{\boldsymbol{p}},\lambda) = 0\,. \tag{3.50}$$

Having listed the projection operators for definite spin projection or helicity, we may now sum over spins to derive the spin-sum identities. These arise when computing squared matrix elements for unpolarized scattering and decay. There are only four basic identities, but for convenience we list each of them with the two index height permutations that can occur in squared amplitudes by following the rules given in this paper. The results can be derived by inspection of the spin projection operators, since summing over $\lambda = \pm 1/2$ simply removes all terms linear in the spin four-vector (which is proportional to λ).

$$\sum_\lambda x_\alpha(\vec{\boldsymbol{p}},\lambda)\bar{x}_{\dot\beta}(\vec{\boldsymbol{p}},\lambda) = p\cdot\sigma_{\alpha\dot\beta}\,, \qquad \sum_\lambda \bar{x}^{\dot\alpha}(\vec{\boldsymbol{p}},\lambda)x^\beta(\vec{\boldsymbol{p}},\lambda) = p\cdot\overline{\sigma}^{\dot\alpha\beta}\,, \tag{3.51}$$

$$\sum_\lambda \bar{y}^{\dot\alpha}(\vec{\boldsymbol{p}},\lambda)y^\beta(\vec{\boldsymbol{p}},\lambda) = p\cdot\overline{\sigma}^{\dot\alpha\beta}\,, \qquad \sum_\lambda y_\alpha(\vec{\boldsymbol{p}},\lambda)\bar{y}_{\dot\beta}(\vec{\boldsymbol{p}},\lambda) = p\cdot\sigma_{\alpha\dot\beta}\,, \tag{3.52}$$

$$\sum_\lambda x_\alpha(\vec{\boldsymbol{p}},\lambda)y^\beta(\vec{\boldsymbol{p}},\lambda) = m\delta_\alpha{}^\beta\,, \qquad \sum_\lambda y_\alpha(\vec{\boldsymbol{p}},s)x^\beta(\vec{\boldsymbol{p}},\lambda) = -m\delta_\alpha{}^\beta\,, \tag{3.53}$$

$$\sum_\lambda \bar{y}^{\dot\alpha}(\vec{\boldsymbol{p}},\lambda)\bar{x}_{\dot\beta}(\vec{\boldsymbol{p}},\lambda) = m\delta^{\dot\alpha}{}_{\dot\beta}\,, \qquad \sum_\lambda \bar{x}^{\dot\alpha}(\vec{\boldsymbol{p}},\lambda)\bar{y}_{\dot\beta}(\vec{\boldsymbol{p}},\lambda) = -m\delta^{\dot\alpha}{}_{\dot\beta}\,. \tag{3.54}$$

These results hold for both massive and massless spin-1/2 fermions.

3.2 Fermion mass diagonalization and external wave functions in a general theory

Consider a collection of free anti-commuting two-component spin-1/2 fields, $\hat\xi_{\alpha i}(x)$, which transform as $(\frac{1}{2},0)$ fields under the Lorentz group. Here, α is the spinor index, and i labels the distinct fields of the collection. The free-field Lagrangian is given by

$$\mathcal{L} = i\bar{\hat\xi}^i\overline{\sigma}^\mu\partial_\mu\hat\xi_i - \tfrac{1}{2}M^{ij}\hat\xi_i\hat\xi_j - \tfrac{1}{2}M_{ij}\bar{\hat\xi}^i\bar{\hat\xi}^j\,, \tag{3.55}$$

where

$$M_{ij} \equiv (M^{ij})^*. \tag{3.56}$$

Note that M^{ij} is a complex symmetric matrix, since the product of anticommuting two-component fields satisfies $\hat\xi_i\hat\xi_j = \hat\xi_j\hat\xi_i$ [with the spinor contraction rule according to eq. (2.15)].

We can diagonalize the mass matrix and rewrite the Lagrangian in terms of mass eigenstates $\xi_{\alpha i}$ that have corresponding real non-negative masses m_i. To do this, we introduce a unitary matrix Ω

$$\hat{\xi}_i = \Omega_i{}^k \xi_k \tag{3.57}$$

and demand that $M^{ij}\Omega_i{}^k\Omega_j{}^\ell = m_k\delta^{k\ell}$ (no sum over k), where the m_k are real and non-negative. Equivalently, in matrix notation with suppressed indices,

$$\Omega^T M\,\Omega = m = \mathrm{diag}(m_1, m_2, \ldots). \tag{3.58}$$

The Takagi factorization of linear algebra [7] states that for an arbitrary complex symmetric matrix M, one can indeed always find such a (complex) unitary matrix Ω. To compute the values of the diagonal elements of m, one may simply note that

$$\Omega^T M M^\dagger \Omega^* = m^2. \tag{3.59}$$

(This is an illustration of that fact that since $MM^\dagger$ is hermitian, it can be diagonalized by a unitary matrix.) Thus, the diagonal elements of m are the non-negative square roots of the corresponding eigenvalues of $MM^\dagger$.

In terms of the mass eigenstates,

$$\mathcal{L} = i\bar{\xi}^i\overline{\sigma}^\mu\partial_\mu\xi_i - \tfrac{1}{2}m_i(\xi_i\xi_i + \bar{\xi}^i\bar{\xi}^i)\,. \tag{3.60}$$

Each $\xi_{\alpha i}$ can now be expanded in a Fourier series, exactly as in the previous subsection:

$$\xi_{\alpha i}(x) = \sum_s \int \frac{d^3p}{(2\pi)^{3/2}(2E_{i\boldsymbol{p}})^{1/2}} \left[x_\alpha(\vec{\boldsymbol{p}},s)a_i(\vec{\boldsymbol{p}},s)e^{-ip\cdot x} + y_\alpha(\vec{\boldsymbol{p}},s)a_i^\dagger(\vec{\boldsymbol{p}},s)e^{ip\cdot x}\right], \tag{3.61}$$

where $E_{i\boldsymbol{p}} \equiv (|\vec{\boldsymbol{p}}|^2 + m_i^2)^{1/2}$, and the creation and annihilation operators, $a_i^\dagger$ and a_i satisfy anticommutation relations:

$$\{a_i(\vec{\boldsymbol{p}},s), a_j^\dagger(\vec{\boldsymbol{p}}',s')\} = \delta^3(\vec{\boldsymbol{p}}-\vec{\boldsymbol{p}}')\delta_{ss'}\delta_{ij}\,. \tag{3.62}$$

We employ covariant normalization of the one particle states, *i.e.*, we act with one creation operator on the vacuum with the following convention

$$|\vec{\boldsymbol{p}},s\rangle \equiv (2\pi)^{3/2}(2E_{i\boldsymbol{p}})^{1/2}a_i^\dagger(\vec{\boldsymbol{p}},s)\,|0\rangle\,, \tag{3.63}$$

so that $\langle\vec{\boldsymbol{p}}|\vec{\boldsymbol{p}}'\rangle = (2\pi)^3(2E_{i\boldsymbol{p}})\delta^3(\vec{\boldsymbol{p}}-\vec{\boldsymbol{p}}')$.

Although the preceding mass diagonalization procedure will always work, there is a modification that is convenient when there are massive Dirac fermions carrying a conserved charge.

The key is to note that what we really need is a diagonal *squared*-mass matrix, so that denominators of propagators will be diagonal. If χ_α is a charged massive field, then there must be an associated independent two-component spinor field η_α of equal mass with the opposite charge. They appear in the Lagrangian as:

$$\mathcal{L} = i\bar{\chi}\overline{\sigma}^\mu\partial_\mu\chi + i\bar{\eta}\overline{\sigma}^\mu\partial_\mu\eta - M(\chi\eta + \bar{\chi}\bar{\eta}) \tag{3.64}$$

Together, χ and $\bar{\eta}$ constitute a single Dirac fermion. We can then write:

$$\chi_\alpha(x) = \sum_s \int \frac{d^3p}{(2\pi)^{3/2}(2E_{\boldsymbol{p}})^{1/2}} \left[x_\alpha(\vec{\boldsymbol{p}},s)a(\vec{\boldsymbol{p}},s)e^{-ip\cdot x} + y_\alpha(\vec{\boldsymbol{p}},s)b^\dagger(\vec{\boldsymbol{p}},s)e^{ip\cdot x}\right], \tag{3.65}$$

$$\eta_\alpha(x) = \sum_s \int \frac{d^3p}{(2\pi)^{3/2}(2E_{\boldsymbol{p}})^{1/2}} \left[x_\alpha(\vec{\boldsymbol{p}},s)b(\vec{\boldsymbol{p}},s)e^{-ip\cdot x} + y_\alpha(\vec{\boldsymbol{p}},s)a^\dagger(\vec{\boldsymbol{p}},s)e^{ip\cdot x}\right], \tag{3.66}$$

where $E_{\boldsymbol{p}} \equiv (|\vec{\boldsymbol{p}}|^2 + m^2)^{1/2}$, and the creation and annihilation operators, $a^\dagger$, $b^\dagger$, a and b satisfy anticommutation relations:

$$\{a(\vec{\boldsymbol{p}},s), a^\dagger(\vec{\boldsymbol{p}}',s')\} = \{b(\vec{\boldsymbol{p}},s), b^\dagger(\vec{\boldsymbol{p}}',s')\} = \delta^3(\vec{\boldsymbol{p}} - \vec{\boldsymbol{p}}')\delta_{s,s'}\,, \tag{3.67}$$

and all other anticommutators vanish. We now must distinguish between two types of one particle states, which we can call fermion (F) and anti-fermion (A):

$$|\vec{\boldsymbol{p}},s;F\rangle \equiv (2\pi)^{3/2}(2E_{\boldsymbol{p}})^{1/2}b^\dagger(\vec{\boldsymbol{p}},s)\,|0\rangle\,, \tag{3.68}$$

$$|\vec{\boldsymbol{p}},s;A\rangle \equiv (2\pi)^{3/2}(2E_{\boldsymbol{p}})^{1/2}a^\dagger(\vec{\boldsymbol{p}},s)\,|0\rangle\,. \tag{3.69}$$

Note that both $\chi(x)$ and $\bar{\eta}(x)$ can create $|\vec{\boldsymbol{p}},s;F\rangle$ from the vacuum, while $\bar{\chi}(x)$ and $\eta(x)$ can create $|\vec{\boldsymbol{p}},s;A\rangle$. The one-particle wave functions are given by:

$$\langle 0|\,\eta_\alpha(x)\,|\vec{\boldsymbol{p}},s;F\rangle = x_\alpha(\vec{\boldsymbol{p}},s)e^{-ip\cdot x}\,, \qquad \langle 0|\,\bar{\chi}_{\dot\alpha}(x)\,|\vec{\boldsymbol{p}},s;F\rangle = \bar{y}_{\dot\alpha}(\vec{\boldsymbol{p}},s)e^{-ip\cdot x}\,, \tag{3.70}$$

$$\langle F;\vec{\boldsymbol{p}},s|\,\chi_\alpha(x)\,|0\rangle = y_\alpha(\vec{\boldsymbol{p}},s)e^{ip\cdot x}\,, \qquad \langle F;\vec{\boldsymbol{p}},s|\,\bar{\eta}_{\dot\alpha}(x)\,|0\rangle = \bar{x}_{\dot\alpha}(\vec{\boldsymbol{p}},s)e^{ip\cdot x}\,, \tag{3.71}$$

$$\langle 0|\,\chi_\alpha(x)\,|\vec{\boldsymbol{p}},s;A\rangle = x_\alpha(\vec{\boldsymbol{p}},s)e^{-ip\cdot x}\,, \qquad \langle 0|\,\bar{\eta}_{\dot\alpha}(x)\,|\vec{\boldsymbol{p}},s;A\rangle = \bar{y}_{\dot\alpha}(\vec{\boldsymbol{p}},s)e^{-ip\cdot x}\,, \tag{3.72}$$

$$\langle A;\vec{\boldsymbol{p}},s|\,\eta_\alpha(x)\,|0\rangle = y_\alpha(\vec{\boldsymbol{p}},s)e^{ip\cdot x}\,, \qquad \langle A;\vec{\boldsymbol{p}},s|\,\bar{\chi}_{\dot\alpha}(x)\,|0\rangle = \bar{x}_{\dot\alpha}(\vec{\boldsymbol{p}},s)e^{ip\cdot x}\,, \tag{3.73}$$

and the eight other single-particle matrix elements vanish.

More generally, consider a collection of such free anti-commuting charged massive spin-1/2 fields, which can be represented by pairs of two-component fields $\hat{\chi}_{\alpha i}(x)$, $\hat{\eta}_{\alpha i}(x)$, where $\hat{\eta}_{\alpha i}(x)$ transforms in a (possibly reducible) representation of the unbroken symmetry group that is the complex conjugate of the representation of $\hat{\chi}_{\alpha i}(x)$. The free-field Lagrangian is given by

$$\mathcal{L} = i\bar{\hat{\chi}}^i\overline{\sigma}^\mu\partial_\mu\hat{\chi}_i + i\bar{\hat{\eta}}^i\overline{\sigma}^\mu\partial_\mu\hat{\eta}_i - M^{ij}\hat{\chi}_i\hat{\eta}_j - M_{ij}\bar{\hat{\chi}}^i\bar{\hat{\eta}}^j\,, \tag{3.74}$$

where M^{ij} is an arbitrary symmetric complex matrix, and $M_{ij} \equiv (M^{ij})^*$ as before. We diagonalize the mass matrix by introducing eigenstates χ_i and η_i and unitary matrices L and R,

$$\hat{\chi}_i = L_i{}^k \chi_k \,, \qquad\qquad \hat{\eta}_i = R_i{}^k \eta_k \,, \tag{3.75}$$

and demand that $M^{ij} L_i{}^k R_j{}^\ell = m_k \delta^{k\ell}$ (no sum over k). In matrix form, this is written as:

$$L^T M R = m = \mathrm{diag}(m_1, m_2, \ldots), \tag{3.76}$$

with the m_i real and non-negative. The singular-value decomposition of linear algebra states that for any complex matrix M, there indeed exist such unitary matrices L and R. It follows that:

$$L^T (M M^\dagger) L^* = m^2, \tag{3.77}$$

$$R^\dagger (M^\dagger M) R = m^2. \tag{3.78}$$

This illustrates the fact that since $MM^\dagger$ and $M^\dagger M$ are both hermitian (these two matrices are not equal in general, although they possess the same real non-negative eigenvalues), they can be diagonalized by unitary matrices. The diagonal elements of m are therefore the non-negative square roots of the corresponding eigenvalues of $MM^\dagger$ (or $M^\dagger M$).

Thus, in terms of the mass eigenstates,

$$\mathcal{L} = i\bar{\chi}^i \overline{\sigma}^\mu \partial_\mu \chi_i + i\bar{\eta}^i \overline{\sigma}^\mu \partial_\mu \eta_i - m_i (\chi_i \eta_i + \bar{\chi}^i \bar{\eta}^i) \,. \tag{3.79}$$

The mass matrix now consists of 2×2 blocks $\begin{pmatrix} 0 & m_i \\ m_i & 0 \end{pmatrix}$ along the diagonal. More importantly, the mass matrix is diagonal with doubly-degenerate entries m_i^2 that will appear in the denominators of the propagators of the theory. It describes a collection of Dirac fermions.[6]

The result of the mass diagonalization procedure in a general theory therefore always consists of a collection of Majorana fermions as in equation (3.60), plus a collection of Dirac fermions as in equation (3.79). This is the basis of the Feynman rules to be presented in the next section.

[6]Of course, one could always choose instead to treat the Dirac fermions in a basis with a fully diagonalized mass matrix, as in equation (3.60), by defining $\xi_{2i-1} = (\chi_i + \eta_i)/\sqrt{2}$ and $\xi_{2i} = i(\chi_i - \eta_i)/\sqrt{2}$. These fermion fields do not carry well-defined charges, and are analogous to writing a charged scalar field ϕ and its oppositely-charged conjugate ϕ^* in terms of their real and imaginary parts. However, it is rarely, if ever, convenient to do so; practical calculations only require that the mass matrix is diagonal, and it is of course more pleasant to use fields that carry well-defined charges.

4 Feynman rules with two-component spinors

4.1 External fermion lines

Let us consider a general theory, for which we may assume that the mass matrix for fermions has been diagonalized as discussed in the previous section. The rules for assigning two-component external state spinors are then as follows. (From now on we suppress the momentum and spin arguments of the spinor wave functions.)

- For an initial-state left-handed $(\frac{1}{2}, 0)$ fermion: x.
- For an initial-state right-handed $(0, \frac{1}{2})$ fermion: $\bar{y}$.
- For a final-state left-handed $(\frac{1}{2}, 0)$ fermion: $\bar{x}$.
- For a final-state right-handed $(0, \frac{1}{2})$ fermion: y.

Note that, in general, the two-component external state fermion wave functions are distinguished by their Lorentz group transformation properties, rather than by their particle or antiparticle status as in four-component Feynman rules. This helps to explain why two-component notation is especially convenient for (i) theories with Majorana particles, in which there is no fundamental distinction between particles and antiparticles, and (ii) theories like the Standard Model and MSSM in which the left and right-handed fermions transform under different representations of the gauge group.

These rules are summarized in the following mnemonic diagram:

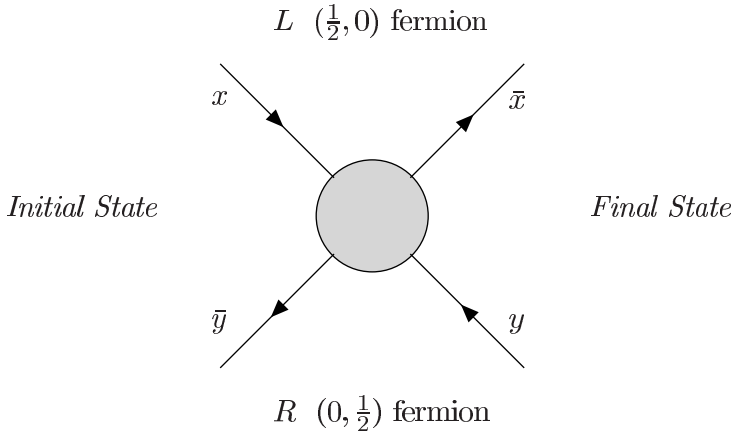

Figure 1: The external wave-function spinors should be assigned as indicated here, for initial-state and final-state left-handed $(\frac{1}{2}, 0)$ and right-handed $(0, \frac{1}{2})$ fermions.

In contrast to four-component Feynman rules, the direction of the arrows do *not* correspond to the flow of charge or fermion number. Nevertheless, the above choice is convenient—the arrows of $(\frac{1}{2},0)$ fermions always point in the direction of their momenta while the arrows of $(0,\frac{1}{2})$ fermions always point opposite to their momenta. These rules simply correspond to the formulas for the one-particle wave functions given in eqs. (3.7) and (3.8) [with the convention that $|\vec{\boldsymbol{p}},s\rangle$ is an initial-state fermion and $\langle\vec{\boldsymbol{p}},s|$ is a final-state fermion].

The rules above apply to any mass eigenstate two-component fermion external wavefunctions. In particular, the same rules apply for the two-component fermions governed by the Lagrangians of eq. (3.60) [Majorana] and eq. (3.79) [Dirac].

4.2 Fermion propagators

Next we turn to the issue of fermion propagators for two-component fermions. These are the Fourier transforms of the free-field vacuum expectation values of time-ordered products of two fermion fields. They are easily obtained by inserting the free-field expansion of the two-component fermion field and evaluating the spin sums using the formulas given in eqs. (3.51) and (3.54). For the case of a single neutral two-component fermion field ξ of mass m [see eqs. (3.60)-(3.63)],

$$\langle 0|\,T\xi_\alpha(x)\bar{\xi}_{\dot\beta}(y)\,|0\rangle_{\rm FT} = \frac{i}{p^2-m^2+i\epsilon}\sum_\lambda x_\alpha(\vec{\boldsymbol{p}},\lambda)\bar{x}_{\dot\beta}(\vec{\boldsymbol{p}},\lambda) = \frac{i}{p^2-m^2+i\epsilon}\,p{\cdot}\sigma_{\alpha\dot\beta}\,, \quad (4.1)$$

$$\langle 0|\,T\bar{\xi}^{\dot\alpha}(x)\xi^\beta(y)\,|0\rangle_{\rm FT} = \frac{i}{p^2-m^2+i\epsilon}\sum_\lambda \bar{y}^{\dot\alpha}(\vec{\boldsymbol{p}},\lambda)y^\beta(\vec{\boldsymbol{p}},\lambda) = \frac{i}{p^2-m^2+i\epsilon}\,p{\cdot}\overline{\sigma}^{\dot\alpha\beta}\,, \quad (4.2)$$

$$\langle 0|\,T\xi_\alpha(x)\xi^\beta(y)\,|0\rangle_{\rm FT} = \frac{i}{p^2-m^2+i\epsilon}\sum_\lambda x_\alpha(\vec{\boldsymbol{p}},\lambda)y^\beta(\vec{\boldsymbol{p}},\lambda) = \frac{i}{p^2-m^2+i\epsilon}\,m\delta_\alpha{}^\beta\,, \quad (4.3)$$

$$\langle 0|\,T\bar{\xi}^{\dot\alpha}(x)\bar{\xi}_{\dot\beta}(y)\,|0\rangle_{\rm FT} = \frac{i}{p^2-m^2+i\epsilon}\sum_\lambda \bar{y}^{\dot\alpha}(\vec{\boldsymbol{p}},\lambda)\bar{x}_{\dot\beta}(\vec{\boldsymbol{p}},\lambda) = \frac{i}{p^2-m^2+i\epsilon}\,m\delta^{\dot\alpha}{}_{\dot\beta}\,, \quad (4.4)$$

where FT indicates the Fourier transform from position to momentum space. These results have an obvious diagrammatic representation, as shown in Figure 2. Note that the direction of the momentum flow p^μ here is determined by the creation operator that appears in the evaluation of the free-field propagator. Arrows on fermion lines always run away from dotted indices at a vertex and toward undotted indices at a vertex.

There are clearly two types of fermion propagators. The first type preserves the direction of arrows, so it has one dotted and one undotted index. For this type of propagator, it is convenient to establish a convention where p^μ in the diagram is defined to be the momentum flowing in the direction of the arrow on the fermion propagator. With this convention, the two

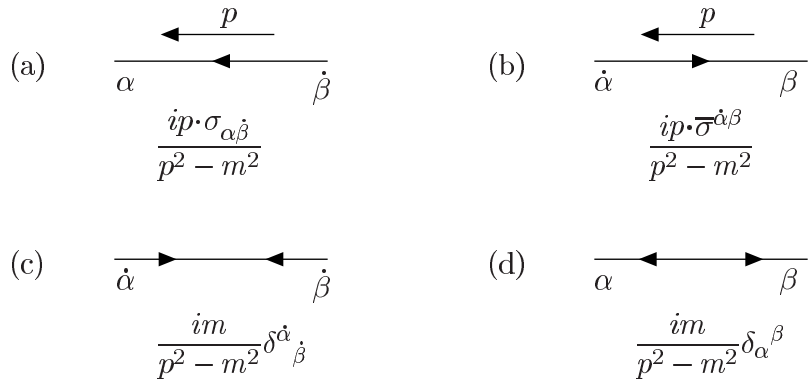

Figure 2: Feynman rules for propagator lines of a neutral two-component fermion. (The $+i\epsilon$ has been omitted for simplicity.)

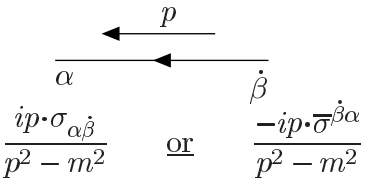

Figure 3: This one rule summarizes the results of Fig. 2(a) and (b).

Figure 4: Fermion mass insertions can be treated as a type of interaction vertex, using the Feynman rules shown here.

rules above for propagators of the first type can be summarized by one rule, as shown in Figure 3. Here the choice of the σ or the $\overline{\sigma}$ version of the rule is uniquely determined by the height of the indices on the vertex to which the propagator is connected. These heights should always be chosen so that they are contracted as in eq. (2.15).

The second type of propagator shown above does not preserve the direction of arrows, and corresponds to an odd number of mass insertions. The indices on $\delta_\alpha{}^\beta$ and $\delta^{\dot\alpha}{}_{\dot\beta}$ are staggered as shown to indicate that α or $\dot\alpha$ are to be contracted with an expression to the left, while β or $\dot\beta$ are to be contracted with an expression to the right, in accord with eq. (2.15).

Mass insertions on fermion lines can instead be handled as interaction vertices, as shown in Figure 4. By summing up an infinite chain of such mass insertions between massless fermion propagators, one can easily reproduce the massive fermion propagators of both types.

It is useful to treat separately the case of charged massive fermions. Consider a charged

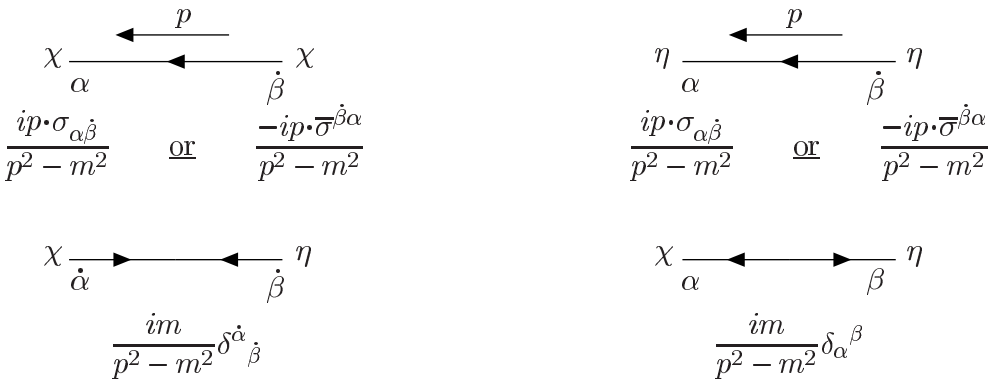

Figure 5: Feynman rules for propagator lines of a charged two-component fermion.

Dirac fermion of mass m, which is described by two two-component fields χ and η, with a mass term:

$$-\mathcal{L}_{\rm mass} = m(\chi\eta + \bar{\chi}\bar{\eta})\,. \tag{4.5}$$

Using the free field expansions given by eqs. (3.65) and (3.66), and the appropriate spin-sums [eqs. (3.51)–(3.54)], the two-component free-field propagators are easily obtained:

$$\langle 0|\,T\chi_\alpha(x)\bar{\chi}_{\dot\beta}(y)\,|0\rangle_{\rm FT} = \langle 0|\,T\eta_\alpha(x)\bar{\eta}_{\dot\beta}(y)\,|0\rangle_{\rm FT} = \frac{i}{p^2-m^2}\,p{\cdot}\sigma_{\alpha\dot\beta}\,, \tag{4.6}$$

$$\langle 0|\,T\bar{\chi}^{\dot\alpha}(x)\chi^\beta(y)\,|0\rangle_{\rm FT} = \langle 0|\,T\bar{\eta}^{\dot\alpha}(x)\eta^\beta(y)\,|0\rangle_{\rm FT} = \frac{i}{p^2-m^2}\,p{\cdot}\bar{\sigma}^{\dot\alpha\beta}\,, \tag{4.7}$$

$$\langle 0|\,T\chi_\alpha(x)\eta^\beta(y)\,|0\rangle_{\rm FT} = \langle 0|\,T\eta_\alpha(x)\chi^\beta(y)\,|0\rangle_{\rm FT} = \frac{i}{p^2-m^2}\,m\,\delta_\alpha{}^\beta\,, \tag{4.8}$$

$$\langle 0|\,T\bar{\chi}^{\dot\alpha}(x)\bar{\eta}_{\dot\beta}(y)\,|0\rangle_{\rm FT} = \langle 0|\,T\bar{\eta}^{\dot\alpha}(x)\bar{\chi}_{\dot\beta}(y)\,|0\rangle_{\rm FT} = \frac{i}{p^2-m^2}\,m\,\delta^{\dot\alpha}{}_{\dot\beta}\,. \tag{4.9}$$

For all other combinations of fermion bilinears, the corresponding two-point functions vanish. These results again have a simple diagrammatic representation, as shown in Figure 5. (Here we have presented the results with the momentum along the arrow direction, as in Fig. 3.) Note that for Dirac fermions, the propagators with opposing arrows (proportional to a mass) necessarily change the identity (χ or η) of the two-component fermion, while the single-arrow propagators never do. In processes involving such a charged fermion, one must of course carefully distinguish between the χ and η fields.

4.3 Fermion interactions

We next examine the possible interaction vertices. Renormalizable Lorentz invariant interactions involving fermions must consist of bilinears in the fermion fields, which transforms as a

Lorentz scalar or vector, coupled to the appropriate bosonic Lorentz scalar or vector field to make an overall Lorentz scalar quantity. Here, we shall first consider the case of fermion pairs coupled to a real scalar field ϕ and a real vector field A_μ. We assume that the two-component fermion mass matrix has been diagonalized as discussed in section 3, so that the fermions consist of a collection $\psi_{\alpha i}$ of two-component $(\frac{1}{2},0)$ fermions. (These may include both neutral two-component fields ξ and/or pairs of oppositely-charged field pairs χ and η.) The interaction Lagrangian is given by

$$\mathcal{L}_{\rm int} = -\tfrac{1}{2}(\lambda^{ij}\psi_i\psi_j + \lambda_{ij}\bar\psi^i\bar\psi^j)\phi - G_i{}^j\,\bar\psi^i\overline{\sigma}_\mu\psi_j\,A^\mu\,, \tag{4.10}$$

where λ is a complex symmetric Yukawa coupling matrix, and G is an hermitian gauge coupling matrix. We have suppressed the spinor indices in eq. (4.10); the product of two component spinors is always performed according to the index convention indicated in eq. (2.15).

In eq. (4.10), we have used the following convention concerning the "flavor" labels i and j. Left-handed $(\frac{1}{2},0)$ fermions always have lowered flavor indices and right-handed $(0,\frac{1}{2})$ fermions always have raised indices. Raised indices can only be contracted with lowered indices and vice versa. Flipping the heights of all flavor indices of an object corresponds to complex conjugation, as in eq. (3.56), so that

$$\lambda_{ij} \equiv (\lambda^{ij})^*\,, \qquad\qquad G^i{}_j \equiv (G_i{}^j)^*\,. \tag{4.11}$$

With this notation, an hermitian matrix $G_i{}^j$ satisfies the condition $G_i{}^j = G^j{}_i$. In the case where the scalar field also possesses a flavor index I, we define $\phi^I(x) \equiv [\phi_I(x)]^*$. The Feynman rules for the vertices that arise from the interaction Lagrangian given in eq. (4.10) are shown in Fig. 6.

One clarification in the labeling is helpful. Consider a line in Fig. 6 labeled ψ_i. This means that the corresponding state is given by $|\psi_i\rangle$ [as in eq. (3.63), (3.68) or (3.69)], independent of the direction of the arrow. The fact that there are two separate rules corresponding to the same pair of outgoing states (differentiated by the arrow directions) is a consequence of the two terms proportional to $\psi_i\psi_j$ and $\bar\psi^i\bar\psi^j$ in eq. (4.10).

In Fig. 6, two versions are given for each of the boson-fermion-fermion Feynman rules. The correct version to use depends in a unique way on the heights of indices used to connect each fermion line to the rest of the diagram. For example, the way of writing the vector-fermion-fermion interaction rule depends on whether we used $-\psi_j\sigma^\mu\bar\psi^i$, or its equivalent form $\bar\psi^i\overline{\sigma}^\mu\psi_j$, from eq. (4.10). Note the different heights of the spinor indices $\dot\alpha$ and β on σ^μ and $\overline{\sigma}^\mu$. The choice of which rule to use is thus dictated by the height of the indices on the lines that connect to the vertex. These heights should always be chosen so that they are contracted as in eq. (2.15). Similarly, for the scalar-fermion-fermion vertices, one should choose the rule which correctly

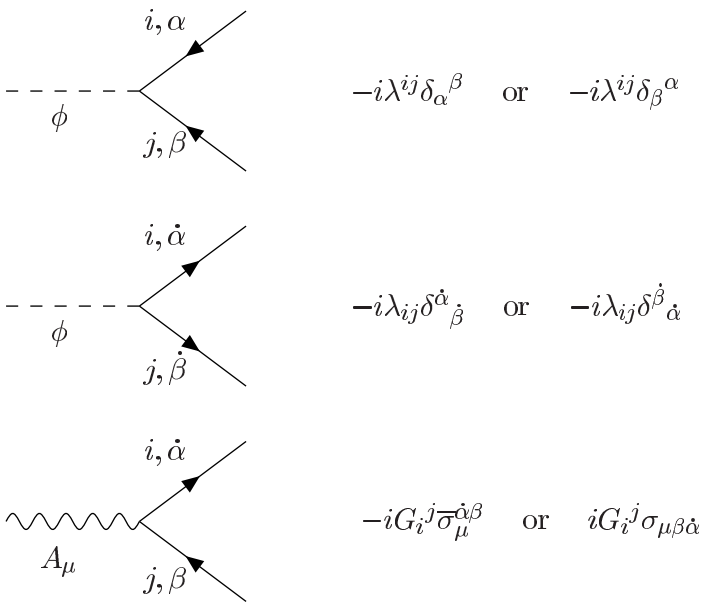

Figure 6: The form of the Feynman rules for two-component fermion interactions with a neutral boson in a general renormalizable field theory.

matches the indices with the rest of the diagram. (However, when all indices are suppressed, the scalar-fermion-fermion rules will have an identical appearance for both cases anyway, since they are just proportional to the identity matrix on the 2×2 spinor space.) These comments will be clarified by examples below.

We can also treat the interactions of fermions to complex scalar and vector fields. We denote a set of neutral fermion fields by ξ_i and a set of charged fermion fields by pairs of oppositely charged fields χ_j and η_j. The charged scalar and vector bosons are complex fields denoted by ϕ and W, respectively. Here, we shall only consider the simplest case where the charges of ϕ, W and χ are assumed to be equal. In this case, the interaction Lagrangian is given by:

$$\begin{aligned}\mathcal{L}_{\rm int} = &-\tfrac{1}{2}\phi^*[\kappa_1^{ij}\chi_i\xi_j + (\kappa_2)_{ij}\overline{\eta}^i\bar{\xi}^j] - \tfrac{1}{2}\phi[\kappa_2^{ij}\eta_i\xi_j + (\kappa_1)_{ij}\bar{\chi}^i\bar{\xi}^j]\\ &-\tfrac{1}{2}W_\mu[(G_1)_i{}^j\bar{\chi}^i\overline{\sigma}^\mu\xi_j + (G_2)_i{}^j\bar{\xi}_i\overline{\sigma}^\mu\eta_j] - \tfrac{1}{2}W_\mu^*[(G_1)_j{}^i\bar{\xi}^j\overline{\sigma}^\mu\chi_i + (G_2)_j{}^i\bar{\eta}^j\overline{\sigma}^\mu\xi_i],\end{aligned} \tag{4.12}$$

where κ_1 and κ_2 are complex symmetric matrices and G_1 and G_2 are hermitian matrices. As in eq. (4.11), we denote $(\kappa_k)_{ij}\equiv(\kappa_k^{ij})^*$. The corresponding Feynman rules are given in Fig. 7.

Let us now work out the specific identification of the Feynman rules in a general renormalizable model. The two-component fermion fields that appear in the Lagrangian are written originally in terms of $(\frac{1}{2},0)$-fermion interaction eigenstates, $\hat{\psi}_i$, which in general may consist of

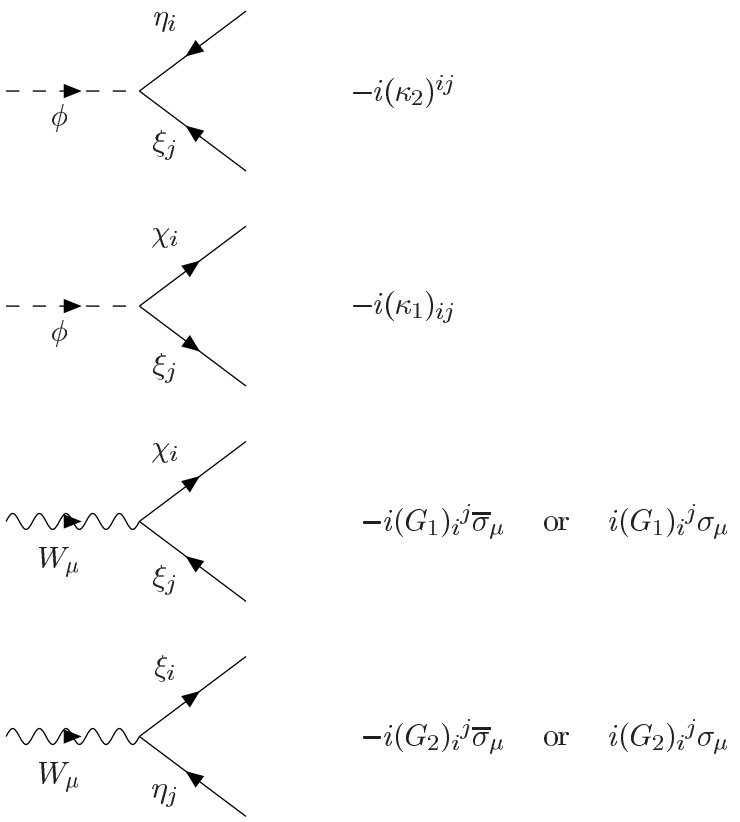

Figure 7: The form of the Feynman rules for two-component fermion interactions with a charged boson in a general renormalizable field theory. For each diagram shown above, there is a charge-conjugated diagram in which all arrows are reversed. The corresponding rules are obtained simply by raising all lowered flavor indices and lowering all raised flavor indices [*c.f.* eq. (4.11)]. Spinor indices are suppressed [*c.f.* Fig. 6]. The arrows on the boson lines and on the charged fermion lines χ and η indicate the flow of charge. On both charged and neutral fermion lines, the arrows also indicate the flow of chirality.

Majorana fermions $\hat{\xi}_i$, and Dirac fermion pairs $\hat{\chi}_i$ and $\hat{\eta}_i$ after mass terms (both explicit and coming from spontaneous symmetry breaking) are taken into account. In order to derive the Feynman rules for the fermion interactions, one expresses these fermion fields in terms of the mass eigenstates, ψ_i. The mass eigenstate basis is achieved by a unitary rotation $U_i{}^j$ on the flavor indices. In matrix form:

$$\hat{\psi} \equiv \begin{pmatrix} \hat{\xi} \\ \hat{\chi} \\ \hat{\eta} \end{pmatrix} = U\psi \equiv \begin{pmatrix} \Omega & 0 & 0 \\ 0 & L & 0 \\ 0 & 0 & R \end{pmatrix} \begin{pmatrix} \xi \\ \chi \\ \eta \end{pmatrix} , \tag{4.13}$$

where Ω, L, and R are constructed as described previously in Section 3.2.

In any theory, the most general set of fermion interaction vertices with a (possibly complex)

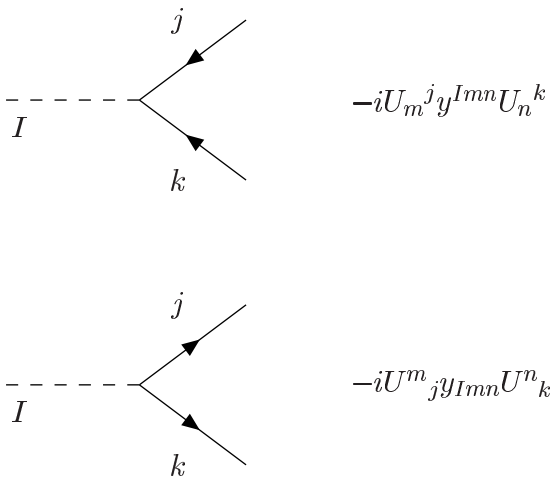

Figure 8: Feynman rule for Yukawa couplings of scalars to two-component fermions. Spinor indices are suppressed; in all cases the interaction is proportional to the identity matrix on the appropriate spinor space with either index raised and the other lowered. Here y^{Imn} are the Yukawa coupling matrices in the interaction-eigenstate basis, and the matrices U achieve the rotation to the mass eigenstate basis.

scalar ϕ_I can be written as follows:

$$\mathcal{L}_{\rm int} = -\tfrac{1}{2} y^{Ijk} \phi_I \hat{\psi}_j \hat{\psi}_k - \tfrac{1}{2} y_{Ijk} \phi^{I*} \bar{\hat{\psi}}^j \bar{\hat{\psi}}^k \,, \tag{4.14}$$

where the $\hat{\psi}_j$ are the original interaction-eigenstate two-component fermions of the theory, and y^{Ijk} is symmetric under interchange of j and k. Therefore, the mass eigenstate Feynman rules take the form shown in Fig. 8: Here, as before, we use the convenient notation $y_{Ijk} \equiv (y^{Ijk})^*$ and $U^i{}_j \equiv (U_i{}^j)^*$. In the case of complex scalars, it is convenient to put an arrow on the scalar line to indicate the flow of "analyticity". In the special case of supersymmetric theories, the index I on the scalar fields coincides with the two-component fermion flavor index i. In the case of superpotential interactions in supersymmetric theories, the three arrows must all flow in (or all out) of a scalar-fermion-fermion vertex.

Finally, we consider the fermion coupling to vector bosons of a gauge theory. In the gauge eigenstate basis, the interactions of two-component fermions with gauge bosons are described by an interaction Lagrangian of the form

$$\mathcal{L}_{\rm int} = -g A^a_\mu \bar{\hat{\psi}}^i \bar{\sigma}^\mu (\mathbf{T}^a)_i{}^j \hat{\psi}_j \,, \tag{4.15}$$

where g is the appropriate real gauge coupling, the $\boldsymbol{T}^a$ are the hermitian representation matrices[7] for the two-component fermions, and the A^a_μ are the gauge bosons. Converting to the

[7]For a $U(1)$ gauge group, the $\boldsymbol{T}^a$ are replaced by real numbers corresponding to the $U(1)$ charges of the left-handed $(\frac{1}{2}, 0)$ fermion.

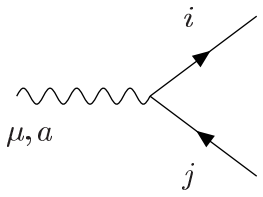

$$-igU_i{}^k(\mathbf{T}^a)_k{}^m U_m{}^j\,\overline{\sigma}_\mu \quad \text{or} \quad igU_i{}^k(\mathbf{T}^a)_k{}^m U_m{}^j\,\sigma_\mu$$

Figure 9: Feynman rule for gauge boson couplings to two-component fermions. Spinor indices are suppressed.

mass eigenstate basis, this interaction results in a Feynman rule shown in Fig. 9.

4.4 General structure and rules for Feynman graphs

When computing an amplitude for a given process, all possible diagrams should be drawn that conform with the rules given above for external wavefunctions, propagators, and interactions. Starting from any external wave function spinor, or from any vertex on a fermion loop, factors corresponding to each propagator and vertex should be written down from left to right, following the line until it ends at another external state wave function or at the original point on the fermion loop. If one starts a fermion line at an x or y external state spinor, it should have a raised undotted index in accord with eq. (2.15). Or, if one starts with an $\bar{x}$ or $\bar{y}$, it should have a lowered dotted spinor index. Then, all spinor indices should always be contracted as in eq. (2.15). If one ends with an x or y external state spinor, it will have a lowered undotted index, while if one ends with an $\bar{x}$ or $\bar{y}$ spinor, it will have a raised dotted index. For arrow-preserving fermion propagators and gauge vertices, the preceding determines whether the σ or $\overline{\sigma}$ rule should be used. With only a little experience, one can write down amplitudes immediately with all spinor indices suppressed.

Symmetry factors for identical particles are implemented in the usual way. Fermi-Dirac statistics are implemented by the following rules:

- Each closed fermion loop gets a factor of -1.
- A relative minus sign is imposed between terms contributing to a given amplitude whenever the ordering of external state spinors (written left-to-right) differs by an odd permutation.

Amplitudes generated according to these rules will contain objects of the form:

$$a = z_1 \Sigma z_2 \tag{4.16}$$

where z_1 and z_2 are each commuting external spinor wave functions x, $\bar{x}$, y, or $\bar{y}$, and Σ is a sequence of alternating σ and $\overline{\sigma}$ matrices. The complex conjugate of this quantity is given by

$$a^* = \bar{z}_2 \overleftarrow{\Sigma} \bar{z}_1 \tag{4.17}$$

where $\overleftarrow{\Sigma}$ is obtained from Σ by reversing the order of all the σ and $\overline{\sigma}$ matrices, and using the same rule for suppressed spinor indices. (Notice that this rule for taking complex conjugates has the same form as for anticommuting spinors.) We emphasize that in principle, it does not matter in what direction a diagram is traversed while applying the rules. However, one must associate a sign with each diagram that depends on the ordering of the external fermions. This sign can be fixed by first choosing some canonical ordering of the external fermions. Then for any graph that contributes to the process of interest, the corresponding sign is positive (negative) if the ordering of external fermions is an even (odd) permutation with respect to the canonical ordering. If one chooses a different canonical ordering, then the resulting amplitude changes by an overall sign (is unchanged) if this ordering is an odd (even) permutation of the original canonical ordering.[8] This is consistent with the fact that the amplitude is only defined up to an overall sign, which is not physically observable.

Note that different graphs contributing to the same process will often have different external state wave function spinors, with different arrow directions, for the same external fermion. Furthermore, there are no arbitrary choices to be made for arrow directions, as there are in some Feynman rules for Majorana fermions. Instead, one must add together *all* Feynman graphs that obey the rules.

4.5 Basic examples of writing down diagrams and amplitudes

A few simple examples based on the vertices of Fig. 6 will help clarify these rules. Let us first consider a theory with a single, uncharged, massive $(\frac{1}{2}, 0)$ fermion ξ, and a real scalar ϕ, with interaction

$$\mathcal{L}_{\rm int} = -\tfrac{1}{2}\left(\lambda\xi\xi + \lambda^*\bar{\xi}\bar{\xi}\right)\phi. \tag{4.18}$$

Consider the decay $\phi \to \xi(\vec{\boldsymbol{p}}_1, s_1)\xi(\vec{\boldsymbol{p}}_2, s_2)$, where by ξ we mean the one particle state given by eq. (3.6), as noted above. Two diagrams contribute to this process, as shown in Figure 10. The matrix element is then given by

[8] For a process with exactly two external fermions, it is convenient to apply the Feynman rules by starting from the same fermion external state in all diagrams. That way, all terms in the amplitude have the same canonical ordering of fermions and there are no additional minus signs between diagrams. If instead there are four or more external fermions, however, it may happen that there is no way to choose the same ordering of external state spinors for all graphs when the amplitude is written down. Then the relative signs between different graphs must be chosen according to the relative sign of the permutation of the corresponding external fermion spinors. This guarantees that the total amplitude is antisymmetric under the interchange of any pair of external fermions.

Figure 10: The two tree-level Feynman diagrams contributing to the decay of a scalar into a Majorana fermion pair.

$$\begin{aligned} i\mathcal{M} &= y(\vec{\boldsymbol{p}}_1, s_1)^\alpha(-i\lambda\delta_\alpha{}^\beta)y(\vec{\boldsymbol{p}}_2, s_2)_\beta + \bar{x}(\vec{\boldsymbol{p}}_1, s_1)_{\dot\alpha}(-i\lambda^*\delta^{\dot\alpha}{}_{\dot\beta})\bar{x}(\vec{\boldsymbol{p}}_2, s_2)^{\dot\beta} \\ &= -i\lambda y(\vec{\boldsymbol{p}}_1, s_1)y(\vec{\boldsymbol{p}}_2, s_2) - i\lambda^*\bar{x}(\vec{\boldsymbol{p}}_1, s_1)\bar{x}(\vec{\boldsymbol{p}}_2, s_2). \end{aligned} \tag{4.19}$$

The second line could be written down directly by recalling that the sum over suppressed spinor indices is taken according to eq. (2.15). Note that if we reverse the ordering for the external fermions, the overall sign of the amplitude changes sign.[9] Of course, this overall sign is not significant and depends on the order used in constructing the two particle state. One could even make the perverse (but correct) choice of starting the first diagram from fermion 1, and the second diagram from fermion 2:

$$i\mathcal{M} = -i\lambda y(\vec{\boldsymbol{p}}_1, s_1)y(\vec{\boldsymbol{p}}_2, s_2) - (-1)i\lambda^*\bar{x}(\vec{\boldsymbol{p}}_2, s_2)\bar{x}(\vec{\boldsymbol{p}}_1, s_1)\,. \tag{4.20}$$

Here the first term establishes the canonical ordering of fermions (1,2), and the contribution from the second diagram therefore includes the relative minus sign in parentheses. It is easily seen that equations (4.19) and (4.20) are indeed equal. Note that when a total decay rate is computed, one must multiply the integral over the total phase space by 1/2 to account for the identical particles, as usual.

Consider next the decay of a massive neutral vector A_μ into a Majorana fermion pair $A_\mu \to \xi(\vec{\boldsymbol{p}}_1, s_1)\xi(\vec{\boldsymbol{p}}_2, s_2)$, following from the interaction

$$\mathcal{L}_{\rm int} = -GA^\mu\bar{\xi}\overline{\sigma}_\mu\xi\,, \tag{4.21}$$

where G is a real coupling parameter. The two diagrams shown in Figure 11 contribute.

Following the rules of Fig. 6, we start from the fermion with momentum p_1 and spin vector s_1, and end at the fermion with momentum p_2 and spin vector s_2. The resulting amplitude for the decay is

$$i\mathcal{M} = \varepsilon^\mu\left[-iG\bar{x}(\vec{\boldsymbol{p}}_1, s_1)\overline{\sigma}_\mu y(\vec{\boldsymbol{p}}_2, s_2) + iGy(\vec{\boldsymbol{p}}_1, s_1)\sigma_\mu\bar{x}(\vec{\boldsymbol{p}}_2, s_2)\right] \tag{4.22}$$

[9] This is easily checked, since for the commuting spinor wave functions ($\bar{x}$ and y), the spinor products in eq. (4.19) change sign when the order is reversed [see eqs. (2.32) and (2.33)].

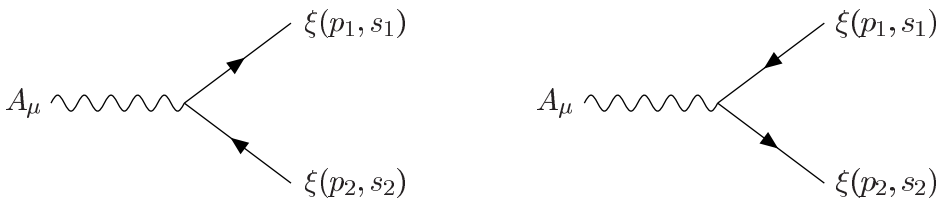

Figure 11: The two tree-level Feynman diagrams contributing to the decay of a massive vector boson A_μ into a pair of Majorana fermions ξ.

where ε^μ is the vector boson polarization vector. As illustrated in Fig. 6, we have used the $\overline{\sigma}$-version of the vector-fermion-fermion rule for the first diagram of Fig. 11 and the σ-version for the second diagram of Fig. 11, as dictated by the implicit spinor indices, which we have suppressed. However, we could have chosen to evaluate the second diagram of Fig. 11 using the $\overline{\sigma}$-version of the vector-fermion-fermion rule by starting from the fermion with momentum p_2. In that case, the factor $+iGy(\vec{\boldsymbol{p}}_1, s_1)\sigma_\mu \bar{x}(\vec{\boldsymbol{p}}_{\boldsymbol{2}}, s_2)$ in eq. (4.22) is replaced by

$$(-1)[-iG\bar{x}(\vec{\boldsymbol{p}}_2, s_2)\overline{\sigma}_\mu y(\vec{\boldsymbol{p}}_{\boldsymbol{1}}, s_1)]\,. \tag{4.23}$$

In eq. (4.23), the factor of $-iG$ arises from the use of the $\overline{\sigma}$-version of the vector-fermion-fermion rule, whereas the overall factor of -1 is due to the fact that the order of the fermion wave functions has been reversed; *i.e* (21) is an odd permutation of (12). This is in accord with the ordering rule stated at the end of Section 4.4. Thus, the resulting amplitude for the decay of the vector boson into the pair of Majorana fermions now takes the form:

$$i\mathcal{M} = \varepsilon^\mu\left[-iG\bar{x}(\vec{\boldsymbol{p}}_1, s_1)\overline{\sigma}_\mu y(\vec{\boldsymbol{p}}_{\boldsymbol{2}}, s_2) + iG\bar{x}(\vec{\boldsymbol{p}}_2, s_2)\overline{\sigma}_\mu y(\vec{\boldsymbol{p}}_{\boldsymbol{1}}, s_1)\right]. \tag{4.24}$$

By using $y\sigma^\mu\bar{x} = \bar{x}\overline{\sigma}^\mu y$, one trivially shows that eqs. (4.22) and (4.24) are identical. The form given in eq. (4.24) is especially convenient because it explicitly exhibits the fact that the amplitude is antisymmetric under the interchange of the two external identical fermions. Again, the absolute sign of the total amplitude is not significant and depends on the choice of ordering of the outgoing states. When computing the total decay rate, one must again multiply the total integral over phase space by 1/2 to account for identical particles in the final state.

Next, we consider the decay of a neutral vector boson into a charged fermion-antifermion pair. Suppose that we identify χ and η as the left-handed fields with charges $Q = 1$ and $Q = -1$, respectively. These charges may or may not correspond to the couplings of χ and η

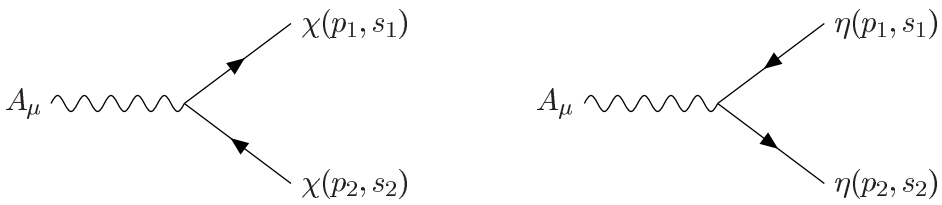

Figure 12: The two tree-level Feynman diagrams contributing to the decay of a massive neutral vector boson A_μ into a Dirac fermion-antifermion pair.

to the vector field, which we write as:

$$\mathcal{L}_{\rm int} = -A^\mu[G_\chi \bar{\chi}\overline{\sigma}_\mu \chi + G_\eta \overline{\eta}\overline{\sigma}_\mu \eta]. \tag{4.25}$$

There are two contributing graphs, as shown in Figure 12. To evaluate the amplitude, we start from the charge $Q = +1$ fermion (with momentum p_1 and spin vector s_1), and end at the charge $Q = -1$ fermion (with momentum p_2 and spin vector s_2). The charge flow follows the direction of the arrow on the fermion line. Note that for the final state fermion lines, the outgoing χ with arrow pointing outward from the vertex and the outgoing η with arrow pointing *inward* to the vertex both correspond to outgoing $Q = +1$ states. The amplitude for the decay is

$$\begin{aligned} i\mathcal{M} &= \varepsilon^\mu \left[-iG_\chi \bar{x}(\vec{\boldsymbol{p}}_1, s_1)\overline{\sigma}_\mu y(\vec{\boldsymbol{p}}_2, s_2) + iG_\eta y(\vec{\boldsymbol{p}}_1, s_1)\sigma_\mu \bar{x}(\vec{\boldsymbol{p}}_2, s_2)\right] \\ &= \varepsilon^\mu \left[-iG_\chi \bar{x}(\vec{\boldsymbol{p}}_1, s_1)\overline{\sigma}_\mu y(\vec{\boldsymbol{p}}_2, s_2) + iG_\eta \bar{x}(\vec{\boldsymbol{p}}_2, s_2)\overline{\sigma}_\mu y(\vec{\boldsymbol{p}}_1, s_1)\right] . \end{aligned} \tag{4.26}$$

As in the case of the decay to a pair of Majorana fermions, we have exhibited two forms for the amplitude in eq. (4.26) that depend on whether the $\overline{\sigma}$-version or the σ-version of the Feynman rule has been employed. Of course, the resulting amplitude is the same in each method (up to an overall sign of the total amplitude which is not determined).

The next level of complexity consists of diagrams that involve fermion propagators. For our first example of this type, consider the tree-level matrix element for the scattering of a neutral scalar and a two-component neutral massive fermion ($\phi\xi \to \phi\xi$), with the interaction Lagrangian given above in eq. (4.18). Using the corresponding Feynman rules, there are eight contributing diagrams. Four are depicted in Fig. 13; there are another four diagrams (not shown) where the initial and final state scalars are crossed (*i.e.*, the initial state scalar is attached to the same vertex as the final state fermion).

We shall write down the amplitudes for these diagrams starting with the final state fermion

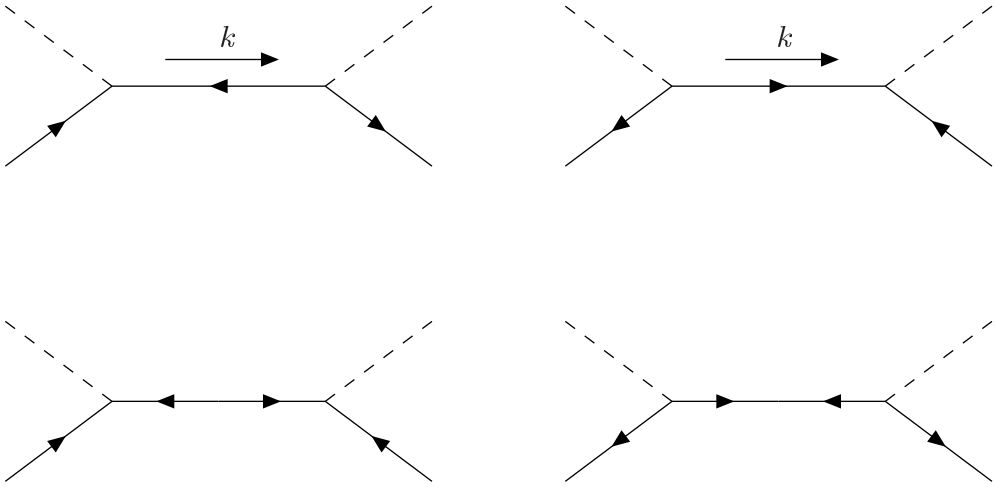

Figure 13: Tree-level Feynman diagrams contributing to the elastic scattering of a neutral scalar and a neutral two-component fermion. There are four more diagrams, obtained from these by crossing the initial and final scalar lines.

line and moving toward the initial state. Then,

$$i\mathcal{M} = \frac{-i}{s - m_\xi^2}\Big\{|\lambda|^2\left[\bar{x}(\vec{\boldsymbol{p}}_{\mathbf{2}}, s_2)\,\overline{\sigma}\cdot k\, x(\vec{\boldsymbol{p}}_{\mathbf{1}}, s_1) + y(\vec{\boldsymbol{p}}_{\mathbf{2}}, s_2)\,\sigma\cdot k\,\bar{y}(\vec{\boldsymbol{p}}_{\mathbf{1}}, s_1)\right] + m_\xi\left[\lambda^2 y(\vec{\boldsymbol{p}}_{\mathbf{2}}, s_2)x(\vec{\boldsymbol{p}}_{\mathbf{1}}, s_1) + (\lambda^*)^2\bar{x}(\vec{\boldsymbol{p}}_{\mathbf{2}}, s_2)\bar{y}(\vec{\boldsymbol{p}}_{\mathbf{1}}, s_1)\right]\Big\} + (\text{crossed})\,. \qquad (4.27)$$

where k^μ is the sum of the two incoming (or outgoing) four-momenta $s = k^2$, (p_1, s_1) are the momentum and spin four-vectors of the incoming fermion, and (p_2, s_2) are those of the outgoing fermion. "Crossed" indicates the same contribution but with the initial and final scalars swapped. Note that we could have evaluated the diagrams above by starting with the initial vertex and moving toward the final vertex. It is easy to check that the resulting amplitude is the negative of the one obtained in eq. (4.27); the overall sign change simply corresponds to swapping the order of the two fermions and has no physical consequence. The overall minus sign is a consequence of eqs. (2.32)–(2.34) and the minus sign difference between the two ways of evaluating the propagator that preserves the arrow direction.

Next, we compute the tree-level matrix element for the scattering of a vector boson and a neutral massive two-component fermion ξ with the interaction Lagrangian of eq. (4.21). Again there are eight diagrams: the four diagrams depicted in Fig. 14 plus another four (not shown) where the initial and final state vector bosons are crossed. Starting with the final state fermion

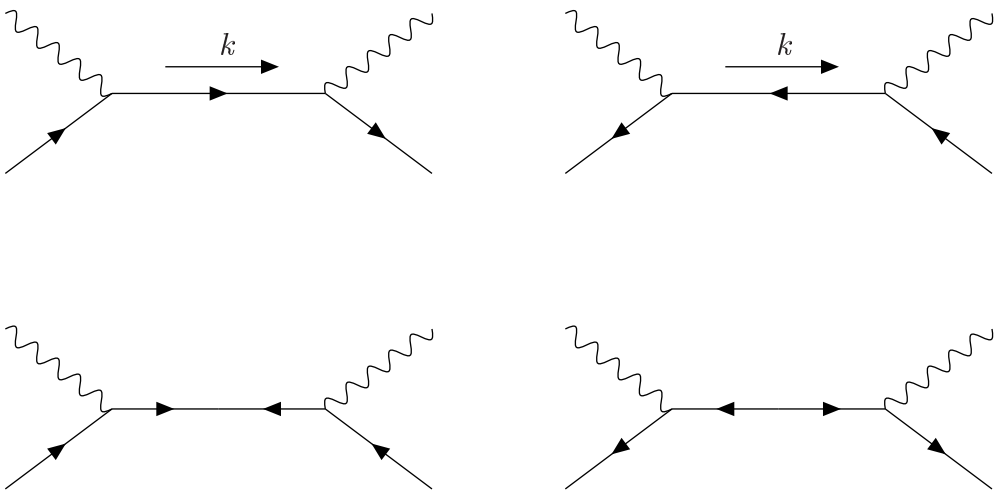

Figure 14: Tree-level Feynman diagrams contributing to the elastic scattering of a neutral vector boson and a neutral two-component fermion. There are four more diagrams, obtained from these by crossing the initial and final scalar lines.

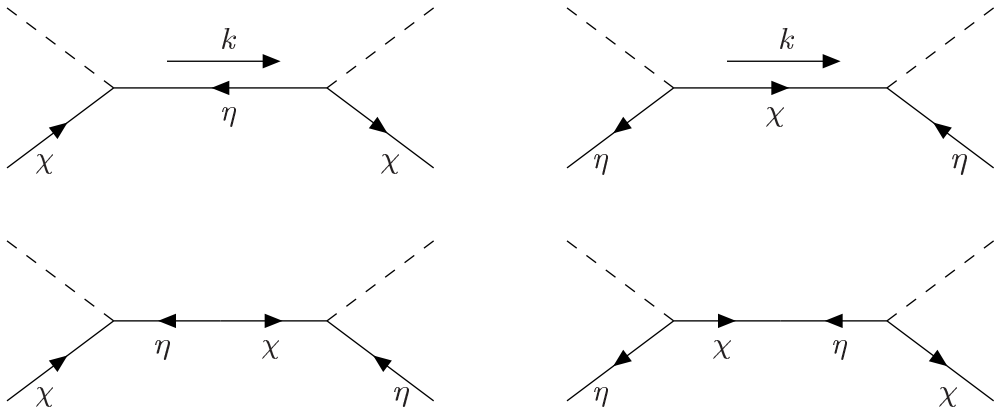

Figure 15: Tree-level Feynman diagrams contributing to the elastic scattering of a neutral scalar and a charged fermion. There are four more diagrams, obtained from these by crossing the initial and final scalar lines.

line and moving toward the initial state, we obtain

$$i\mathcal{M} = \frac{-iG^2}{s - m_\xi^2}\Big\{\bar{x}(\vec{\boldsymbol{p}}_{\mathbf{2}}, s_2)\,\overline{\sigma}\cdot\varepsilon_2^*\,\sigma\cdot k\,\overline{\sigma}\cdot\varepsilon_1\,x(\vec{\boldsymbol{p}}_{\mathbf{1}}, s_1) + y(\vec{\boldsymbol{p}}_{\mathbf{2}}, s_2)\,\sigma\cdot\varepsilon_2^*\,\overline{\sigma}\cdot k\,\sigma\cdot\varepsilon_1\,\bar{y}\,(\vec{\boldsymbol{p}}_{\mathbf{1}}, s_1)$$

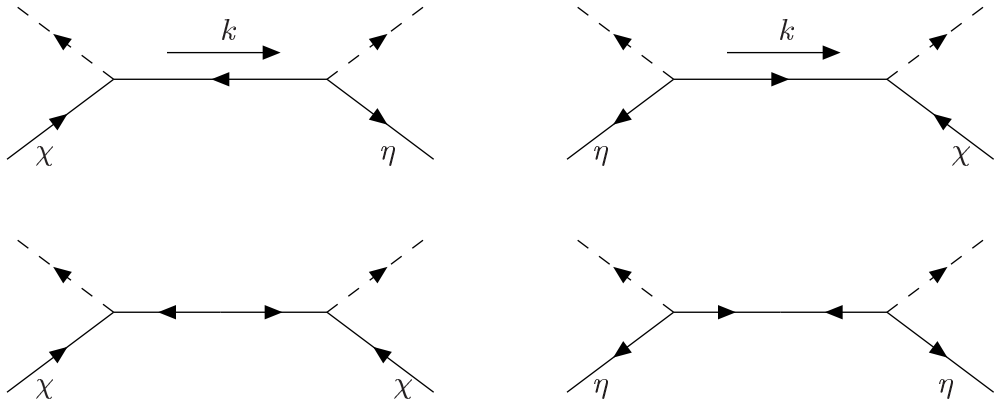

Figure 16: Tree-level Feynman diagrams contributing to the scattering of an initial charged scalar and a charged fermion into its charge-conjugated final state. The unlabeled intermediate state is a neutral fermion. There are four more diagrams, obtained from these by crossing the initial and final scalar lines.

$$-m_\xi \left[y(\vec{\boldsymbol{p}}_{\mathbf{2}}, s_2)\, \sigma{\cdot}\varepsilon_2^*\, \overline{\sigma}{\cdot}\varepsilon_1\, x(\vec{\boldsymbol{p}}_{\mathbf{1}}, s_1) + \bar{x}(\vec{\boldsymbol{p}}_{\mathbf{2}}, s_2)\, \overline{\sigma}{\cdot}\varepsilon_2^*\, \sigma{\cdot}\varepsilon_1\, \bar{y}(\vec{\boldsymbol{p}}_{\mathbf{1}}, s_1) \right] \Big\} + (\text{crossed})\,, \quad (4.28)$$

where ε_1 and ε_2 are the initial and final vector boson polarization four-vectors, respectively. As before, k^μ is the sum of the two incoming (or outgoing) four-momenta and $s = k^2$, and (p_1, s_1) are the momentum and spin four-vectors of the incoming fermion, and (p_2, s_2) are those of the outgoing fermion. "Crossed" indicates the same contribution but with the initial and final vector bosons swapped. If one evaluates the diagrams above by starting with the initial vertex and moving toward the final vertex, the resulting amplitude is the negative of the one obtained in eq. (4.28), as expected.

Next, consider the scattering of a charged Dirac fermion with a neutral scalar. The left-handed fields χ and η have opposite charges $Q = +1$ and -1 respectively, and interact with the scalar ϕ according to

$$\mathcal{L}_{\text{int}} = -\phi[\kappa\chi\eta + \kappa^*\bar{\chi}\bar{\eta}]\,, \quad (4.29)$$

where κ is a coupling parameter. Then, for the elastic scattering of a $Q = +1$ fermion and a scalar, the diagrams of Fig. 15 contribute at tree-level plus another four diagrams (not shown) where the initial and final state scalars are crossed. Now, these diagrams match precisely those of Fig. 13. Thus, applying the Feynman rules yields the same matrix element, eq. (4.27), previously obtained for the scattering of a neutral scalar and neutral two-component fermion, with the replacement of λ with κ.

Consider next the scattering of a charged Dirac fermion and a charged scalar, where both

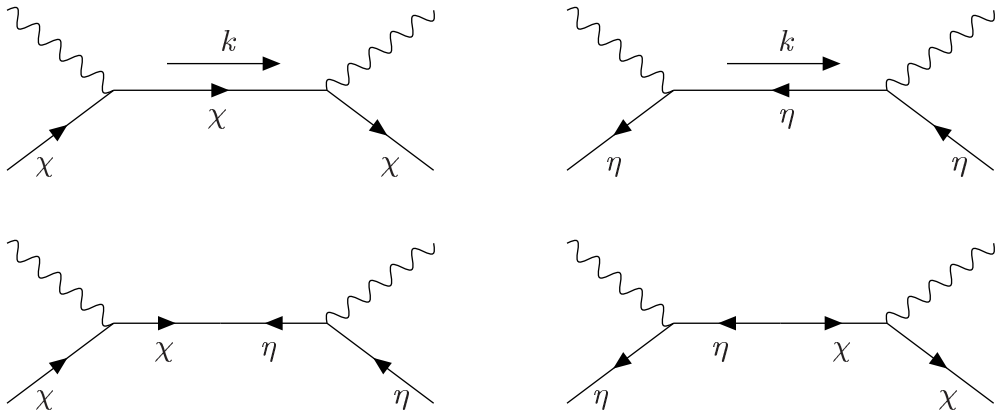

Figure 17: Tree-level Feynman diagrams contributing to the elastic scattering of a neutral vector boson and a charged Dirac fermion. There are four more diagrams, obtained from these by crossing the initial and final vector lines.

the scalar and fermion have the same absolute value of the charge. As usual, we denote the charged $Q = +1$ fermion by the pair of two-component fermions χ and η and the (intermediate state) neutral two-component fermion by ξ. The charged $Q = \pm 1$ scalar is represented by the scalar field ϕ and its complex conjugate, and the corresponding interaction Lagrangian takes the form:

$$\mathcal{L}_{\rm int} = -\phi^*[\kappa_1 \chi\xi + \kappa_2^* \bar{\eta}\bar{\xi}] - \phi[\kappa_2 \eta\xi + \kappa_1^* \bar{\chi}\bar{\xi}]\,. \tag{4.30}$$

One scattering process which requires special attention is the scattering of an initial boson-fermion state into its charge-conjugated final state via the exchange of a neutral fermion. The relevant diagrams are shown in Fig. 16 plus the corresponding diagrams with the initial and final scalars crossed. The derivation is similar to the ones given previously, and we end up with

$$\begin{aligned} i\mathcal{M} = \frac{-i}{s - m_\xi^2}\Big\{ & \kappa_1\kappa_2^*[\bar{x}(\vec{\boldsymbol{p}}_{\boldsymbol{2}}, s_2)\,\overline{\sigma}\cdot k\, x(\vec{\boldsymbol{p}}_{\boldsymbol{1}}, s_1) + y(\vec{\boldsymbol{p}}_{\boldsymbol{2}}, s_2)\,\sigma\cdot k\,\bar{y}(\vec{\boldsymbol{p}}_{\boldsymbol{1}}, s_1)] \\ & + m_\xi\left[\kappa_1^2 y(\vec{\boldsymbol{p}}_{\boldsymbol{2}}, s_2)x(\vec{\boldsymbol{p}}_{\boldsymbol{1}}, s_1) + (\kappa_2^*)^2\bar{x}(\vec{\boldsymbol{p}}_{\boldsymbol{2}}, s_2)\bar{y}(\vec{\boldsymbol{p}}_{\boldsymbol{1}}, s_1)\right]\Big\} + (\text{crossed})\,, \end{aligned} \tag{4.31}$$

where the four-momentum k is defined as shown in Fig. 16.

The scattering of a charged fermion and a neutral spin-1 vector boson can be similarly treated. For example, consider the amplitude for the elastic scattering of a charged fermion and a neutral vector boson. Again taking the interactions as given in eq. (4.25), the relevant diagrams are those shown in Fig. 17, plus four diagrams (not shown) obtained from these by crossing the initial and final state vectors. Applying the Feynman rules following from eq. (4.21)

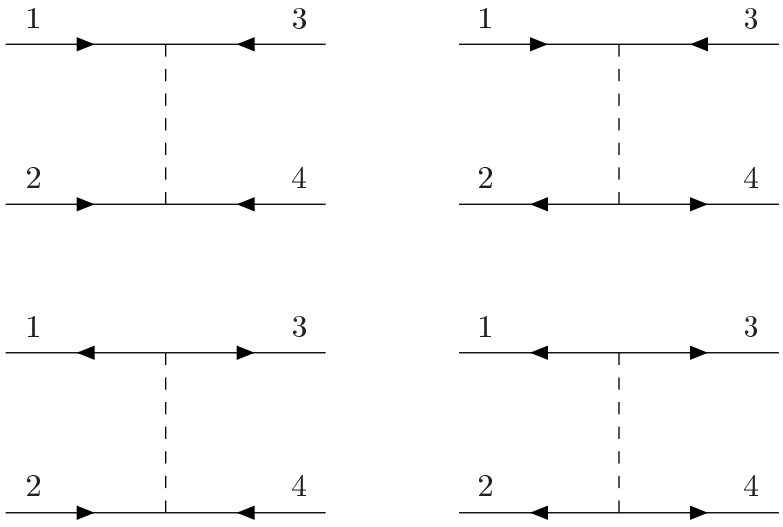

Figure 18: Tree-level Feynman diagrams contributing to the elastic scattering of identical neutral Majorana fermions via scalar exchange in the t-channel. Additionally, there are four u-channel diagrams obtained from these by crossing either the initial or final fermion lines. Finally, one must also evaluate four s-channel diagrams in which the two-component fermions 1 and 2 annihilate into an intermediate scalar which subsequently decays into two-component fermions 3 and 4.

as before, one obtains the following matrix element

$$i\mathcal{M} = \frac{-i}{s-m_\xi^2}\Big\{G_\chi^2 \bar{x}(\vec{\boldsymbol{p}}_{\mathbf{2}},s_2)\,\overline{\sigma}\cdot\varepsilon_2^*\,\sigma\cdot p\,\overline{\sigma}\cdot\varepsilon_1\,x(\vec{\boldsymbol{p}}_{\mathbf{1}},s_1) + G_\eta^2 y(\vec{\boldsymbol{p}}_{\mathbf{2}},s_2)\,\sigma\cdot\varepsilon_2^*\,\overline{\sigma}\cdot p\,\sigma\cdot\varepsilon_1\bar{y}\,(\vec{\boldsymbol{p}}_{\mathbf{1}},s_1)$$
$$-mG_\chi G_\eta\left[y(\vec{\boldsymbol{p}}_{\mathbf{2}},s_2)\,\sigma\cdot\varepsilon_2^*\,\overline{\sigma}\cdot\varepsilon_1\,x(\vec{\boldsymbol{p}}_{\mathbf{1}},s_1) + \bar{x}(\vec{\boldsymbol{p}}_{\mathbf{2}},s_2)\,\overline{\sigma}\cdot\varepsilon_2^*\,\sigma\cdot\varepsilon_1\,\bar{y}(\vec{\boldsymbol{p}}_{\mathbf{1}},s_1)\right]\Big\} + (\text{crossed}) \quad (4.32)$$

and the assignments of momenta and spins are as before.

The computation of the amplitude for the scattering of a charged fermion and a charged vector boson is straightforward and will not be given explicitly here.

Finally, let us do an example with four external-state fermions. Consider the case of elastic scattering of two identical Majorana fermions due to scalar exchange, governed by the interaction of eq. (4.18). The t-channel diagrams for scattering initial fermions labeled $1,2$ into final state fermions labeled $3,4$ are shown in Fig. 18. There are also four u-channel and four s-channel annihilation diagrams (not shown). The resulting matrix element is:

$$i\mathcal{M} = \frac{-i}{s-m_\phi^2}\left\{\lambda^2(x_1x_2)(y_3y_4) + (\lambda^*)^2(\bar{y}_1\bar{y}_2)(\bar{x}_3\bar{x}_4) + |\lambda|^2\left[(x_1x_2)(\bar{x}_3\bar{x}_4) + (\bar{y}_1\bar{y}_2)(y_3y_4)\right]\right\}$$
$$+(-1)\frac{-i}{t-m_\phi^2}\left\{\lambda^2(y_3x_1)(y_4x_2) + (\lambda^*)^2(\bar{x}_3\bar{y}_1)(\bar{x}_4\bar{y}_2) + |\lambda|^2\left[(\bar{x}_3\bar{y}_1)(y_4x_2) + (y_3x_1)(\bar{x}_4\bar{y}_2)\right]\right\}$$

$$+\frac{-i}{u-m_\phi^2}\left\{\lambda^2(y_4x_1)(y_3x_2)+(\lambda^*)^2(\bar{x}_4\bar{y}_1)(\bar{x}_3\bar{y}_2)+|\lambda|^2\left[(\bar{x}_4\bar{y}_1)(y_3x_2)+(y_4x_1)(\bar{x}_3\bar{y}_2)\right]\right\}, \tag{4.33}$$

where $x_i \equiv x(\vec{\boldsymbol{p}}_{\boldsymbol{i}}, s_i)$, $y_i \equiv y(\vec{\boldsymbol{p}}_{\boldsymbol{i}}, s_i)$, m_ϕ is the mass of the exchanged scalar, $s = (p_1+p_2)^2$, $t = (p_1-p_3)^2$ and $u = (p_1-p_4)^2$. The relative minus sign (in parentheses) between the t-channel diagram and the s and u-channel diagrams is obtained by observing that 3142 is an odd permutation and 4132 is an even permutation of 1234.[10]

5 Conventions for fermion and anti-fermion names and fields

When treating the Standard Model and its minimal supersymmetric extension, one must adopt a naming convention for the external fermion lines.

Table 1: Fermion and anti-fermion names and two-component fields in the Standard Model (with massless neutrinos) and the MSSM

Fermion name	Two-component fields
ℓ^- (lepton)	ℓ , $\overline{\ell^c}$
ℓ^+ (anti-lepton)	ℓ^c , $\overline{\ell}$
ν (neutrino)	ν , $-$
$\bar{\nu}$ (antineutrino)	$-$, $\overline{\nu}$
q (quark)	q , $\overline{q^c}$
$\bar{q}$ (anti-quark)	q^c , $\overline{q}$
f (quark or lepton)	f , $\overline{f^c}$
$\bar{f}$ (anti-quark or anti-lepton)	f^c , $\overline{f}$
$\widetilde{N}_i$ (neutralino)	χ_i^0 , $\overline{\chi_i^0}$
$\widetilde{C}_i^+$ (chargino)	χ_i^+ , $\overline{\chi_i^-}$
$\widetilde{C}_i^-$ (anti-chargino)	χ_i^- , $\overline{\chi_i^+}$
$\widetilde{g}$ (gluino)	$\widetilde{g}$, $\overline{\widetilde{g}}$

[10]Note that we would have obtained the same sign for the u-channel diagram had we crossed the initial state fermion lines instead of the final state fermion lines.

To label incoming and outgoing fermions, one can either use symbols for the two-component fields or for the particle names. In Table 1, we list the corresponding names and symbols for the Standard Model and the MSSM fermions.[11] In the case of Majorana fermions, there is a one-to-one correspondence between the particle names and the left-handed fields, but for Dirac fermions there are always two distinct two-component fields that correspond to each particle name. Therefore, in the Dirac case, one has the option of labeling graphs by particle names or field names; each choice has advantages and disadvantages.[12] Employing symbols for two-component fields is more convenient for applying two-component Feynman rules. Thus, it is convenient to display a translation between the two labeling conventions, as shown in Fig. 19.

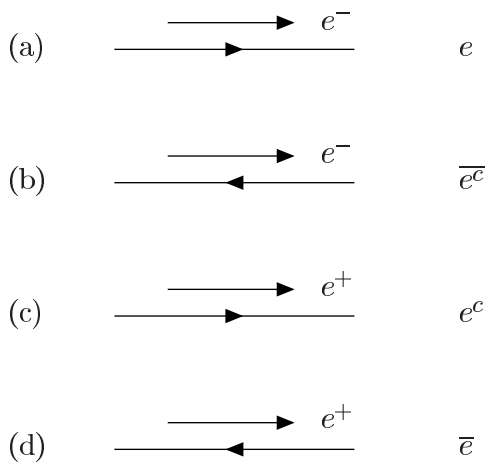

Figure 19: The translation between the particle name and the two-component field name conventions for external lines in a Feynman diagram. The diagrams represent an electron or positron whose momentum points from left to right (as specified by the arrow above each line). The corresponding two-component field label is indicated to the right of each line.

Note that the two-component fields e and $\overline{e^c}$ both represent the negatively charged electron, conventionally denoted by e^-, whereas both e^c and $\overline{e}$ represent the positively charged positron, conventionally denoted by e^+ (as indicated in Table 1).

To evaluate the invariant amplitude for a given process, we apply the Feynman rules of Appendices C and D. However, we first need to establish a convention for labeling the two-component fermion fields that appear in the Feynman rules. As an example, consider the two-component Feynman rules for the QED coupling of electrons and positrons to the photon,

[11] In the original version of the Standard Model, neutrinos are exactly massless and the right-handed neutrino is absent from the spectrum. Hence, no ν^c appears in Table 1. If necessary, it is straightforward to add ν^c to the Standard Model and generate neutrino masses via the seesaw mechanism.

[12] Unfortunately, the notation for fermion names can be ambiguous since some of the symbols used also appear as names for one of the two-component fermion fields. In practice, it should be clear from the context which set of names are being employed.

which are exhibited in Fig. 20.[13]

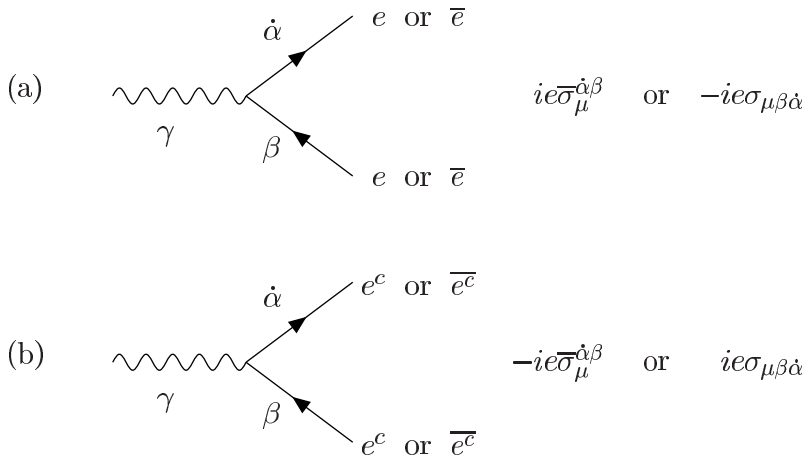

Figure 20: The two-component Feynman rules for the QED vertex. The choice of the two-component field label depends on the direction of momentum flow (which is independent of the direction of the arrow on the fermion lines), following the prescription of Fig. 19.

In general, two-component fermion lines with dotted indices always correspond to arrows going away from the vertex, and two-component fermion lines with undotted indices always correspond to arrows going toward the vertex. When employing the Feynman rules of Fig. 20, the choice of the two-component field label depends on the direction of momentum flow of the corresponding fermion, following the prescription of Fig. 19. For example, if the direction of the momentum flow in Fig. 20 follows the direction of the arrows of the two-component fermion fields, then one should label the two-component fermion lines with unbarred fields. We have followed this latter convention in labeling all the Feynman rules given in Appendices C and D, which results in the relevant two-component fermion Feynman rules for vertices in the Standard Model and the MSSM. That is, the Feynman rules are labeled with two-component (unbarred) fields; they can be applied to processes involving either fermions or anti-fermions (following the prescription of Fig. 19).

A simple example should make this clear. Consider the s-channel tree-level Feynman diagrams that contribute to Bhabha scattering ($e^-e^+ \to e^-e^+$). If we label the external fermion lines according to the corresponding particle names, the result is shown in Figure 21. However, when using the particle name convention, one must discern the identity of the external two-component fermion fields by carefully observing the direction of the arrow of each fermion line. If the arrow coincides with the direction of propagation, then we identify the electron [positron]

[13] See Fig. 52; note that $Q_e = -1$ for the two-component electron field.

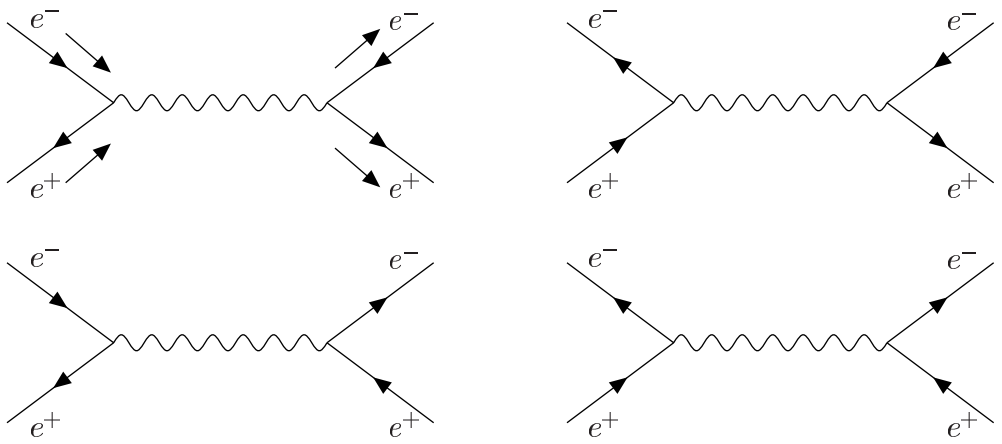

Figure 21: Tree-level s-channel Feynman diagrams for $e^-e^+ \to e^-e^+$, with the external lines labeled according to the particle names. The momentum flow of the external particles is indicated by the arrows above the corresponding fermion lines in the upper left diagram.

line with e [e^c]. If the arrow is opposite to the direction of propagation, then we identify the electron [positron] line with $\overline{e^c}$ [$\overline{e}$], in accord with the prescription of Fig. 19. Thus, in order to employ the two-component QED Feynman rules given in Fig. 20, we relabel the graphs of eq. (21) by employing the two-component fermion field labels, as shown in Fig. 22.

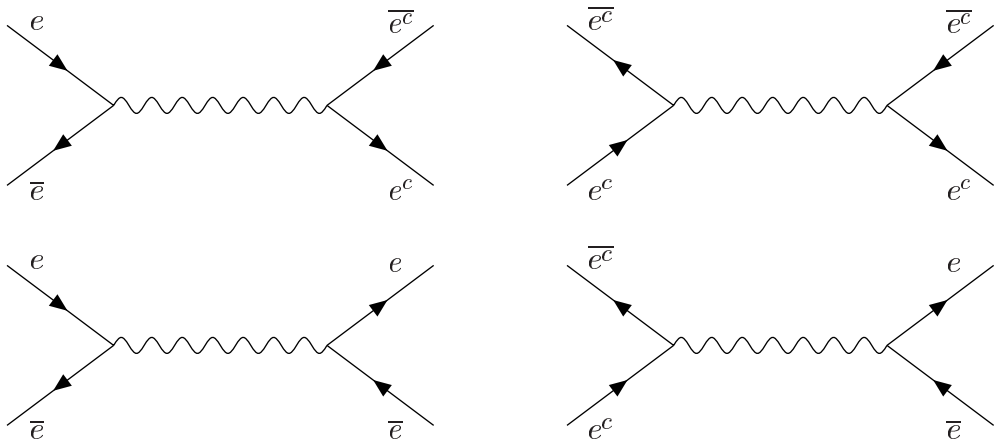

Figure 22: Tree-level s-channel Feynman diagrams for $e^+e^- \to e^+e^-$, with the external lines labeled according to the two-component fermion fields. Note that all momenta flow from left to right.

One can now employ the Feynman rules of Fig. 20 directly to compute the invariant amplitude. Note that the choice of rule involving either the fields e and $\overline{e}$ in Fig. 20(a) or the fields e^c and $\overline{e^c}$ in Fig. 20(b) is unambiguous.

6 Examples from the Standard Model and Minimal Supersymmetry

In this section we will present some examples to illustrate the use of the rules presented in this paper. These examples are chosen from the Standard Model and the MSSM, in order to provide an unambiguous point of reference. In all cases, the fermion lines in Feynman diagrams are labeled by two-component field names, rather than particle names, as explained in Section 5.

6.1 Top quark decay: $t \to bW^+$

We begin by calculating the decay width of a top quark into a bottom quark and W^+ vector boson. Let the four-momenta and helicities of these particle be (p_t, λ_t), (k_b, λ_b) and (k_W, λ_W), respectively. Then $p_t^2 = m_t^2$, $k_b^2 = m_b^2$ and $k_W^2 = m_W^2$ and

$$2p_t{\cdot}k_W = m_t^2 - m_b^2 + m_W^2\,, \tag{6.1}$$

$$2p_t{\cdot}k_b = m_t^2 + m_b^2 - m_W^2\,, \tag{6.2}$$

$$2k_W{\cdot}k_b = m_t^2 - m_b^2 - m_W^2\,. \tag{6.3}$$

Because only left-handed top quarks couple to the W boson, the only Feynman diagram for $t \to bW^+$ is the one shown in Fig. 23. The corresponding amplitude can be read off of the Feynman rule of Fig. 52 in Appendix C. Here the initial-state top quark is a two-component field t going into the vertex and the final-state bottom quark is created by a two-component field $\bar{b}$. Therefore the amplitude (ignoring CKM mixing) is given by:

$$i\mathcal{M} = -\frac{i}{\sqrt{2}} g \varepsilon_\mu^*(p_W) \bar{x}(p_b) \overline{\sigma}^\mu x(p_t)\,, \tag{6.4}$$

where ε_μ is the polarization vector of the W^+. Squaring this amplitude yields:

$$|\mathcal{M}|^2 = \tfrac{1}{2} g^2 \varepsilon_\mu^*(k_W) \varepsilon_\nu(k_W) \bar{x}(p_b) \overline{\sigma}^\mu x(p_t)\, \bar{x}(p_t) \overline{\sigma}^\nu x(p_b)\,, \tag{6.5}$$

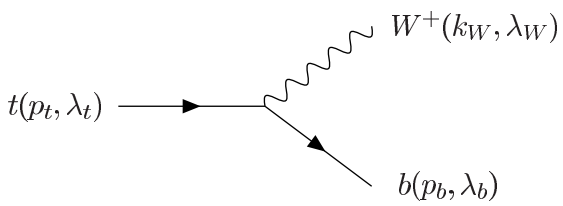

Figure 23: The Feynman diagram for $t \to bW^+$ at tree level.

where we have used equation (2.21). Next, we can average over the top quark spin polarizations using eq. (3.51):

$$\tfrac{1}{2}\sum_{\lambda_t}|\mathcal{M}|^2 = \tfrac{1}{4}g^2\varepsilon^*_\mu(k_W)\varepsilon_\nu(k_W)\bar{x}(p_b)\overline{\sigma}^\mu\, p_t{\cdot}\sigma\,\overline{\sigma}^\nu x(p_b)\,, \tag{6.6}$$

and then sum over the bottom quark spin polarizations. This yields a trace over spinor indices:

$$\begin{aligned}\tfrac{1}{2}\sum_{\lambda_t,\lambda_b}|\mathcal{M}|^2 &= \tfrac{1}{4}g^2\varepsilon^*_\mu(k_W)\varepsilon_\nu(k_W)\,\mathrm{Tr}[\overline{\sigma}^\mu p_t{\cdot}\sigma\,\overline{\sigma}^\nu k_b{\cdot}\sigma] \\ &= \tfrac{1}{2}g^2\varepsilon^*_\mu(k_W)\varepsilon_\nu(k_W)\left[p_t^\mu k_b^\nu + k_b^\mu p_t^\nu - g^{\mu\nu}p_t{\cdot}k_b\right]\,, \end{aligned}\tag{6.7}$$

where we have used eq. (2.30). Finally we can sum over the W^+ polarizations according to:

$$\sum_{\lambda_W}\varepsilon^*_\mu(k_W)\varepsilon_\nu(k_W) = -g_{\mu\nu} + \frac{(k_W)_\mu(k_W)_\nu}{m_W^2}\,. \tag{6.8}$$

The final result is:

$$\tfrac{1}{2}\sum_{\lambda_t,\lambda_b}|\mathcal{M}|^2 = \tfrac{1}{2}g^2\left[p_t{\cdot}k_b + \frac{2(p_t{\cdot}k_W)(k_b{\cdot}k_W)}{m_W^2}\right]. \tag{6.9}$$

After performing the phase space integration, one obtains:

$$\Gamma(t\to bW^+) = \frac{1}{16\pi m_t}\lambda^{1/2}\left(1,\frac{m_W^2}{m_t^2},\frac{m_b^2}{m_t^2}\right)\left(\frac{1}{2}\sum_{\lambda_t,\lambda_b}|\mathcal{M}|^2\right) \tag{6.10}$$

$$= \frac{g^2\left[(m_t^2-m_b^2-2m_W^2)(m_t^2-m_b^2-m_W^2)+2m_b^2m_W^2\right]}{64\pi m_W^2 m_t}\lambda^{1/2}\left(1,\frac{m_W^2}{m_t^2},\frac{m_b^2}{m_t^2}\right)\,, \tag{6.11}$$

where

$$\lambda(x,y,z) \equiv x^2+y^2+z^2-2xy-2xz-2yz. \tag{6.12}$$

In the approximation where $m_b \ll m_W, m_t$, one ends up with the well-known result

$$\Gamma(t\to bW^+) = \frac{g^2 m_t}{64\pi}\left(\frac{m_t^2}{m_W^2}\right)\left(1+\frac{2m_W^2}{m_t^2}\right)\left(1-\frac{m_W^2}{m_t^2}\right)^2\,, \tag{6.13}$$

which exhibits the Nambu-Goldstone enhancement factor (m_t^2/m_W^2).

6.2 Z^0 vector boson decay: $Z^0 \to f\bar{f}$

Consider the partial decay width of the Z^0 boson into Standard Model fermion-antifermion final states. There are two Feynman diagrams (as in the generic example of Fig. 12), shown in Fig. 24. The particle labels refer to the particle names rather than the two-component fermion fields (see Section 5). Let us call the initial Z^0 four-momentum and helicity (p, λ_Z) and the

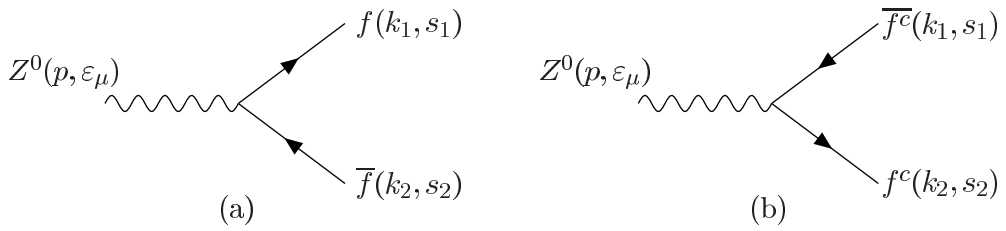

Figure 24: The Feynman diagrams for Z^0 decay into a fermion-antifermion pair. Fermion lines are labeled according to the two-component fermion labeling convention (see Section 5).

final state fermion (f) and anti-fermion ($\bar{f}$) momentum and helicities (k_1,λ_1) and (k_2,λ_2), respectively. Then, $k_1^2 = k_2^2 = m_f^2$ and $p^2 = m_Z^2$, and

$$k_1{\cdot}k_2 = \tfrac{1}{2}m_Z^2 - m_f^2\,, \tag{6.14}$$

$$p{\cdot}k_1 = p{\cdot}k_2 = \tfrac{1}{2}m_Z^2\,. \tag{6.15}$$

According to the rules of Fig. 52, the matrix elements for the two Feynman graphs are:

$$i\mathcal{M}_a = -i\frac{g}{c_W}(T_3^f - Q_f s_W^2)\,\varepsilon_\mu \bar{x}_1\overline{\sigma}^\mu y_2 \tag{6.16}$$

$$\begin{aligned} i\mathcal{M}_b &= igQ_f\frac{s_W^2}{c_W}\,\varepsilon_\mu y_1\sigma^\mu\bar{x}_2 \\ &= igQ_f\frac{s_W^2}{c_W}\varepsilon_\mu\bar{x}_2\overline{\sigma}^\mu y_1\,, \end{aligned} \tag{6.17}$$

where $x_i \equiv x(\vec{\boldsymbol{k}}_{\boldsymbol{i}}, s_i)$ and $y_i \equiv y(\vec{\boldsymbol{k}}_{\boldsymbol{i}}, s_i)$, for $i = 1,2$, and $\varepsilon_\mu \equiv \varepsilon_\mu(p)$. For $i\mathcal{M}_b$, we have exhibited two identical forms for the amplitude depending on whether one makes use of the σ-version or $\overline{\sigma}$-version of the Feynman rule (see the discussion in Section 4.5). It is convenient to define:

$$a_f \equiv T_3^f - Q_f s_W^2\,; \qquad\qquad b_f \equiv -Q_f s_W^2\,. \tag{6.18}$$

In terms of these quantities the squared matrix element for the decay is given by

$$|\mathcal{M}|^2 = \frac{g^2}{c_W^2}\varepsilon_\mu\varepsilon_\nu^*\left[a_f\bar{x}_1\overline{\sigma}^\mu y_2 + b_f y_1\sigma^\mu\bar{x}_2\right]\left[a_f\bar{y}_2\overline{\sigma}^\nu x_1 + b_f x_2\sigma^\nu\bar{y}_1\right]. \tag{6.19}$$

Summing over the anti-fermion helicity using eqs. (3.51)–(3.54) gives:

$$\begin{aligned} \sum_{\lambda_2}|\mathcal{M}|^2 = \frac{g^2}{c_W^2}\varepsilon_\mu\varepsilon_\nu^*\Big[&a_f^2\bar{x}_1\overline{\sigma}^\mu k_2{\cdot}\sigma\overline{\sigma}^\nu x_1 + b_f^2 y_1\sigma^\mu k_2{\cdot}\overline{\sigma}\sigma^\nu\bar{y}_1 \\ &- m_f a_f b_f\bar{x}_1\overline{\sigma}^\mu\sigma^\nu\bar{y}_1 - m_f a_f b_f y_1\sigma^\mu\overline{\sigma}^\nu x_1\Big]. \end{aligned} \tag{6.20}$$

Next, we sum over the fermion helicity:

$$\sum_{\lambda_1,\lambda_2} |\mathcal{M}|^2 = \frac{g^2}{c_W^2}\varepsilon_\mu\varepsilon_\nu^*\Big[a_f^2\mathrm{Tr}(\overline{\sigma}^\mu k_2{\cdot}\sigma\overline{\sigma}^\nu k_1{\cdot}\sigma) + b_f^2\mathrm{Tr}(\sigma^\mu k_2{\cdot}\overline{\sigma}\sigma^\nu k_1{\cdot}\overline{\sigma}) \\ -m_f^2 a_f b_f \mathrm{Tr}(\overline{\sigma}^\mu\sigma^\nu) - m_f^2 a_f b_f \mathrm{Tr}(\sigma^\mu\overline{\sigma}^\nu)\Big]. \tag{6.21}$$

Finally, averaging over the Z^0 polarization using

$$\tfrac{1}{3}\sum_{\lambda_Z}\varepsilon^\mu\varepsilon^{\nu *} = \tfrac{1}{3}\left(-g^{\mu\nu} + \frac{p^\mu p^\nu}{m_Z^2}\right) \tag{6.22}$$

and applying eqs. (2.28)–(2.30), one gets:

$$\tfrac{1}{3}\sum_{\text{spins}} |\mathcal{M}|^2 = \frac{g^2}{3c_W^2}\left[(a_f^2+b_f^2)\left(2k_1{\cdot}k_2 + \frac{4\,k_1{\cdot}p\,k_2{\cdot}p}{m_Z^2}\right) + 12a_f b_f m_f^2\right] \tag{6.23}$$

$$= \frac{2g^2}{3c_W^2}\left[(a_f^2+b_f^2)(m_Z^2-m_f^2) + 6a_f b_f m_f^2\right], \tag{6.24}$$

where we have used eqs. (6.14) and (6.15). After the phase-space integration, we obtain the well-known result for the partial width of the Z^0:

$$\Gamma(Z^0\to f\bar{f}) = \frac{1}{16\pi m_Z}\left(1-\frac{4m_f^2}{m_Z^2}\right)^{1/2}\left(\tfrac{1}{3}\sum_{\text{spins}}|\mathcal{M}|^2\right) \tag{6.25}$$

$$= \frac{g^2 m_Z}{24\pi c_W^2}\left(1-\frac{4m_f^2}{m_Z^2}\right)^{1/2}\left[(a_f^2+b_f^2)\left(1-\frac{m_f^2}{m_Z^2}\right) + 6a_f b_f\frac{m_f^2}{m_Z^2}\right]. \tag{6.26}$$

Finally, we note that if the final state fermions are colored, then one must also sum over colors. Since the Z^0 is a color singlet, the resulting color factor is simply equal to the dimension of the color representation of the outgoing fermions (that is, 1 for leptons and 3 for quarks).

6.3 Bhabha scattering: $e^+e^-\to e^+e^-$

In our next example, we consider the computation of Bhabha scattering in QED (that is, we we consider photon exchange but neglect Z^0-exchange). We denote the initial state electron and positron momenta and helicities by (p_1,λ_1) and (p_2,λ_2) and the final state electron and positron momenta and helicities by (p_3,λ_3) and (p_4,λ_4), respectively. Neglecting the electron mass (so that $p_i^2=0$ for $i=1,\ldots 4$), we have in terms of the usual Mandelstam variables s,t,u:

$$p_1{\cdot}p_2 = p_3{\cdot}p_4 \equiv \tfrac{1}{2}s\,, \tag{6.27}$$

$$p_1{\cdot}p_3 = p_2{\cdot}p_4 \equiv -\tfrac{1}{2}t\,, \tag{6.28}$$

$$p_1{\cdot}p_4 = p_2{\cdot}p_3 \equiv -\tfrac{1}{2}u\,. \tag{6.29}$$

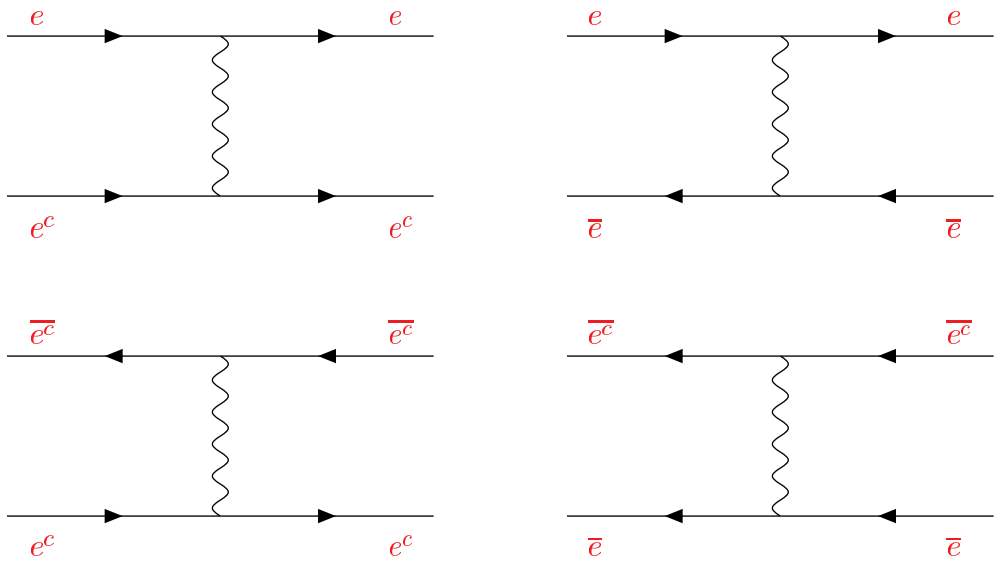

Figure 25: Tree-level t-channel Feynman diagrams for $e^+e^- \to e^+e^-$, with the external lines labeled according to the two-component field names. The momentum flow of the external particles is from left to right. (Comment: I have changed all the labels so that the upper line is the electron and the lower the positron, as in Fig. 22.)

There are eight distinct Feynman diagrams. First, there are four s-channel diagrams, as shown in Fig. 22 with amplitudes that follow from the Feynman rules of Fig. 20 (more generally, see Fig. 52 in Appendix C):

$$i\mathcal{M}_s = \left[\frac{-ig^{\mu\nu}}{s}\right]\Big([-ie\,x_1\sigma_\mu\bar{y}_2][ie\,y_3\sigma_\nu\bar{x}_4] + [-ie\,\bar{y}_1\overline{\sigma}_\mu x_2][ie\,y_3\sigma_\nu\bar{x}_4] \\ +[-ie\,x_1\sigma_\mu\bar{y}_2][ie\,\bar{x}_3\overline{\sigma}_\nu y_4] + [-ie\,\bar{y}_1\overline{\sigma}_\mu x_2][ie\,\bar{x}_3\overline{\sigma}_\nu y_4]\Big)\,, \tag{6.30}$$

where $x_i \equiv x(\vec{\boldsymbol{p}}_{\boldsymbol{i}}, \lambda_i)$ and $y_i \equiv y(\vec{\boldsymbol{p}}_{\boldsymbol{i}}, \lambda_i)$, for $i = 1, 4$. The photon propagator in Feynman gauge is $-ig^{\mu\nu}/p^2 = -ig^{\mu\nu}/s$. Here, we have chosen to follow the fermion lines in the order $1, 2, 3, 4$, which dictates the use of either the $\overline{\sigma}$ or σ forms of the Feynman rules of Fig. 20. One can group the terms of eq. (6.30) together more compactly:

$$i\mathcal{M}_s = e^2\left[\frac{-ig^{\mu\nu}}{s}\right]\Big[x_1\sigma_\mu\bar{y}_2 + \bar{y}_1\overline{\sigma}_\mu x_2\Big]\Big[y_3\sigma_\nu\bar{x}_4 + \bar{x}_3\overline{\sigma}_\nu y_4\Big]. \tag{6.31}$$

There are also four t-channel diagrams, as shown in Fig. 25. The corresponding amplitudes for these four diagrams can be written:

$$i\mathcal{M}_t = (-1)e^2\left[\frac{-ig^{\mu\nu}}{t}\right][x_1\sigma_\mu\bar{x}_3 + \bar{y}_1\overline{\sigma}_\mu y_3]\,[x_2\sigma_\nu\bar{x}_4 + \bar{y}_2\overline{\sigma}_\nu y_4]\,. \tag{6.32}$$

(Comm. factored out e^2 and the i's.) Here, the overall factor of (-1) comes from Fermi-Dirac statistics, since the external fermion wave functions are written in an odd permutation $(1, 3, 2, 4)$ of the original order $(1, 2, 3, 4)$ established by the first term in eq. (6.30).

Fierzing each term using eqs. (2.38)–(2.40), and using eqs. (2.32) and (2.33), the total amplitude can be written as:

$$\mathcal{M} = \mathcal{M}_s + \mathcal{M}_t = 2e^2\Bigg[\frac{1}{s}(x_1y_3)(\bar{y}_2\bar{x}_4) + \frac{1}{s}(\bar{y}_1\bar{x}_3)(x_2y_4) + \left(\frac{1}{s}+\frac{1}{t}\right)(\bar{y}_1\bar{x}_4)(x_2y_3)$$
$$+\left(\frac{1}{s}+\frac{1}{t}\right)(x_1y_4)(\bar{y}_2\bar{x}_3) - \frac{1}{t}(x_1x_2)(\bar{x}_3\bar{x}_4) - \frac{1}{t}(\bar{y}_1\bar{y}_2)(y_3y_4)\Bigg]. \tag{6.33}$$

Squaring this amplitude and summing over spins, all of the cross-terms will vanish in the $m_e \to 0$ limit. This is because any cross term will have an x or an $\bar{x}$ for some electron or positron combined with a y or a $\bar{y}$ for the same particle, and the corresponding spin sum is proportional to m_e [see eqs. (3.53) and (3.54)]. Hence, summing over final state spins and averaging over initial state spins, the end result contains the sum of the squares of the six terms in eq. (6.33):

$$\tfrac{1}{4}\sum_{\text{spins}}|\mathcal{M}|^2 = e^4 \sum_{\lambda_1,\lambda_2,\lambda_3,\lambda_4}\Bigg\{\frac{1}{s^2}\left[(x_1y_3(\bar{y}_3\bar{x}_1)(\bar{y}_2\bar{x}_4)(x_4y_2) + (\bar{y}_1\bar{x}_3)(x_3y_1)(x_2y_4)(\bar{y}_4\bar{x}_2)\right]$$
$$+\left(\frac{1}{s}+\frac{1}{t}\right)^2\left[(\bar{y}_1\bar{x}_4)(x_4y_1)(x_2y_3)(\bar{y}_3\bar{x}_2) + (x_1y_4)(\bar{y}_4\bar{x}_1)(\bar{y}_2\bar{x}_3)(x_3y_2)\right]$$
$$+\frac{1}{t^2}\left[(x_1x_2)(\bar{x}_2\bar{x}_1)(\bar{x}_3\bar{x}_4)(x_4x_3) + (\bar{y}_1\bar{y}_2)(y_2y_1)(y_3y_4)(\bar{y}_4\bar{y}_3)\right]\Bigg\}. \tag{6.34}$$

(Comment: I reversed the order of the spinors twice. This changes nothing, it is just what you get directly from the previous equation.) Performing the remaining spin sums using eqs. (3.51) and (3.52) and using the trace identities eq. (A.3):

$$\tfrac{1}{4}\sum_{\text{spins}}|\mathcal{M}|^2 = 8e^4\left[\frac{p_2\cdot p_4\, p_1\cdot p_3}{s^2} + \frac{p_1\cdot p_2\, p_3\cdot p_4}{t^2} + \left(\frac{1}{s}+\frac{1}{t}\right)^2 p_1\cdot p_4\, p_2\cdot p_3\right]$$
$$= 2e^4\left[\frac{t^2}{s^2}+\frac{s^2}{t^2}+u^2\left(\frac{1}{s}+\frac{1}{t}\right)^2\right]. \tag{6.35}$$

Thus, the differential cross section for Bhabha scattering is given by:

$$\frac{d\sigma}{dt} = \frac{1}{16\pi s^2}\left(\tfrac{1}{4}\sum_{\text{spins}}|\mathcal{M}|^2\right) = \frac{2\pi\alpha^2}{s^2}\left[\frac{t^2}{s^2}+\frac{s^2}{t^2}+u^2\left(\frac{1}{s}+\frac{1}{t}\right)^2\right]. \tag{6.36}$$

This agrees with the result of, for example, problem 5.2 of ref. [4].

6.4 Neutral CP-even Higgs scalar decay in the MSSM: $h^0, H^0 \to f\bar{f}$

In this subsection, we consider the decay of the CP-even neutral Higgs scalar bosons h^0 and H^0 of the MSSM into Standard Model fermion-antifermion pairs. First consider the decay

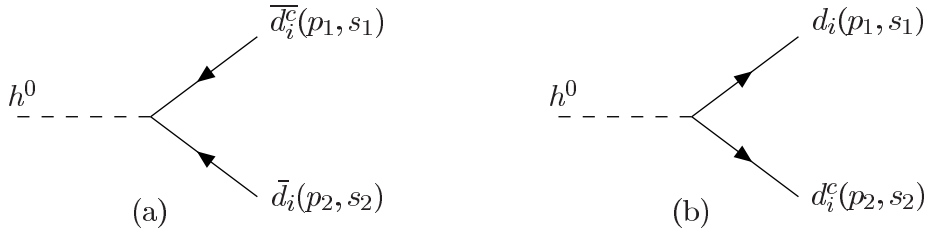

Figure 26: The Feynman diagrams for the decay $h^0 \to d_i \bar{d}_i$. We have labeled the external quarks according to the two-component down-like quark field names.

of h^0 into down-like quark and anti-quark, with momenta and spin polarizations (p_1, λ_1) and (p_2, λ_2), respectively. The external wave functions are denoted $x_1 \equiv x(d)$, $y_1 \equiv y(d)$ and $x_2 \equiv x(\bar{d})$, $y_2 \equiv y(\bar{d})$, respectively. There are two Feynman diagrams for $h^0 \to d_i \bar{d}_i$, as shown in Fig. 26. The rules of Figure 56 of Appendix D tell us that the resulting amplitudes are:

$$i\mathcal{M}_a = \frac{i}{\sqrt{2}}\, y_{di}\, \sin\alpha\, y_1 y_2\,, \tag{6.37}$$

$$i\mathcal{M}_b = \frac{i}{\sqrt{2}}\, y_{di}\, \sin\alpha\, \bar{x}_1 \bar{x}_2\,. \tag{6.38}$$

Now, let us specialize to the $b\bar{b}$ final state. Assuming a diagonal basis in which the bottom quark mass and the diagonal Yukawa coupling y_b are real and positive, we have a total amplitude:

$$i\mathcal{M} = i\mathcal{M}_a + i\mathcal{M}_b = \frac{i}{\sqrt{2}}\, y_b \sin\alpha\, \left[y_1 y_2 + \bar{x}_1 \bar{x}_2\right]\,. \tag{6.39}$$

Squaring this yields:

$$|\mathcal{M}|^2 = \frac{1}{2}\, y_b^2\, \sin^2\alpha\, \left[y_1 y_2 + \bar{x}_1 \bar{x}_2\right] \left[\bar{y}_2 \bar{y}_1 + x_2 x_1\right]\,. \tag{6.40}$$

Summing over the quark and anti-quark spins we obtain

$$\sum_{\lambda_1,\lambda_2} |\mathcal{M}|^2 = \frac{1}{2}\, y_b^2\, \sin^2\alpha\, \Big[\mathrm{Tr}(p_2{\cdot}\sigma p_1{\cdot}\overline{\sigma}) + \mathrm{Tr}(p_2{\cdot}\overline{\sigma} p_1{\cdot}\sigma) - 2m_b^2 - 2m_b^2\Big] \tag{6.41}$$

$$= +2\, y_b^2\, \sin^2\alpha\, (+p_1{\cdot}p_2 - m_b^2) \tag{6.42}$$

$$= y_b^2\, \sin^2\alpha\, (m_{h^0}^2 - 4m_b^2), \tag{6.43}$$

where we have used $p_1{\cdot}p_2 = \frac{1}{2}m_{h^0}^2 - m_b^2$. Therefore,

$$\Gamma(h^0 \to b\bar{b}) = \frac{1}{16\pi m_{h^0}} \left(1 - \frac{4m_b^2}{m_{h^0}^2}\right)^{1/2} \sum_{\text{color}} \sum_{\lambda_1,\lambda_2} |\mathcal{M}|^2 \tag{6.44}$$

$$= \frac{3}{16\pi}\, y_b^2\, \sin^2\alpha\, m_{h^0} \left(1 - \frac{4m_b^2}{m_{h^0}^2}\right)^{3/2} \tag{6.45}$$

which checks with the expression in Appendix B of the Higgs Hunter's Guide [3].

Other decays of h^0 and H^0 proceed in exactly the same way, with appropriate substitutions of the coupling parameters and the obvious accounting for color. Therefore, with no further work one obtains from eq. (6.45) the results:

- $H^0 \to b\bar{b}$ by taking $\sin^2\alpha \to \cos^2\alpha$ and $m_{h^0} \to m_{H^0}$.
- $h^0 \to c\bar{c}$ by taking $y_b^2 \sin^2\alpha \to y_c^2 \cos^2\alpha$ and $m_b \to m_c$.
- $H^0 \to c\bar{c}$ by taking $y_b^2 \to y_c^2$ and $m_b \to m_c$ and $m_{h^0} \to m_{H^0}$.
- $h^0 \to \tau^+\tau^-$ by taking $3y_b^2 \to y_\tau^2$ and $m_b \to m_\tau$.
- $H^0 \to \tau^+\tau^-$ by taking $3y_b^2 \sin^2\alpha \to y_\tau^2 \cos^2\alpha$ and $m_b \to m_\tau$ and $m_{h^0} \to m_{H^0}$.

6.5 Neutral CP-odd Higgs decay in the MSSM: $A^0 \to f\bar{f}$

Let us next consider the decay $A^0 \to b\bar{b}$. There are two Feynman diagrams, exactly as in the previous example with $h^0 \to A^0$. The external wave functions are also labeled as in the previous section. However, the sum of the amplitudes is given by:

$$i\mathcal{M} = i\mathcal{M}_a + i\mathcal{M}_b = \frac{1}{\sqrt{2}}\, y_b \sin\beta [y_1 y_2 - \bar{x}_1\bar{x}_2]\,. \tag{6.46}$$

Notice the relative minus sign between the amplitudes, which follows directly from the Feynman rules in Figure 57 of Appendix D, and is a crucial hallmark of a pseudoscalar coupling to fermion pairs with real positive masses. (It is *not* due to Fermi-Dirac statistics.) Summing and squaring yields:

$$|\mathcal{M}|^2 = \frac{1}{2}\, y_b^2 \sin^2\beta\, [y_1 y_2 - \bar{x}_1\bar{x}_2]\,[\bar{y}_2\bar{y}_1 - x_2 x_1]\ . \tag{6.47}$$

Now sum over the spin polarization of the $\bar{b}$ and the b:

$$\sum_{\lambda_1,\lambda_2} |\mathcal{M}|^2 = \frac{1}{2}\, y_b^2 \sin^2_\beta \left[\mathrm{Tr}(p_2\cdot\sigma\, p_1\cdot\overline{\sigma}) + \mathrm{Tr}(p_2\cdot\overline{\sigma}\, p_1\cdot\sigma) + 2m_b^2 + 2m_b^2\right] \tag{6.48}$$

$$= +2\, y_b^2 \sin^2_\beta\, (p_1\cdot p_2 + m_b^2) \tag{6.49}$$

$$= y_b^2 \sin^2_\beta\, m_{A^0}^2\,. \tag{6.50}$$

Therefore:

$$\Gamma(A^0 \to b\bar{b}) = \frac{1}{16\pi m_{A^0}} \left(1 - \frac{4m_b^2}{m_{A^0}^2}\right)^{1/2} \sum_{\text{color}} \sum_{\lambda_1,\lambda_2} |\mathcal{M}|^2 \tag{6.51}$$

$$= \frac{N_c}{16\pi}\, y_b^2 \sin^2\beta\, m_{A^0} \left(1 - \frac{4m_b^2}{m_{A^0}^2}\right)^{1/2}\,, \tag{6.52}$$

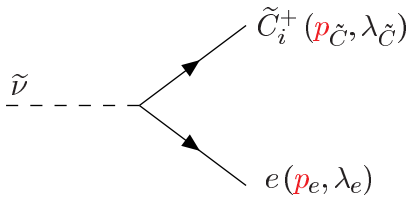

Figure 27: The Feynman diagram for $\widetilde{\nu} \to \widetilde{C}_i^+ e^+$ in the MSSM. Note we have used the two-component field names.

where $N - c = 3$ is the color factor. This again agrees with the expression in Appendix B of the Higgs Hunter's Guide [3]. The different threshold behavior [compared to eq. (6.45)] is due to the relative minus sign between the contributions of the two diagrams to the amplitude.

By appropriate substitutions of coupling parameters and masses, and no further work, one obtains:

- $A^0 \to \tau^+\tau^-$ by taking $3y_b^2 \to y_\tau^2$ and $m_b \to m_\tau$.
- $A^0 \to t\bar{t}$ by taking $y_b^2 \sin^2\beta \to y_t^2 \cos^2\beta$ and $m_b \to m_t$.
- $A^0 \to c\bar{c}$ by taking $y_b^2 \sin^2\beta \to y_c^2 \cos^2\beta$ and $m_b \to m_c$.

6.6 Sneutrino decay $\widetilde{\nu} \to \widetilde{C}_i^+ e^-$ in the MSSM

Next we consider the process of $\widetilde{\nu} \to \widetilde{C}_i^+ e^-$ in minimal supersymmetry. Because only the left-handed electron can couple to the chargino and sneutrino (with the excellent approximation that the electron Yukawa coupling is 0), there is just one Feynman diagram, shown in Fig. 27. The external wave functions of the electron and chargino are denoted as x_e, and $x_{\widetilde{C}}$, respectively. From the corresponding Feynman rule given in Figure 60 of Appendix D, the amplitude is:

$$i\mathcal{M} = -igV_{i1}\,\bar{x}_{\widetilde{C}}\bar{x}_e, \tag{6.53}$$

where V_{ij} is one of the two matrices used to diagonalize the chargino masses. Squaring this yields:

$$|\mathcal{M}|^2 = g^2|V_{i1}|^2\,(\bar{x}_{\widetilde{C}}\bar{x}_e)(x_e x_{\widetilde{C}})\,. \tag{6.54}$$

Now summing over the electron and chargino spin polarizations yields

$$\sum_{\lambda_e,\lambda_{\tilde{C}}} |\mathcal{M}|^2 = g^2|V_{i1}|^2 \mathrm{Tr}[p_e{\cdot}\overline{\sigma}\, p_{\tilde{C}}{\cdot}\sigma] = 2g^2|V_{i1}|^2\, p_e{\cdot}p_{\tilde{C}} = g^2|V_{i1}|^2(m_{\tilde{\nu}}^2 - m_{\tilde{C}}^2)\,, \tag{6.55}$$

where we have used $2p_e{\cdot}p_{\tilde{C}} = m_{\tilde{\nu}}^2 - m_{\tilde{C}}^2$ and have neglected the electron mass. Therefore, the decay width is:

$$\Gamma(\widetilde{\nu} \to \widetilde{C}_i^+ e^-) = \frac{1}{16\pi m_{\tilde{\nu}}}\left(1 - \frac{m_{\tilde{C}}^2}{m_{\tilde{\nu}}^2}\right)\sum_{\lambda_e,\lambda_{\tilde{C}}} |\mathcal{M}|^2 = \frac{g^2}{16\pi}|V_{i1}|^2 m_{\tilde{\nu}}\left(1 - \frac{m_{\tilde{C}}^2}{m_{\tilde{\nu}}^2}\right)^2\,. \tag{6.56}$$

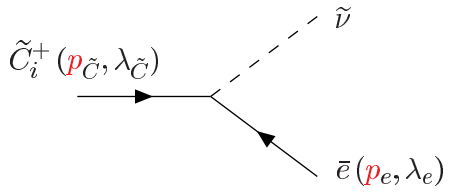

Figure 28: The Feynman diagram for $\widetilde{C}_i^+ \to \widetilde{\nu} e^-$ in the MSSM.

6.7 Chargino decay $\widetilde{C}_i^+ \to \widetilde{\nu} e^+$ in the MSSM

Here again there is just one Feynman diagram (neglecting the electron mass in the Yukawa coupling) shown in Fig. 28. The external wave functions for the chargino and the positron are denoted by $x_{\widetilde{C}}$ and y_{e^+}, respectively. The momenta and helicities are denoted as in Fig. 28. The amplitude can be directly determined using the Feynman rule given in Fig. 60 in App. D

$$\mathcal{M} = -igV_{i1}^*\, x_{\widetilde{C}}\, y_{e^+}\,. \tag{6.57}$$

Squaring this yields:

$$|\mathcal{M}|^2 = g^2|V_{i1}|^2\,(x_{\widetilde{C}} y_{e^+})\,(\bar{y}_{e^+}\bar{x}_{\widetilde{C}})\,. \tag{6.58}$$

Summing over the electron helicity and averaging over the chargino helicity we obtain:

$$\tfrac{1}{2}\sum_{\lambda_e,\lambda_{\widetilde{C}}} |\mathcal{M}|^2 = \tfrac{1}{2}g^2|V_{i1}|^2 \mathrm{Tr}[p_e\cdot\sigma\, p_{\widetilde{C}}\cdot\overline{\sigma}] = +g^2|V_{i1}|^2 p_e\cdot p_{\widetilde{C}} = \frac{g^2}{2}|V_{i1}|^2(m_{\widetilde{C}}^2 - m_{\widetilde{\nu}}^2)\,. \tag{6.59}$$

So the decay width is, neglecting the electron mass:

$$\Gamma(\widetilde{C}_i^+ \to \widetilde{\nu} e^+) = \frac{1}{16\pi m_{\widetilde{C}_i}}\left(1 - \frac{m_{\widetilde{\nu}}^2}{m_{\widetilde{C}_i}^2}\right)\left[\frac{1}{2}\sum_{\lambda_e,\lambda_{\widetilde{C}_i}} |\mathcal{M}|^2\right] = \frac{g^2}{32\pi}|V_{i1}|^2 m_{\widetilde{C}_i}\left(1 - \frac{m_{\widetilde{\nu}}^2}{m_{\widetilde{C}_i}^2}\right)^2. \tag{6.60}$$

6.8 Selectron production: $e^-e^- \to \widetilde{e}_L^-\widetilde{e}_R^-$

Here there are 2 Feynman graphs (if we again neglect the electron mass in the Yukawa couplings). Note that these two graphs are related by interchange of the identical initial state electrons. Let the electrons have momenta p_1 and p_2 and the selectrons have momenta k_1 and k_2, so that $p_1^2 = p_2^2 = 0$; $k_1^2 = m_{\widetilde{e}_L}^2$; $k_2^2 = m_{\widetilde{e}_R}^2$; $t = (p_1 - k_1)^2$; $u = (p_2 - k_1)^2$; and (I have modified many signs here due to the metric.)

$$2p_1\cdot p_2 = s; \qquad 2k_1\cdot k_2 = s - m_{\widetilde{e}_L}^2 - m_{\widetilde{e}_R}^2; \tag{6.61}$$

$$2p_1\cdot k_1 = -t + m_{\widetilde{e}_L}^2; \qquad 2p_1\cdot k_2 = -u + m_{\widetilde{e}_R}^2; \tag{6.62}$$

$$2p_2\cdot k_1 = -u + m_{\widetilde{e}_L}^2; \qquad 2p_2\cdot k_2 = -t + m_{\widetilde{e}_R}^2\,. \tag{6.63}$$

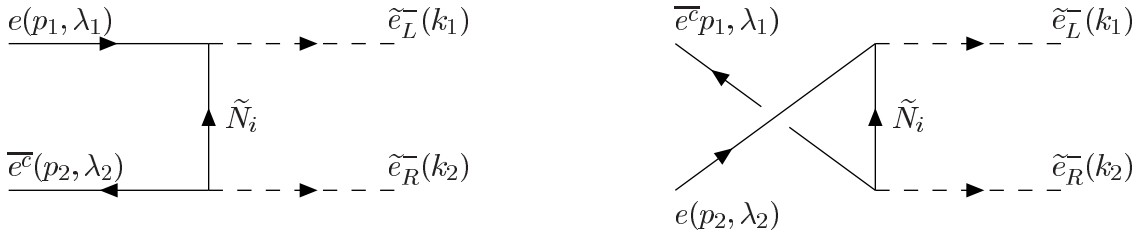

Figure 29: Feynman diagrams for $e^-e^- \to \widetilde{e}_L^-\widetilde{e}_R^-$ using the two component field labels. I have played around with this figure. So please check completely.

The matrix element for the first graph, for each exchanged neutralino $\widetilde{N}_i$, is then:

$$\mathcal{M}_a = \left[-i\sqrt{2}g\frac{s_W}{c_W}N_{i1}\right]\left[i\frac{g}{\sqrt{2}}\left(N_{i2}^* + \frac{s_W}{c_W}N_{i1}^*\right)\right]\, x_1\left[\frac{+i(k_1-p_1)\cdot\sigma}{(k_1-p_1)^2-m^2_{\widetilde{N}_i}}\right]\bar{y}_2\,, \tag{6.64}$$

while the matrix elements for the second graph are the same with the two incoming electrons exchanged, $e_1 \leftrightarrow e_2$:

$$\mathcal{M}_b = (-1)\left[-i\sqrt{2}g\frac{s_W}{c_W}N_{i1}\right]\left[i\frac{g}{\sqrt{2}}\left(N_{i2}^* + \frac{s_W}{c_W}N_{i1}^*\right)\right]\, x_2\left[\frac{+i(k_1-p_2)\cdot\sigma}{(k_1-p_2)^2-m^2_{\widetilde{N}_i}}\right]\bar{y}_1\,. \tag{6.65}$$

Note that since we have written the fermion wave function spinors in the opposite order in $\mathcal{M}_2$ compared to $\mathcal{M}_1$, there is a factor (-1) for Fermi-Dirac statistics. Alternatively, starting at the electron with momentum p_1 and using the Feynman rules as above, we can directly write:

$$\mathcal{M}_b = \left[-i\sqrt{2}g\frac{s_W}{c_W}N_{i1}\right]\left[i\frac{g}{\sqrt{2}}\left(N_{i2}^* + \frac{s_W}{c_W}N_{i1}^*\right)\right]\, \bar{y}_1\left[\frac{-i(k_1-p_2)\cdot\overline{\sigma}}{(k_1-p_2)^2-m^2_{\widetilde{N}_i}}\right]x_2\,. \tag{6.66}$$

This has no Fermi-Dirac factor (-1) because the wave function spinors are written in the same order as in $\mathcal{M}_1$. However, now the Feynman rule for the propagator has an extra minus sign, as can be seen in Fig. 3. We can also obtain eq. (6.66) from eq. (6.65) using eq. (2.34). So we can write for the total amplitude:

$$\mathcal{M} = \mathcal{M}_b + \mathcal{M}_b = x_1 a\cdot\sigma\bar{y}_2 + \bar{y}_1 b\cdot\overline{\sigma}x_2\,, \tag{6.67}$$

where

$$a^\mu \equiv i\frac{g^2 s_W}{c_W}(k_1^\mu - p_1^\mu)\sum_{i=1}^{4} N_{i1}(N_{i2}^* + \frac{s_W}{c_W}N_{i1}^*)\frac{1}{t-m^2_{\widetilde{N}_i}}\,, \tag{6.68}$$

$$b^\mu \equiv -i\frac{g^2 s_W}{c_W}(k_1^\mu - p_2^\mu)\sum_{i=1}^{4} N_{i1}(N_{i2}^* + \frac{s_W}{c_W}N_{i1}^*)\frac{1}{u-m^2_{\widetilde{N}_i}}\,. \tag{6.69}$$

So:

$$|\mathcal{M}|^2 = [x_1(a\cdot\sigma)\bar{y}_2]\,[y_2(a^*\cdot\sigma)\bar{x}_1] + [\bar{y}_1(b\cdot\overline{\sigma})x_2]\,[\bar{x}_2(b^*\cdot\overline{\sigma})y_1] + [x_1(a\cdot\sigma)\bar{y}_2]\,[\bar{x}_2(b^*\cdot\overline{\sigma})y_1] + [\bar{y}_1(b\cdot\overline{\sigma})x_2]\,[y_2(a^*\cdot\sigma)\bar{x}_1]\ . \tag{6.70}$$

Averaging over the initial state electron spins, the a, b^* and a^*, b cross terms are proportional to m_e and can thus be neglected in our approximation. We get:

$$\frac{1}{4}\sum_{\text{spins}}|\mathcal{M}|^2 = \frac{1}{4}\mathrm{Tr}[a\cdot\sigma\ p_2\cdot\overline{\sigma}\ a^*\cdot\sigma\ p_1\cdot\overline{\sigma}] + \frac{1}{4}\mathrm{Tr}[b\cdot\overline{\sigma}\ p_2\cdot\sigma\ b^*\cdot\overline{\sigma}\ p_1\cdot\sigma]\,. \tag{6.71}$$

These terms can be simplified using the identities:

$$\mathrm{Tr}[(k_1-p_1)\cdot\sigma\ p_2\cdot\overline{\sigma}\ (k_1-p_1)\cdot\sigma\ p_1\cdot\overline{\sigma}] = \mathrm{Tr}[(k_1-p_2)\cdot\overline{\sigma}\ p_2\cdot\sigma\ (k_1-p_2)\cdot\overline{\sigma}\ p_1\cdot\sigma] \tag{6.72}$$

$$= tu - m^2_{\widetilde{e}_L}\, m^2_{\widetilde{e}_R}\,, \tag{6.73}$$

resulting in:

$$\frac{1}{4}\sum_{\text{spins}}|\mathcal{M}|^2 = \frac{g^4 s_W^2}{4c_W^2}(tu - m^2_{\widetilde{e}_L}\, m^2_{\widetilde{e}_R})\sum_{i,j=1}^{4} N_{j1}N^*_{i1}(N^*_{j2} + \frac{s_W}{c_W}N^*_{j1})(N_{i2} + \frac{s_W}{c_W}N_{i1}) \left[\frac{1}{(t-m^2_{\widetilde{N}_i})(t-m^2_{\widetilde{N}_j})} + \frac{1}{(u-m^2_{\widetilde{N}_i})(u-m^2_{\widetilde{N}_j})}\right]. \tag{6.74}$$

To get the differential cross-section $d\sigma/dt$, multiply this by $1/(16\pi s^2)$:

$$\frac{d\sigma}{dt} = \frac{\pi\alpha^2}{4s_W^2c_W^2}\left(\frac{tu - m^2_{\widetilde{e}_L}\, m^2_{\widetilde{e}_R}}{s^2}\right)\sum_{i,j=1}^{4} N_{j1}N^*_{i1}(N^*_{j2} + \frac{s_W}{c_W}N^*_{j1})(N_{i2} + \frac{s_W}{c_W}N_{i1}) \left[\frac{1}{(t-m^2_{\widetilde{N}_i})(t-m^2_{\widetilde{N}_j})} + \frac{1}{(u-m^2_{\widetilde{N}_i})(u-m^2_{\widetilde{N}_j})}\right]. \tag{6.75}$$

To compare with eq. E26, p. 244 in Haber and Kane, note that for a pure photino exchange, $N_{i1} \to c_W\delta_{i1}$ and $N_{i2} \to s_W\delta_{i1}$, so that

$$\frac{1}{4s_W^2c_W^2}|N_{i1}|^2|N_{i2} + \frac{s_W}{c_W}N_{i1}|^2 \ \to\ 1\,, \tag{6.76}$$

and it checks.

6.9 $e^-e^- \to \widetilde{e}^-_R\widetilde{e}^-_R$ (done)

In the following we again neglect the electron mass and thus the Higgsino coupling to the electron. There are then 2 Feynman graphs related by the exchange of identical electrons in the initial state or equivalently by exchange of the identical selectrons in the final state, as shown

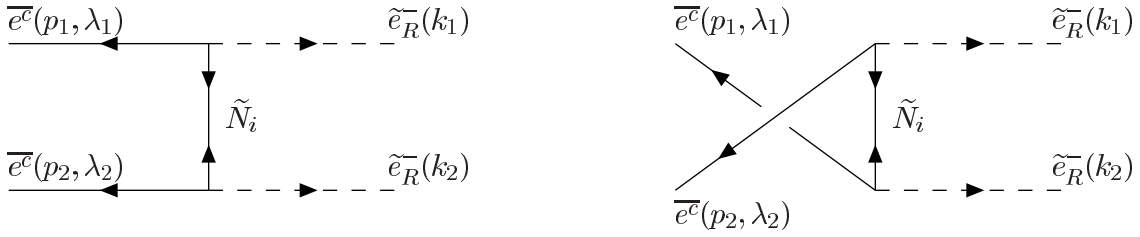

Figure 30: The two Feynman diagrams for $e^-e^- \to \widetilde{e}_R^-\widetilde{e}_R^-$ in the limit where $m_e \to 0$.

in Fig. 30. Let the electrons have momenta p_1 and p_2 and the selectrons have momenta k_1 and k_2, so that $p_1^2 = p_2^2 = 0$; $k_1^2 = k_2^2 = m^2_{\widetilde{e}_R}$; $t = (k_1 - p_1)^2$; $u = (k_1 - p_2)^2$; and

$$2p_1{\cdot}p_2 = +s; \qquad 2k_1{\cdot}k_2 = +s-2m^2_{\widetilde{e}_R}\,; \tag{6.77}$$

$$2p_1{\cdot}k_1 = 2p_2{\cdot}k_2 = -t+m^2_{\widetilde{e}_R}; \tag{6.78}$$

$$2p_1{\cdot}k_2 = 2p_2{\cdot}k_1 = -u+m^2_{\widetilde{e}_R}. \tag{6.79}$$

The amplitude for the first graph is:

$$\mathcal{M}_1 = \left(-i\sqrt{2}g\frac{s_W}{c_W}N_{i1}\right)^2\left[\frac{+i\,m_{\widetilde{N}_i}}{(p_1-k_1)^2-m^2_{\widetilde{N}_i}}\right]\bar{y}_1\bar{y}_2 \tag{6.80}$$

for each exchanged neutralino. The amplitudes for the second graph are the same, but with electrons exchanged:

$$\mathcal{M}_2 = \left(-i\sqrt{2}g\frac{s_W}{c_W}N_{i1}\right)^2\left[\frac{+i\,m_{\widetilde{N}_i}}{(p_2-k_1)^2-m^2_{\widetilde{N}_i}}\right]\bar{y}_1\bar{y}_2\,. \tag{6.81}$$

Since we have chosen to write the external state wave function spinors in the same order in $\mathcal{M}_1$ and $\mathcal{M}_2$, there is no factor of (-1) for Fermi-Dirac statistics. So, the total amplitude squared is:

$$|\mathcal{M}|^2 = \frac{4g^4s_W^4}{c_W^4}(y_1\bar{y}_2)(y_2y_1)\sum_{i,j=1}^{4}(N_{i1})^2(N^*_{j1})^2 m_{\widetilde{N}_i}m_{\widetilde{N}_j} \left(\frac{1}{t-m^2_{\widetilde{N}_i}}+\frac{1}{u-m^2_{\widetilde{N}_i}}\right)\left(\frac{1}{t-m^2_{\widetilde{N}_j}}+\frac{1}{u-m^2_{\widetilde{N}_j}}\right) \tag{6.82}$$

The sum over the electron spins is given by

$$\sum_{\lambda_1,\lambda_2}(\bar{y}_1\bar{y}_2)(y_2y_1) = \mathrm{Tr}[p_2{\cdot}\overline{\sigma}p_1{\cdot}\sigma] = +2p_2{\cdot}p_1 = s\,. \tag{6.83}$$

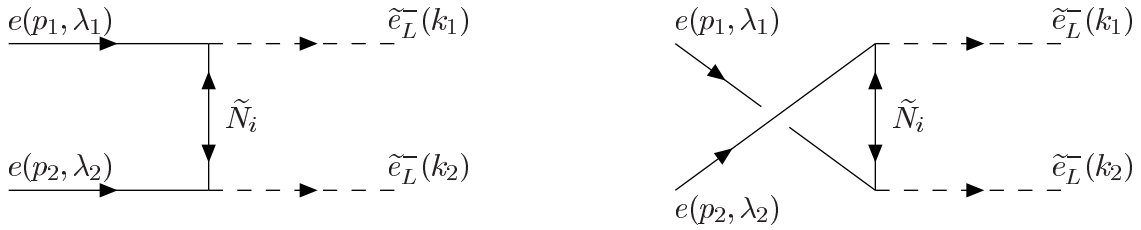

Figure 31: The two Feynman diagrams for $e^-e^- \to \widetilde{e}_L^-\widetilde{e}_L^-$ in the limit of vanishing electron mass.

So the spin-averaged differential cross-section is:

$$\frac{d\sigma}{dt} = \left(\frac{1}{2}\right)\frac{1}{16\pi s^2}\left(\frac{1}{4}\sum_{s_1,s_2}|\mathcal{M}|^2\right) \tag{6.84}$$

$$= \frac{\pi\alpha^2}{2c_W^4}\sum_{i,j=1}^{4}(N_{i1})^2(N_{j1}^*)^2\frac{m_{\widetilde{N}_i}m_{\widetilde{N}_j}}{s}\left(\frac{1}{t-m^2_{\widetilde{N}_i}}+\frac{1}{u-m^2_{\widetilde{N}_i}}\right)\left(\frac{1}{t-m^2_{\widetilde{N}_j}}+\frac{1}{u-m^2_{\widetilde{N}_j}}\right) \tag{6.85}$$

where the first factor of (1/2) in eq. (6.84) comes from the fact that there are identical sleptons in the final state and thus the phase space is degenerate.

To compare with eq. E27, p. 245 in Haber and Kane, note that for a pure photino exchange, $N_{i1} \to c_W\delta_{i1}$, so it checks.

6.10 $e^-e^- \to \widetilde{e}_L^-\widetilde{e}_L^-$ (done)

Again, in the limit of vanishing electron mass, there are 2 Feynman graphs related by the exchange of identical electrons in the initial state or equivalently by exchange of the identical selectrons in the final state. As shown in Fig. 31, they are exactly like the previous example, but with all arrows reversed. The amplitude for the first graph is:

$$\mathcal{M}_1 = \left(i\frac{g}{\sqrt{2}}[N_{i2}^* + \frac{s_W}{c_W}N_{i1}^*]\right)^2\left[\frac{+i\,m_{\widetilde{N}_i}}{(p_1-k_1)^2-m^2_{\widetilde{N}_i}}\right]x_1x_2 \tag{6.86}$$

for each exchanged neutralino. The amplitudes for the second graph are the same, but with $p_1 \leftrightarrow p_2$:

$$\mathcal{M}_2 = \left(i\frac{g}{\sqrt{2}}[N_{i2}^* + \frac{s_W}{c_W}N_{i1}^*]\right)^2\left[\frac{+i\,m_{\widetilde{N}_i}}{(p_2-k_1)^2-m^2_{\widetilde{N}_i}}\right]x_1x_2 \tag{6.87}$$

Since we have chosen to write the external state wave function spinors in the same order in $\mathcal{M}_1$ and $\mathcal{M}_2$, there is no factor of (-1) for Fermi-Dirac statistics. The total amplitude squared is:

$$|\mathcal{M}|^2 = \frac{g^4}{4}(x_1x_2)(\bar{x}_2\bar{x}_1)\sum_{i,j=1}^{4}(N_{i2}^* + \frac{s_W}{c_W}N_{i1}^*)^2(N_{j2} + \frac{s_W}{c_W}N_{j1})^2 m_{\widetilde{N}_i}m_{\widetilde{N}_j}$$

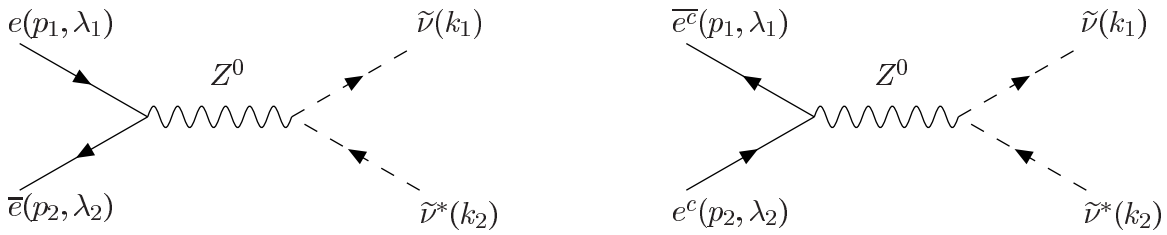

Figure 32: Two Feynman diagrams for $e^+e^- \to \widetilde{\nu}\widetilde{\nu}^*$ via s-channel Z^0 exchange.

$$\left(\frac{1}{t-m^2_{\widetilde{N}_i}}+\frac{1}{u-m^2_{\widetilde{N}_i}}\right)\left(\frac{1}{t-m^2_{\widetilde{N}_j}}+\frac{1}{u-m^2_{\widetilde{N}_j}}\right). \tag{6.88}$$

The average over the electron spins is given by

$$\sum_{\lambda_1,\lambda_2}(x_1x_2)(x_2x_1) = \mathrm{Tr}[p_2{\cdot}\sigma p_1{\cdot}\overline{\sigma}] = -2p_2{\cdot}p_1 = s\,. \tag{6.89}$$

So the spin-averaged differential cross-section is:

$$\frac{d\sigma}{dt} = \left(\frac{1}{2}\right)\frac{1}{16\pi s^2}\left(\frac{1}{4}\sum_{s_1,s_2}|\mathcal{M}|^2\right) \tag{6.90}$$

$$= \frac{\pi\alpha^2}{32 s_W^4}\sum_{i,j=1}^{4}(N^*_{i2}+\frac{s_W}{c_W}N^*_{i1})^2(N_{j2}+\frac{s_W}{c_W}N_{j1})^2\frac{m_{\widetilde{N}_i}m_{\widetilde{N}_j}}{s}$$
$$\left(\frac{1}{t-m^2_{\widetilde{N}_i}}+\frac{1}{u-m^2_{\widetilde{N}_i}}\right)\left(\frac{1}{t-m^2_{\widetilde{N}_j}}+\frac{1}{u-m^2_{\widetilde{N}_j}}\right) \tag{6.91}$$

where the first factor of (1/2) in eq. (6.90) comes from the fact that there are identical sleptons in the final state. To compare with eq. E27, p. 245 in Haber and Kane, note that for a pure photino exchange, $N_{i1} \to c_W\delta_{i1}$ and $N_{i2} \to s_W\delta_{i1}$, so it checks.

6.11 $e^+e^- \to \widetilde{\nu}\widetilde{\nu}^*$

There are two graphs featuring the s-channel exchange of the Z^0, shown in Fig. 32, where we have also defined the helicities and momenta of the particles. Since we shall neglect the electron mass, there is only one graph featuring the t-channel exchange of a chargino, shown in Fig. 33. The Mandelstam variables can be expressed in terms of the momenta and the sneutrino mass

$$2p_1{\cdot}p_2 = s\,; \qquad 2k_1{\cdot}k_2 = s - 2m^2_{\widetilde{\nu}_L}\,; \tag{6.92}$$

$$2p_1{\cdot}k_1 = -t + m^2_{\widetilde{\nu}_L}\,; \qquad 2p_1{\cdot}k_2 = -u + m^2_{\widetilde{\nu}_L}\,; \tag{6.93}$$

$$2p_2{\cdot}k_1 = -u + m^2_{\widetilde{\nu}_L}\,; \qquad 2p_2{\cdot}k_2 = -t + m^2_{\widetilde{\nu}_L}\,. \tag{6.94}$$

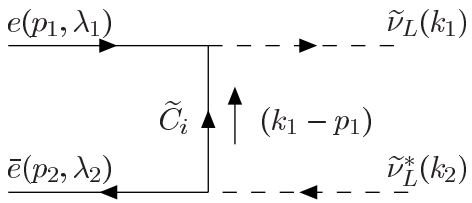

Figure 33: The one Feynman diagram for $e^+e^- \to \widetilde{\nu}\widetilde{\nu}^*$ via the t-channel exchange of a chargino in the limit where $m_e \to 0$.

The amplitude for the two graphs in Fig. 32 are given by

$$\mathcal{M}_1 = (-1)\frac{ig^2(-\frac{1}{2}+s_W^2)}{2c_W^2}\frac{1}{D_Z}\left[\bar{y}_2(k_1-k_2)\cdot\overline{\sigma}x_1\right], \tag{6.95}$$

$$\mathcal{M}_2 = \frac{-ig^2 s_W^2}{2c_W^2}\frac{1}{D_Z}\left[\bar{y}_1(k_1-k_2)\cdot\overline{\sigma}x_2\right], \tag{6.96}$$

where $D_Z \equiv s - M_Z^2 + i\Gamma_Z M_Z$ and Γ_Z is the Z^0 decay width. We have inserted an extra overall minus sign in the first amplitude, due to the different ordering of the spinors. This could have also been inserted in the second amplitude. The Feynman rules for the Z^0ee vertices are given in Figs. 52 a,b, for the $Z^0\widetilde{\nu}_L\widetilde{\nu}_L$ vertex in Fig. 72c, ref. [2]. The amplitude for the Feynman graph in Fig. 33 is given by

$$\mathcal{M}_3 = (-1)\frac{ig^2|V_{i1}|^2}{t-m^2_{\widetilde{C}_i}}\left[\bar{y}_2(k_1-p_1)\cdot\overline{\sigma}x_1\right], \tag{6.97}$$

where the relevant Feynman rule is given in Fig. 60b. Again we have inserted an extra overall minus sign due to the ordering of the spinors. Squaring each amplitude and summing over the incoming helicities we obtain

$$\sum_{\lambda_1\lambda_2}|\mathcal{M}_1|^2 = (-1)\frac{g^4(-\frac{1}{2}+s_W^2)^2}{c_W^4}\frac{1}{|D_Z|^2}\left[(t-m^2_{\widetilde{\nu}_L})^2+ts\right], \tag{6.98}$$

$$\sum_{\lambda_1\lambda_2}|\mathcal{M}_2|^2 = (-1)\frac{g^4 s_W^4}{c_W^4}\frac{1}{|D_Z|^2}\left[(t-m^2_{\widetilde{\nu}_L})^2+ts\right], \tag{6.99}$$

$$\sum_{\lambda_1\lambda_2}|\mathcal{M}_3|^2 = -g^4\left[(t-m^2_{\widetilde{\nu}_L})^2+ts\right]\sum_{i,j=1}^{2}\frac{|V_{i1}|^2|V_{j1}|^2}{(t-m^2_{\widetilde{C}_i})(t-m^2_{\widetilde{C}_j})}. \tag{6.100}$$

The interference terms between the first and the second as well as between the second and third amplitudes are proportional to m_e^2 and can thus be neglected. For the remaining interference term we obtain

$$2\Re(\mathcal{M}_1\mathcal{M}_3^\dagger) = \frac{g^4(1-2s_W^2)}{c_W^2}\frac{(s-M_Z^2)}{|D_Z|^2}\left[(t-m^2_{\widetilde{\nu}_L})^2+ts\right]\sum_{i=1}^{2}\frac{|V_{i1}|^2}{(t-m^2_{\widetilde{C}_i})}. \tag{6.101}$$

In computing eqs. (6.98)-(6.101) we have used

$$\mathrm{Tr}\left[p_1{\cdot}\sigma\,(k_1-k_2){\cdot}\overline{\sigma}\,p_2{\cdot}\sigma\,(k_1-k_2){\cdot}\overline{\sigma}\right]=4\,\mathrm{Tr}\left[p_2{\cdot}\sigma\,(k_1-p_1){\cdot}\overline{\sigma}\,p_1{\cdot}\sigma\,(k_1-p_1){\cdot}\overline{\sigma}\right]=$$
$$2\,\mathrm{Tr}\left[p_1{\cdot}\sigma\,(k_1-p_1){\cdot}\overline{\sigma}\,p_2{\cdot}\sigma\,(k_1-k_2){\cdot}\overline{\sigma}\right]=-4\left[(t-m^2_{\widetilde{\nu}_L})^2+st\right]\,. \tag{6.102}$$

This agrees with eqs. E46-E48 of ref. [2][14]. We can compute the total cross section via

$$\sigma=\int_{t_-}^{t_+}\frac{d\sigma}{dt}dt=\frac{1}{16\pi s^2}\int_{t_-}^{t_+}\left(\frac{1}{4}\sum_{\lambda_1\lambda_2}|\mathcal{M}|^2\right)dt\,, \tag{6.103}$$

where the integration limits are given by

$$t_\pm\equiv m^2_{\widetilde{\nu}_L}-\frac{s}{2}(1\mp\beta),\quad\text{and}\quad\beta\equiv\left(1-\frac{4m^2_{\widetilde{\nu}_L}}{s}\right)^{1/2}\,. \tag{6.104}$$

Denoting the terms corresponding to the matrix elements squared as

$$\sigma(e^+e^-\to\widetilde{\nu}_L\widetilde{\nu}_L^*)=\frac{g^4}{64\pi s}\left(S_1+S_2+S_3+S_{13}\right) \tag{6.105}$$

we obtain

$$S_1+S_2=\frac{s^2\beta^3}{48c_W^4|D_Z|^2}\left[(4s_W^2-1)^2+1\right] \tag{6.106}$$

$$S_{3,i}=|V_{i1}^4|\left[-2\beta+(1-2\gamma_i)\ln\left(\frac{t_--M^2_{\widetilde{C}_i}}{t_+-M^2_{\widetilde{C}_i}}\right)\right] \tag{6.107}$$

$$S_{3,12}=|V_{11}^2|V_{21}^2|\left[-2\beta+\frac{2s}{M^2_{\widetilde{C}_2}-M^2_{\widetilde{C}_1}}\sum_{i=1}^{2}(\gamma_i^2+\frac{M^2_{\widetilde{C}_i}}{s})\ln\left(\frac{t_--M^2_{\widetilde{C}_i}}{t_+-M^2_{\widetilde{C}_i}}\right)\right] \tag{6.108}$$

$$S_{13}=\frac{(-\frac{1}{2}+s_W^2)(1-\frac{M_Z^2}{s})s^2}{c_W^2|D_Z|^2}\sum_{i=1}^{2}|V_{i1}|^2\left(\tfrac{1}{2}\beta(1-2\gamma_i)-(\gamma_i^2+\frac{M^2_{\widetilde{C}_i}}{s})\ln\left(\frac{t_--M^2_{\widetilde{C}_i}}{t_+-M^2_{\widetilde{C}_i}}\right)\right) \tag{6.109}$$

which agrees with eqs. E49-E52 of ref. [2] in the limit of a single wino chargino. Here

$$\gamma_i=(m^2_{\widetilde{\nu}_L}-M^2_{\widetilde{C}_i})/s \tag{6.110}$$

$$S_3=S_{3,1}+S_{3,2}+S_{3,12} \tag{6.111}$$

6.12 $e^+e^-\to\widetilde{N}_i\widetilde{N}_j$

Next we consider the pair production of neutralinos via e^+e^--annihilation. Here there are 8 Feynman graphs shown in Figs. 34 and 35: four for s-channel Z^0 exchange and 4 for t-channel selectron exchange. The momenta are as labeled in the graphs. We denote the neutralino

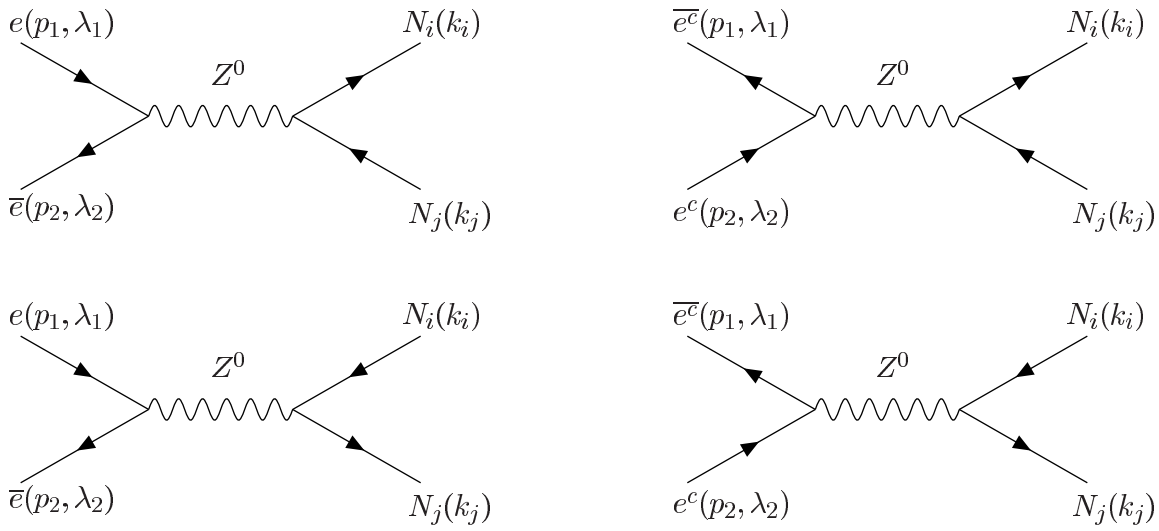

Figure 34: Four Feynman diagrams for $e^+e^- \to \widetilde{N}_i\widetilde{N}_j$ via s-channel Z^0 exchange.

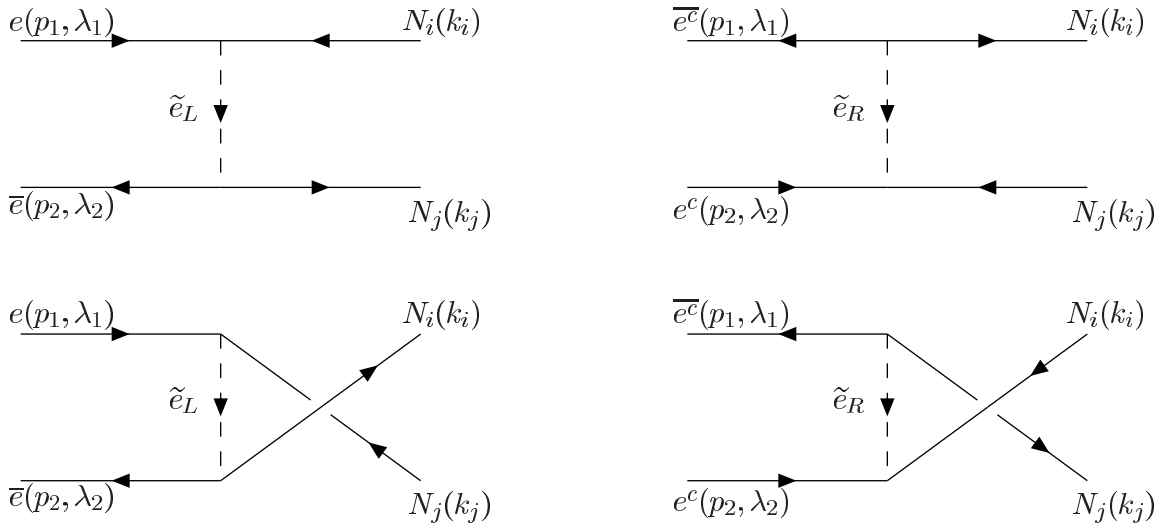

Figure 35: Four Feynman diagrams for $e^+e^- \to \widetilde{N}_i\widetilde{N}_j$ via t-channel selectron exchange.

masses as $M_{\widetilde{N}_{i,j}}$ and the selectron masses as $\widetilde{m}_{eL/R}$, respectively. The electron mass will be

[14]There is a typo in eq. E48 of [2], it should be multiplied by $1/\cos^2\theta_{\rm w}$.

neglected. The kinematical variables are then given by

$$s = (p_1+p_2)^2 = 2p_1{\cdot}p_2 = (k_i+k_j)^2 = 2k_i{\cdot}k_j + M^2_{\widetilde{N}_i} + M^2_{\widetilde{N}_j}\,, \tag{6.112}$$

$$t = (p_1-k_i)^2 = -2p_1{\cdot}k_i + M^2_{\widetilde{N}_i} = (p_2-k_j)^2 = -2p_2{\cdot}k_j + M_{\widetilde{N}_1}M^2_{\widetilde{N}_j}\,, \tag{6.113}$$

$$u = (p_1-k_j)^2 = -2p_1{\cdot}k_j + M^2_{\widetilde{N}_j} = (p_2-k_i)^2 = -2p_2{\cdot}k_i + M^2_{\widetilde{N}_i}\,. \tag{6.114}$$

Numbering the Feynman graphs in each figure from left to right and from top to bottom we obtain for the 8 amplitudes

$$\mathcal{M}_1 = (-1)\frac{(-i)g^2\mathcal{O}''^L_{ij}(-\frac{1}{2}+s^2_W)}{c^2_W D_Z}\,(\bar{x}_i\overline{\sigma}_\mu y_j)\,(\bar{y}_2\overline{\sigma}^\mu x_1)\,, \tag{6.115}$$

$$\mathcal{M}_2 = \frac{ig^2 s^2_W\mathcal{O}''^L_{ij}}{c^2_W D_Z}\,(\bar{x}_i\overline{\sigma}_\mu y_j)\,(\bar{y}_1\overline{\sigma}^\mu x_2)\,, \tag{6.116}$$

$$\mathcal{M}_3 = \frac{(-i)g^2\mathcal{O}''^{L*}_{ij}(-\frac{1}{2}+s^2_W)}{c^2_W D_Z}\,(\bar{x}_j\overline{\sigma}_\mu y_i)\,(\bar{y}_2\overline{\sigma}^\mu x_1)\,, \tag{6.117}$$

$$\mathcal{M}_4 = (-1)\frac{ig^2 s^2_W\mathcal{O}''^{L*}_{ij}}{c^2_W D_Z}\,(\bar{x}_j\overline{\sigma}_\mu y_i)\,(\bar{y}_1\overline{\sigma}^\mu x_2)\,, \tag{6.118}$$

$$\mathcal{M}_5 = (-1)\frac{(-i)2g^2 A^*_i A_j}{(t-\widetilde{m}^2_{eL})}\,(y_i x_1)\,(\bar{x}_j\bar{y}_2)\,, \tag{6.119}$$

$$\mathcal{M}_6 = (-1)\frac{(-i)2g^2 s^2_W N_{i1}N^*_{j1}}{c^2_W(t-\widetilde{m}^2_{eR})}\,(\bar{x}_i\bar{y}_1)\,(y_j x_2)\,, \tag{6.120}$$

$$\mathcal{M}_7 = \frac{(-i)2g^2 A_i A^*_j}{(u-\widetilde{m}^2_{eL})}\,(y_j x_1)\,(\bar{x}_i\bar{y}_2)\,, \tag{6.121}$$

$$\mathcal{M}_8 = \frac{(-i)2g^2 s^2_W N^*_{i1}N_{j1}}{c^2_W(u-\widetilde{m}^2_{eR})}\,(\bar{x}_j\bar{y}_1)\,(y_i x_2)\,, \tag{6.122}$$

where $\mathcal{O}''^L_{ij} = \mathcal{O}''^{L*}_{ji}$ is given in eq. (D.5), $A_i \equiv -\frac{1}{2}N_{i2} - \frac{s_W}{2c_W}N_{i1}$ and $D_Z \equiv 1/(s-M^2_Z+i\Gamma_z M_Z)$, as before. We have chosen the order $(ij12)$ of the spinors in $\mathcal{M}_2$ to have an overall plus sign. Thus the amplitudes $\mathcal{M}_{1,4,5,6}$ receive an overall minus sign, since the order of their spinors is an odd permutation of $(ij12)$. We now must sum the amplitudes and then square them. We first list the individual amplitudes squared, summed over incoming and outgoing spins.

$$\sum_{\lambda_{1,2},i,j}|\mathcal{M}_1|^2 = \frac{2g^4|\mathcal{O}''^L_{ij}|^2(-\frac{1}{2}+s^2_W)^2}{c^4_W|D_Z|^2}\left[(M^2_{\widetilde{N}_i}-u)(M^2_{\widetilde{N}_j}-u)+(M^2_{\widetilde{N}_i}-t)(M^2_{\widetilde{N}_j}-t)\right] \tag{6.123}$$

$$\sum_{\lambda_{1,2},i,j}|\mathcal{M}_2|^2 = \frac{2g^4 s^4_W|\mathcal{O}''^L_{ij}|^2}{c^4_W|D_Z|^2}\left[(M^2_{\widetilde{N}_i}-u)(M^2_{\widetilde{N}_j}-u)+(M^2_{\widetilde{N}_i}-t)(M^2_{\widetilde{N}_j}-t)\right] \tag{6.124}$$

$$\sum_{\lambda_{1,2},i,j}|\mathcal{M}_3|^2 = \frac{2g^4|\mathcal{O}''^L_{ij}|^2(-\frac{1}{2}+s^2_W)^2}{c^4_W|D_Z|^2}\left[(M^2_{\widetilde{N}_i}-u)(M^2_{\widetilde{N}_j}-u)+(M^2_{\widetilde{N}_i}-t)(M^2_{\widetilde{N}_j}-t)\right] \tag{6.125}$$

$$\sum_{\lambda_{1,2},i,j} |\mathcal{M}_4|^2 = \frac{2g^4 s_W^4 |\mathcal{O}''^L_{ij}|^2}{c_W^4 |D_Z|^2} \left[(M^2_{\widetilde{\widetilde{N}}_i} - u)(M^2_{\widetilde{\widetilde{N}}_j} - u) + (M^2_{\widetilde{\widetilde{N}}_i} - t)(M^2_{\widetilde{\widetilde{N}}_j} - t) \right] \tag{6.126}$$

$$\sum_{\lambda_{1,2},i,j} |\mathcal{M}_5|^2 = \frac{4g^4 |A_i A_j|^2}{(t - \widetilde{m}^2_{eL})^2} (M^2_{\widetilde{\widetilde{N}}_i} - t)(M^2_{\widetilde{\widetilde{N}}_j} - t) \tag{6.127}$$

$$\sum_{\lambda_{1,2},i,j} |\mathcal{M}_6|^2 = \frac{4g^4 s_W^4 |N_{i1} N_{j1}|^2}{c_W^4 (t - \widetilde{m}^2_{eR})^2} (M^2_{\widetilde{\widetilde{N}}_i} - t)(M^2_{\widetilde{\widetilde{N}}_j} - t) \tag{6.128}$$

$$\sum_{\lambda_{1,2},i,j} |\mathcal{M}_7|^2 = \frac{4g^4 |A_i A_j|^2}{(u - \widetilde{m}^2_{eL})^2} (M^2_{\widetilde{\widetilde{N}}_i} - u)(M^2_{\widetilde{\widetilde{N}}_j} - u) \tag{6.129}$$

$$\sum_{\lambda_{1,2},i,j} |\mathcal{M}_8|^2 = \frac{4g^4 s_W^4 |N_{i1} N_{j1}|^2}{c_W^4 (u - \widetilde{m}^2_{eR})^2} (M^2_{\widetilde{\widetilde{N}}_i} - u)(M^2_{\widetilde{\widetilde{N}}_j} - u) \tag{6.130}$$

Since we are neglecting the electron mass, interference term pairs containing $x_1 y_1$, $\bar{x}_1 \bar{y}_1$ or $1 \to 2$ vanish. Therefore, we must only compute the pairings: (13),(15),(17),(24),(26),(28),(35),(37), (46),(48),(57), and (68): (must include $i\Gamma_Z$ in numerator and take real part $\Re[\mathcal{O}''^{L2}_{ij}(s - M_Z^2 - i\Gamma_Z M_Z)]$)

$$2 \sum_{\lambda_{1,2},i,j} \Re(\mathcal{M}_1 \mathcal{M}_3^\dagger) = (-1) \frac{8g^4 \Re(\mathcal{O}''^L_{ij})^2 (\frac{1}{2} - s_W^2)^2}{c_W^4 |D_Z|^2} M_{\widetilde{N}_i} M_{\widetilde{N}_j} s\,, \tag{6.131}$$

$$2 \sum_{\lambda_{1,2},i,j} \Re(\mathcal{M}_1 \mathcal{M}_5^\dagger) = (-1) \frac{8g^4 (-\frac{1}{2} + s_W^2) \Re(\mathcal{O}''^L_{ij} A_i A_j^* D_Z^{-1})}{c_W^2 (t - \widetilde{m}_L^2) |D_Z|^2} M_{\widetilde{N}_i} M_{\widetilde{N}_j} s\,, \tag{6.132}$$

$$2 \sum_{\lambda_{1,2},i,j} \Re(\mathcal{M}_1 \mathcal{M}_7^\dagger) = \frac{8g^4 (s_W^2 - \frac{1}{2}) \Re(\mathcal{O}''^L_{ij} A_i^* A_j D_Z^{-1})}{c_W^2 (u - \widetilde{m}_L^2)} (s + t - M^2_{\widetilde{\widetilde{N}}_i})(s + t - M^2_{\widetilde{\widetilde{N}}_j})\,, \tag{6.133}$$

$$2 \sum_{\lambda_{1,2},i,j} \Re(\mathcal{M}_2 \mathcal{M}_4^\dagger) = (-1) \frac{8g^4 s_W^4 \Re(\mathcal{O}''^L_{ij})^2}{c_W^4 |D_Z|^2} s M_{\widetilde{N}_i} M_{\widetilde{N}_j}\,, \tag{6.134}$$

$$2 \sum_{\lambda_{1,2},i,j} \Re(\mathcal{M}_2 \mathcal{M}_6^\dagger) = \frac{-8g^4 s_W^4 \Re(N_{i1}^* N_{j1} \mathcal{O}''^L_{ij} D_Z^{-1})}{c_W^4 (t - \widetilde{m}_R^2)} (M^2_{\widetilde{\widetilde{N}}_i} - t)(M^2_{\widetilde{\widetilde{N}}_j} - t)\,, \tag{6.135}$$

$$2 \sum_{\lambda_{1,2},i,j} \Re(\mathcal{M}_2 \mathcal{M}_8^\dagger) = \frac{8g^4 s_W^4 \Re(N_{j1}^* N_{i1} \mathcal{O}''^L_{ij} D_Z^{-1})}{c_W^4 (u - \widetilde{m}_R^2)} M_{\widetilde{N}_i} M_{\widetilde{N}_j} s, \tag{6.136}$$

$$2 \sum_{\lambda_{1,2},i,j} \Re(\mathcal{M}_3 \mathcal{M}_5^\dagger) = \frac{8g^4 (-\frac{1}{2} + s_W^2) \Re(\mathcal{O}''^{L*}_{ij} A_i A_j^* D_Z^{-1})}{c_W^2 (t - \widetilde{m}_L^2)} (M^2_{\widetilde{\widetilde{N}}_i} - t)(M^2_{\widetilde{\widetilde{N}}_j} - t)\,, \tag{6.137}$$

$$2 \sum_{\lambda_{1,2},i,j} \Re(\mathcal{M}_3 \mathcal{M}_7^\dagger) = (-1) \frac{8g^4 \mathcal{O}''^{L*}_{ij} A_i^* A_j (-\frac{1}{2} + s_W^2)}{c_W^2 (u - \widetilde{m}_L^2) |D_Z|^2} (s - M_Z^2) s M_{\widetilde{N}_i} M_{\widetilde{N}_j}\,, \tag{6.138}$$

$$2 \sum_{\lambda_{1,2},i,j} \Re(\mathcal{M}_4 \mathcal{M}_6^\dagger) = \frac{8g^4 s_W^4 \mathcal{O}''^{L*}_{ij} N_{i1}^* N_{j1}}{c_W^4 (t - \widetilde{m}_R^2) |D_Z|^2} (s - M_Z^2) s M_{\widetilde{N}_i} M_{\widetilde{N}_j}\,, \tag{6.139}$$

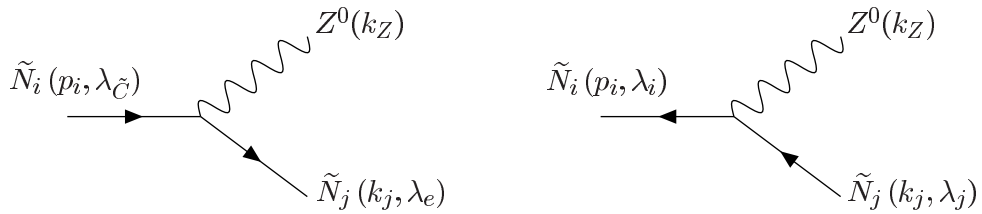

Figure 36: The Feynman diagrams for $\widetilde{N}_i \to \widetilde{N}_j Z^0$ in the MSSM.

$$2\sum_{\lambda_{1,2},i,j}\Re(\mathcal{M}_4\mathcal{M}_8^\dagger) = \frac{-8g^4 s_W^4 \mathcal{O}''^{L*}_{ij} N_{i1} N^*_{j1}}{c_W^4(u-\tilde{m}_R^2)|D_Z|^2}(s-M_Z^2)(s+t-M^2_{\widetilde{N}_i})(s+t-M^2_{\widetilde{N}_j})\,, \quad (6.140)$$

$$2\sum_{\lambda_{1,2},i,j}\Re(\mathcal{M}_5\mathcal{M}_7^\dagger) = \frac{-8g^4(A_i^* A_j)^2}{(t-\tilde{m}_L^2)(u-\tilde{m}_L^2)} s M_{\widetilde{N}_i} M_{\widetilde{N}_j}\,., \quad (6.141)$$

$$2\sum_{\lambda_{1,2},i,j}\Re(\mathcal{M}_6\mathcal{M}_8^\dagger) = \frac{-8g^4 s_W^4 (N_{i1}N^*_{j1})^2}{c_W^4(t-\tilde{m}_R^2)(u-\tilde{m}_R^2)} s M_{\widetilde{N}_i} M_{\widetilde{N}_j}\,. \quad (6.142)$$

The total cross section is now given as in eq. (6.103), where the integration limits are now given by

$$t_\pm \equiv \quad (6.143)$$

what kind of integrals do we have?

$$\int (C+t+t^2)dt\,, \qquad \int (C+t+t^2)/(t-m^2)\,dt\,, \quad (6.144)$$

$$\int (C+t+t^2)/(t-m^2)^2\,dt\,, \qquad \int (C+t+t^2)/[(t-m_1^2)(t-m_2^2)]\,dt\,. \quad (6.145)$$

6.13 $\widetilde{N}_i \to Z^0 \widetilde{N}_j$

For this two-body decay there are two tree-level Feynman diagrams shown in Fig. 36, where we have also defined the momenta. The scalar products of the momenta can be expressed in terms of the masses as

$$2k_j\cdot k_Z = M^2_{\widetilde{N}_i} - M^2_{\widetilde{N}_j} - M_Z^2 \quad (6.146)$$

$$2p_i\cdot k_j = M^2_{\widetilde{N}_i} + M^2_{\widetilde{N}_j} - M_Z^2 \quad (6.147)$$

$$2p_i\cdot k_Z = M^2_{\widetilde{N}_i} - M^2_{\widetilde{N}_j} + M_Z^2 \quad (6.148)$$

The two amplitudes are given by[15]

$$\mathcal{M}_1 = \frac{ig\mathcal{O}''^{L*}_{ij}}{c_W}(\bar{x}_j\overline{\sigma}_\mu x_i)\epsilon^{\mu *}\,, \quad (6.149)$$

[15]When comparing with the 4-component Feynman rule in ref. [2] note that $\mathcal{O}''^{L}_{ij} = \mathcal{O}''^{R*}_{ij}$, *c.f.* eq. (D.5).

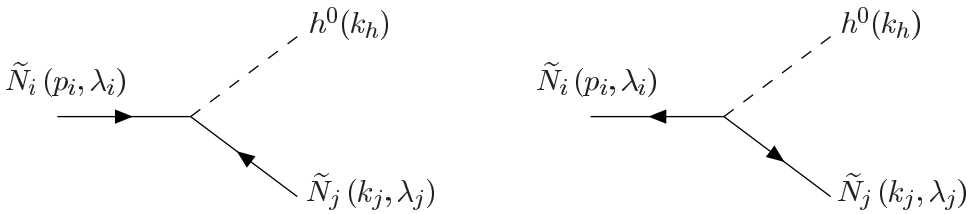

Figure 37: The Feynman diagrams for $\widetilde{N}_i \to \widetilde{N}_j h^0$ in the MSSM.

$$\mathcal{M}_2 = \frac{ig\mathcal{O}''^L_{ij}}{c_W}(\bar{y}_i\overline{\sigma}_\mu y_j)\epsilon^{\mu *}\,. \tag{6.150}$$

Squaring the individual amplitudes, summing over initial and final state spins and using

$$\sum_{\text{pol}} \epsilon^{\mu *}\epsilon^{\nu} = -g^{\mu\nu} + \frac{k_Z^\mu k_Z^\nu}{M_Z^2}\,, \tag{6.151}$$

we obtain

$$\sum_{\lambda_{i,j,Z}} |\mathcal{M}_1|^2 = \sum_{\lambda_{i,j,Z}} |\mathcal{M}_2|^2 = \frac{g^2|\mathcal{O}''^L_{ij}|^2}{c_W^2}\left[M^2_{\widetilde{N}_i} + M^2_{\widetilde{N}_j} - 2M_Z^2 + \frac{(M^2_{\widetilde{N}_i} - M^2_{\widetilde{N}_j})^2}{M_Z^2}\right]. \tag{6.152}$$

For the interference term we observe that in $\mathcal{M}_1$ and $\mathcal{M}_2$ $\bar{x}_j\,(x_i)$ is matched with $y_j\,(\bar{y}_i)$. Therefore it must be proportional to $M_{\widetilde{N}_i} M_{\widetilde{N}_j}$.

$$2\Re(\mathcal{M}_1\mathcal{M}_2^\dagger) = 12\frac{g^2\Re(\mathcal{O}''^L_{ij})^2}{c_W^2} M_{\widetilde{N}_i} M_{\widetilde{N}_j}\,. \tag{6.153}$$

$$\Gamma(\widetilde{N}_i \to Z^0\widetilde{N}_j) = \frac{1}{16\pi M_{\widetilde{N}_i}}\lambda^{1/2}\left(1, \frac{M_Z^2}{M^2_{\widetilde{N}_i}}, \frac{M^2_{\widetilde{N}_j}}{M^2_{\widetilde{N}_i}}\right)\left(\frac{1}{2}\sum_{\lambda_{i,j,Z}} |\mathcal{M}|^2\right) \tag{6.154}$$

$$= x \tag{6.155}$$

where

$$\lambda(x,y,z) \equiv x^2 + y^2 + z^2 - 2xy - 2xz - 2yz. \tag{6.156}$$

6.14 $\widetilde{N}_i \to h^0\widetilde{N}_j$

Next we consider the decay of a neutralino to a lighter neutralino and the lightest neutral CP-even Higgs boson. The two tree-level Feynman graphs are shown in Fig. 37, where we have also labeled the momenta and helicities. We denote the masses for the neutralinos and Higgs boson

respectively as $M_{\widetilde{N}_i,\widetilde{N}_j}$, M_{h^0}. The invariant momentum scalar products are then given by

$$2k_j\cdot k_h = M^2_{\widetilde{N}_i} - M^2_{\widetilde{N}_j} - M^2_{h^0} \tag{6.157}$$

$$2p_i\cdot k_j = M^2_{\widetilde{N}_i} + M^2_{\widetilde{N}_j} - M^2_{h^0} \tag{6.158}$$

$$2p_i\cdot k_h = M^2_{\widetilde{N}_i} - M^2_{\widetilde{N}_j} + M^2_{h^0} \tag{6.159}$$

Using the Feynman rules of Fig. 59, the amplitudes are given by

$$\mathcal{M}_1 = igA^*_{ij}(x_i y_i)\,, \tag{6.160}$$

$$\mathcal{M}_2 = igA_{ij}(\bar{y}_i \bar{x}_j)\,, \tag{6.161}$$

where we have defined the mixing matrix $A_{ij} \equiv S''_{ij}\cos\alpha + Q''_{ij}\sin\alpha$ (*c.f.* eqs. (D.24) and (D.25)). Summing over initial and final state spins we obtain for the parts of the total matrix element squared

$$\sum_{\lambda_{i,j}} |\mathcal{M}_1^2| = \sum_{\lambda_{i,j}} |\mathcal{M}_1^2| = g^2|A_{ij}|^2(M^2_{\widetilde{N}_i} + M^2_{\widetilde{N}_j} - M^2_{h^0})\,, \tag{6.162}$$

$$2\Re(\mathcal{M}_1\mathcal{M}_2^\dagger) = 4g^2\Re(A^2_{ij})M_{\widetilde{N}_i}M_{\widetilde{N}_j} \tag{6.163}$$

The total decay rate is given by

$$\Gamma(\widetilde{N}_i \to h^0\widetilde{N}_j) = \frac{1}{16\pi M_{\widetilde{N}_i}}\lambda^{1/2}\left(1, \frac{M^2_{h^0}}{M^2_{\widetilde{N}_i}}, \frac{M^2_{\widetilde{N}_j}}{M^2_{\widetilde{N}_i}}\right)\left(\frac{1}{2}\sum_{\lambda_{i,j,Z}}|\mathcal{M}|^2\right) \tag{6.164}$$

$$= x \tag{6.165}$$

where

$$\lambda(x,y,z) \equiv x^2 + y^2 + z^2 - 2xy - 2xz - 2yz. \tag{6.166}$$

The decay rates for the processes $\widetilde{N}_i \to \widetilde{N}_j H^0$ and $\widetilde{N}_i \to \widetilde{N}_j A^0$ can be obtained from the above by replacing

6.15 $\widetilde{N}_i \to \widetilde{N}_j\widetilde{N}_k\widetilde{N}_\ell$

Next we consider the decay of a neutralino $\widetilde{N}_i$ to three lighter neutralinos: $\widetilde{N}_j, \widetilde{N}_k, \widetilde{N}_\ell$. At tree-level, this can proceed via a Z^0 boson for which the Feynman graphs are shown in Fig. 38, where we have also defined the momenta. In addition, it can proceed via the exchange of either of the neutral scalar Higgs bosons: h^0, H^0, A^0 as shown in Fig. 39. Since either of the final state neutralinos can directly couple to the initial state neutralino there are two more diagrams for each diagram shown in Figs. 38 and 39 for a total of 48 tree-level diagrams. The computation

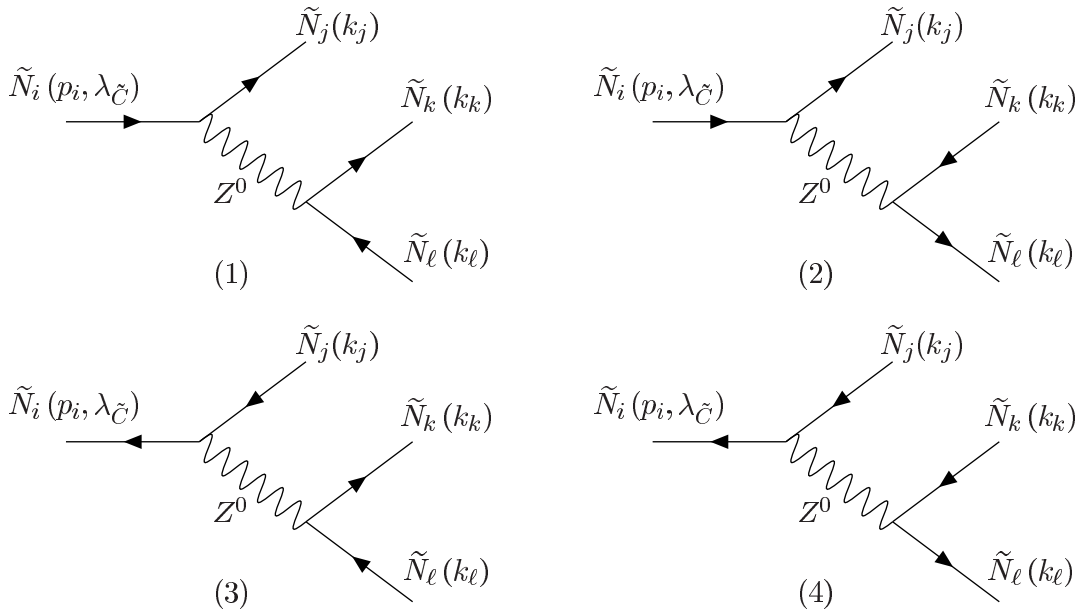

Figure 38: Four Feynman diagrams for $\widetilde{N}_i \to \widetilde{N}_j \widetilde{N}_k \widetilde{N}_\ell$ in the MSSM via Z^0 exchange. There are four more where $\widetilde{N}_j \leftrightarrow \widetilde{N}_k$ are interchanged and another four where $\widetilde{N}_j \leftrightarrow \widetilde{N}_\ell$ are interchanged.

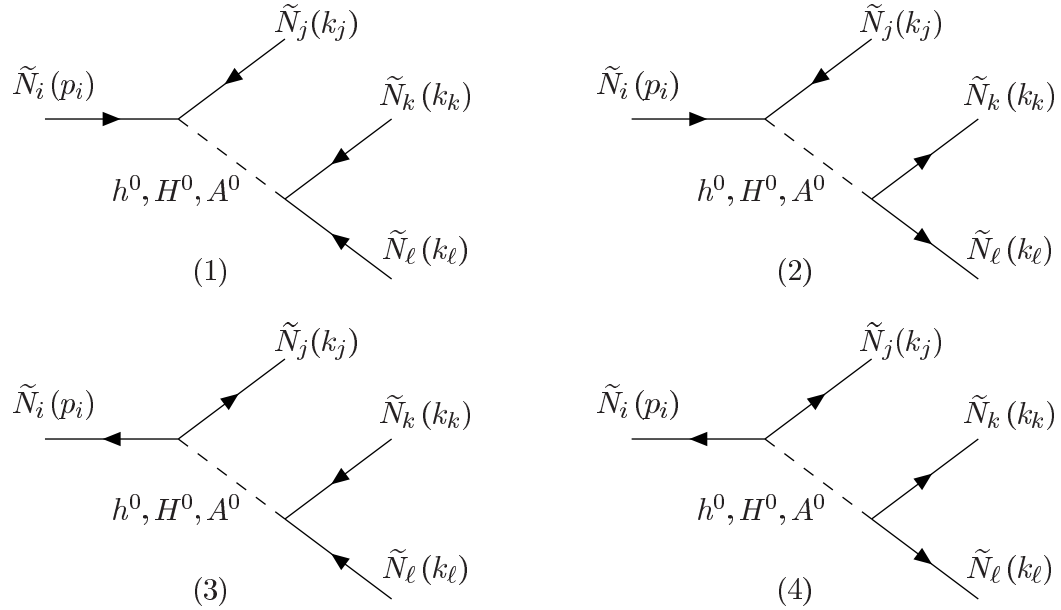

Figure 39: Four Feynman diagrams for $\widetilde{N}_i \to \widetilde{N}_j \widetilde{N}_k \widetilde{N}_\ell$ in the MSSM via h^0, H^0, A^0 exchange. There are four more where the labels $\widetilde{N}_j \leftrightarrow \widetilde{N}_k$ are interchanged and another four where $\widetilde{N}_j \leftrightarrow \widetilde{N}_\ell$ are interchanged.

of the total decay rate is correspondingly elaborate and we restrict ourselves here to recording

the contributing amplitudes:

$$\mathcal{M}_{Z1} = (-1)\frac{ig^2\mathcal{O}''^L_{ji}\mathcal{O}''^L_{k\ell}}{c_W^2 D_Z}(\bar{x}_j\overline{\sigma}_\mu x_i)(\bar{x}_k\overline{\sigma}^\mu y_\ell)\,, \tag{6.167}$$

$$\mathcal{M}_{Z2} = \frac{ig^2\mathcal{O}''^L_{ji}\mathcal{O}''^L_{\ell k}}{c_W^2 D_Z}(\bar{x}_j\overline{\sigma}_\mu x_i)(\bar{x}_\ell\overline{\sigma}^\mu y_k)\,, \tag{6.168}$$

$$\mathcal{M}_{Z3} = \frac{ig^2\mathcal{O}''^L_{ij}\mathcal{O}''^L_{k\ell}}{c_W^2 D_Z}(\bar{y}_i\overline{\sigma}_\mu x_j)(\bar{x}_k\overline{\sigma}^\mu y_\ell)\,, \tag{6.169}$$

$$\mathcal{M}_{Z4} = (-1)\frac{ig^2\mathcal{O}''^L_{ij}\mathcal{O}''^L_{\ell k}}{c_W^2 D_Z}(\bar{y}_i\overline{\sigma}_\mu x_j)(\bar{x}_\ell\overline{\sigma}^\mu y_k)\,, \tag{6.170}$$

$$\mathcal{M}_{\text{Higgs1}} = -g^2\mathcal{C}^*_{ij}\mathcal{C}^*_{k\ell}(x_i y_j)(y_k y_\ell)\,, \tag{6.171}$$

$$\mathcal{M}_{\text{Higgs2}} = -g^2\mathcal{C}^*_{ij}\mathcal{C}_{k\ell}(x_i y_j)(\bar{y}_k \bar{y}_\ell)\,, \tag{6.172}$$

$$\mathcal{M}_{\text{Higgs3}} = -g^2\mathcal{C}_{ij}\mathcal{C}^*_{k\ell}(\bar{y}_i \bar{x}_j)(y_k y_\ell)\,, \tag{6.173}$$

$$\mathcal{M}_{\text{Higgs4}} = -g^2\mathcal{C}_{ij}\mathcal{C}_{k\ell}(\bar{y}_i \bar{x}_j)(\bar{y}_k \bar{y}_\ell)\,, \tag{6.174}$$

where the Higgs-boson coupling constants are given by (*c.f.* eqs. (D.24) and (D.25))

$$\mathcal{C}_{ij} \equiv \mathcal{C}^{h^0}_{ij} + \mathcal{C}^{H^0}_{ij} + \mathcal{C}^{A^0}_{ij} \tag{6.175}$$

$$\mathcal{C}^{h^0}_{ij} \equiv S''_{ij}\cos\alpha + Q''_{ij}\sin\alpha \tag{6.176}$$

$$\mathcal{C}^{H^0}_{ij} \equiv S''_{ij}\sin\alpha - Q''_{ij}\cos\alpha \tag{6.177}$$

$$\mathcal{C}^{A^0}_{ij} \equiv (-i)\left(S''_{ij}\cos\beta - Q''_{ij}\sin\beta\right)\,. \tag{6.178}$$

For each amplitude in eqs. (6.167)-(6.174), there are two further amplitudes: one where the indices $j \leftrightarrow k$ are swapped and another where the indices $j \leftrightarrow \ell$ are swapped. The additional amplitudes all have a further factor of (-1) due to the ordering of the spinors. When computing the total decay rate, additional attention must be paid to the case where two or more final state indices are equal, since the phase space is then reduced by the corresponding factor.

6.16 $e^+e^- \to \widetilde{C}_i^+\widetilde{C}_j^-$

Next we consider the pair production of charginos. We denote the chargino masses as $M_{\widetilde{C}_{i,j}}$ and neglect the electron mass. The s-channel Feynman diagrams are shown in Fig. 40, where we have also introduced the notation for the momenta and helicities. The t-channel Feynman diagram via sneutrino exchange is shown in Fig. 41. The invariant scalar products can be expressed in terms of the chargino masses and the Mandelstam variables:

$$p_1{\cdot}p_2 = \tfrac{1}{2}s\,, \qquad k_i{\cdot}k_j = \tfrac{1}{2}(s - M^2_{\widetilde{C}_i} + M^2_{\widetilde{C}_j})\,, \tag{6.179}$$

$$p_1{\cdot}k_j = \tfrac{1}{2}(M^2_{\widetilde{C}_j} - t)\,, \qquad p_2{\cdot}k_i = \tfrac{1}{2}(M^2_{\widetilde{C}_i} - t)\,, \tag{6.180}$$

$$p_1{\cdot}k_i = \tfrac{1}{2}(M^2_{\widetilde{C}_i} - u)\,, \qquad p_2{\cdot}k_j = \tfrac{1}{2}(M^2_{\widetilde{C}_j} - u)\,. \tag{6.181}$$

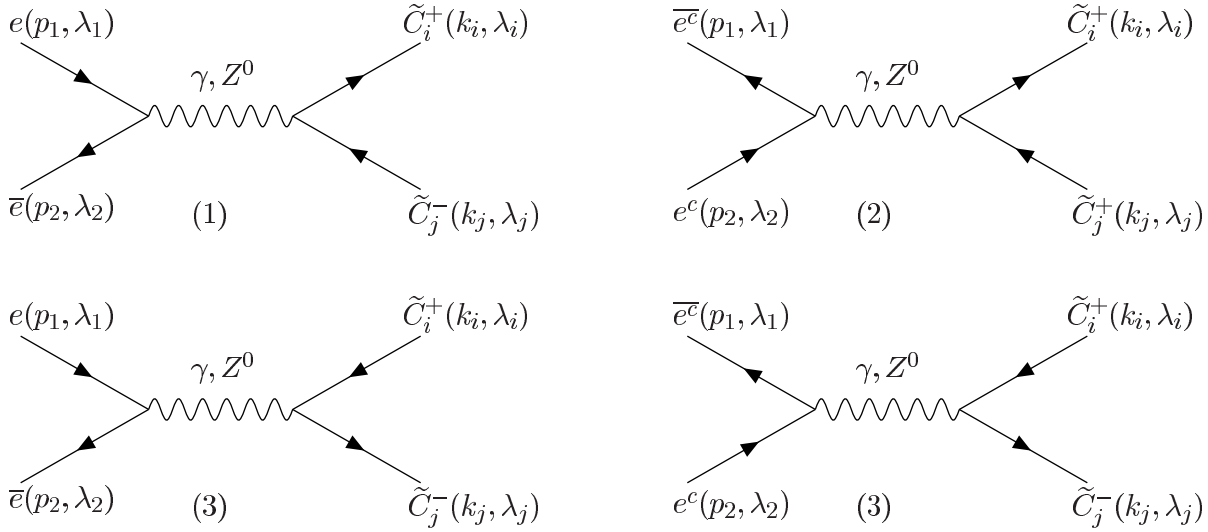

Figure 40: Feynman diagrams for $e^+e^- \to \widetilde{C}_i^+\widetilde{C}_j^-$ via s-channel γ and Z^0 exchange.

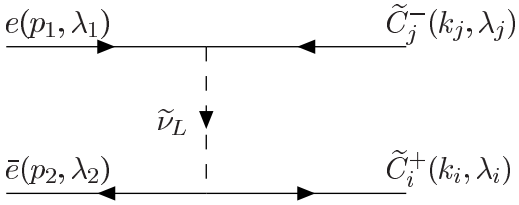

Figure 41: The Feynman diagram for $e^+e^- \to \widetilde{C}_i^+\widetilde{C}_j^-$ via the t-channel exchange of a chargino.

The s-channel Z and γ amplitudes are given by

$$\mathcal{M}_{\gamma Z^0,1} = (-1)\frac{ig^2}{c_W^2}\left(-\frac{\mathcal{C}_e}{s} - \frac{A_e\mathcal{O}'^L_{ij}}{D_Z}\right)(\bar{x}_i\overline{\sigma}_\mu y_j)(\bar{y}_2\overline{\sigma}^\mu x_1)\,, \tag{6.182}$$

$$\mathcal{M}_{\gamma Z^0,2} = (+1)\frac{ig^2}{c_W^2}\left(\frac{\mathcal{C}_e}{s} - \frac{B_e\mathcal{O}'^L_{ij}}{D_Z}\right)(\bar{x}_i\overline{\sigma}_\mu y_j)(\bar{y}_1\overline{\sigma}^\mu x_2)\,, \tag{6.183}$$

$$\mathcal{M}_{\gamma Z^0,3} = (+1)\frac{ig^2}{c_W^2}\left(\frac{\mathcal{C}_e}{s} + \frac{A_e\mathcal{O}'^R_{ij}}{D_Z}\right)(\bar{x}_j\overline{\sigma}_\mu y_i)(\bar{y}_2\overline{\sigma}^\mu x_1)\,, \tag{6.184}$$

$$\mathcal{M}_{\gamma Z^0,4} = (-1)\frac{ig^2}{c_W^2}\left(-\frac{\mathcal{C}_e}{s} + \frac{B_e\mathcal{O}'^R_{ij}}{D_Z}\right)(\bar{x}_j\overline{\sigma}_\mu y_i)(\bar{y}_1\overline{\sigma}^\mu x_2)\,, \tag{6.185}$$

where $A_e \equiv -\frac{1}{2} + s_W^2$, $B_e \equiv Q_e s_W^2$ and $\mathcal{C}_e \equiv -Q_e e^2 c_W^2/g^2$. The t-channel amplitude is given by

$$\mathcal{M}_{\widetilde{\nu}} = (+1)\frac{-ig^2 V_{i1} V_{j1}^*}{t - m_{\widetilde{\nu}}^2}(y_j x_1)(\bar{x}_i \bar{y}_2) \tag{6.186}$$

Squaring the individual amplitudes and summing over initial and final state spins we obtain

$$|\mathcal{M}_{\gamma Z^0,1}|^2 = \frac{2g^4}{c_W^2}\left|\frac{\mathcal{C}_e}{s} + \frac{A_e \mathcal{O}'^L_{ij}}{D_Z}\right|^2 \left[(M^2_{\widetilde{C}_i} - t)(M^2_{\widetilde{C}_j} - t) + (s + t - M^2_{\widetilde{C}_i})(s + t - M^2_{\widetilde{C}_j})\right], \tag{6.187}$$

$$|\mathcal{M}_{\gamma Z^0,2}|^2 = \frac{2g^4}{c_W^2}\left|\frac{\mathcal{C}_e}{s} - \frac{B_e \mathcal{O}'^L_{ij}}{D_Z}\right|^2 \left[(M^2_{\widetilde{C}_i} - t)(M^2_{\widetilde{C}_j} - t) + (s + t - M^2_{\widetilde{C}_i})(s + t - M^2_{\widetilde{C}_j})\right], \tag{6.188}$$

$$|\mathcal{M}_{\gamma Z^0,3}|^2 = \frac{2g^4}{c_W^2}\left|\frac{\mathcal{C}_e}{s} + \frac{A_e \mathcal{O}'^R_{ij}}{D_Z}\right|^2 \left[(M^2_{\widetilde{C}_i} - t)(M^2_{\widetilde{C}_j} - t) + (s + t - M^2_{\widetilde{C}_i})(s + t - M^2_{\widetilde{C}_j})\right], \tag{6.189}$$

$$|\mathcal{M}_{\gamma Z^0,4}|^2 = \frac{2g^4}{c_W^2}\left|\frac{\mathcal{C}_e}{s} - \frac{B_e \mathcal{O}'^R_{ij}}{D_Z}\right|^2 \left[(M^2_{\widetilde{C}_i} - t)(M^2_{\widetilde{C}_j} - t) + (s + t - M^2_{\widetilde{C}_i})(s + t - M^2_{\widetilde{C}_j})\right], \tag{6.190}$$

$$|\mathcal{M}_{\widetilde{\nu}}|^2 = \frac{g^4 |V_{i1} V_{j1}|^2}{(t - m_{\widetilde{\nu}}^2)^2}(M^2_{\widetilde{C}_i} - t)(M^2_{\widetilde{C}_j} - t)\,. \tag{6.191}$$

Next we must consider the interference terms. Since we neglect the electron mass only the amplitude pairings $(13)(1\widetilde{\nu})(24)$ and $(3\widetilde{\nu})$ contribute

$$2\Re\left(\mathcal{M}_{\gamma Z^0,1}\mathcal{M}^\dagger_{\gamma Z^0,3}\right) = \frac{8g^4}{c_W^4}\Re\left[\left(\frac{\mathcal{C}_e}{s} + \frac{A_e \mathcal{O}'^L_{ij}}{D_Z}\right)\left(\frac{\mathcal{C}_e}{s} + \frac{A_e \mathcal{O}'^{R*}_{ij}}{D_Z^*}\right)\right] M_{\widetilde{C}_i} M_{\widetilde{C}_j}\, s\,, \tag{6.192}$$

$$2\Re\left(\mathcal{M}_{\gamma Z^0,1}\mathcal{M}^\dagger_{\widetilde{\nu}}\right) = \frac{4g^4}{c_W^2(t - m_{\widetilde{\nu}}^2)}\Re\left[V_{i1}^* V_{j1}\left(\frac{\mathcal{C}_e}{s} + \frac{A_e \mathcal{O}'^L_{ij}}{D_Z}\right)\right](M^2_{\widetilde{C}_i} - t)(M^2_{\widetilde{C}_j} - t)\,, \tag{6.193}$$

$$2\Re\left(\mathcal{M}_{\gamma Z^0,2}\mathcal{M}^\dagger_{\gamma Z^0,4}\right) = \frac{8g^4}{c_W^4}\Re\left[\left(\frac{\mathcal{C}_e}{s} - \frac{B_e \mathcal{O}'^L_{ij}}{D_Z}\right)\left(\frac{\mathcal{C}_e}{s} - \frac{B_e \mathcal{O}'^{R*}_{ij}}{D_Z^*}\right)\right] M_{\widetilde{C}_i} M_{\widetilde{C}_j}\, s\,, \tag{6.194}$$

$$2\Re\left(\mathcal{M}_{\gamma Z^0,3}\mathcal{M}^\dagger_{\widetilde{\nu}}\right) = \frac{4g^4}{c_W^2(t - m_{\widetilde{\nu}}^2)}\Re\left[V_{i1}^* V_{j1}\left(\frac{\mathcal{C}_e}{s} + \frac{A_e \mathcal{O}'^R_{ij}}{D_Z}\right)\right] M_{\widetilde{C}_i} M_{\widetilde{C}_j}\, s\,. \tag{6.195}$$

The total cross section can be computed via

$$\sigma = \int_{t_-}^{t_+} \frac{d\sigma}{dt} dt = \frac{1}{16\pi^2 s}\int_{t_-}^{t_+}\left(\frac{1}{4}\sum_{\lambda_1\lambda_2}|\mathcal{M}|^2\right) dt\,. \tag{6.196}$$

where the integration limits are given by

$$t_\pm \equiv M^2_{\widetilde{C}_j} - \frac{s}{2}(1 \mp \beta_j)\,, \quad \text{and} \quad \beta_j \equiv \left(1 - \frac{4M^2_{\widetilde{C}_j}}{s}\right)^{1/2}. \tag{6.197}$$

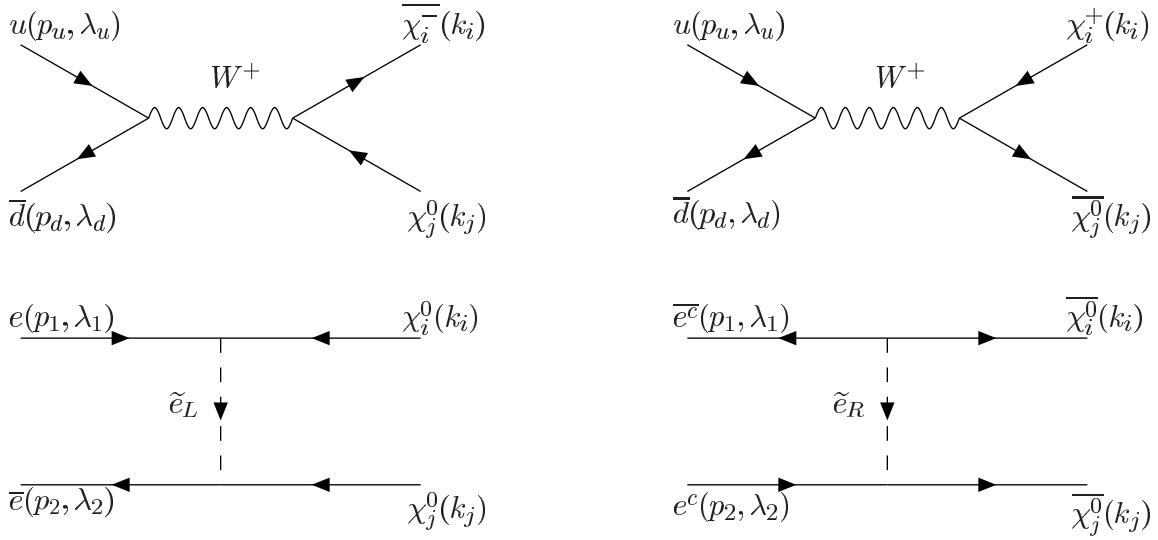

Figure 42: The four tree-level Feynman diagrams for $u\overline{d} \to \widetilde{C}_i^+ \widetilde{N}_j$.

6.17 $f f'^* \to \widetilde{C}_i^+ \widetilde{N}_j$

$$\mathcal{M}_1 = \frac{-ig^2 \mathcal{O}_{ji}^{L*}}{\sqrt{2} D_W} (\bar{y}_d \overline{\sigma}_\mu x_u)(\bar{x}_i \overline{\sigma}^\mu y_j) \tag{6.198}$$

$$\mathcal{M}_2 = \frac{-ig^2 \mathcal{O}_{ji}^{R*}}{\sqrt{2} D_W} (\bar{y}_d \overline{\sigma}_\mu x_u)(\bar{x}_j \overline{\sigma}^\mu y_i) \tag{6.199}$$

$$\mathcal{M}_3 = \frac{-i\sqrt{2} g^2 U_{i1}^* X_{\tilde{N}jd}}{u - m_{\tilde{d}_L}^2} (x_u y_i)(\bar{y}_d \bar{x}_j) \tag{6.200}$$

$$\mathcal{M}_4 = \frac{i\sqrt{2} g^2 V_{i1} X_{\tilde{N}ju}^*}{t - m_{\tilde{u}_L}^2} (\bar{y}_d \bar{x}_i)(x_u y_j) \tag{6.201}$$

where the neutralino couplings are given by

$$X_{\tilde{N}id} \equiv -\tfrac{1}{2} N_{j2} + \frac{s_W}{6 c_W} N_{j1}\,, \qquad X_{\tilde{N}id} \equiv \tfrac{1}{2} N_{j2} + \frac{s_W}{6 c_W} N_{j1}\,. \tag{6.202}$$

Next we compute the individual amplitudes squared.

$$|\mathcal{M}_1|^2 = \frac{g^4 |\mathcal{O}_{ji}^L|^2}{|D_W|^2} \left[(M_{\widetilde{C}_i}^2 - t)(M_{\widetilde{N}_j}^2 - t) + (s + t - M_{\widetilde{C}_i}^2)(s + t - M_{\widetilde{N}_j}^2) \right], \tag{6.203}$$

$$|\mathcal{M}_2|^2 = \frac{g^4 |\mathcal{O}_{ji}^R|^2}{|D_W|^2} \left[(M_{\widetilde{C}_i}^2 - t)(M_{\widetilde{N}_j}^2 - t) + (s + t - M_{\widetilde{C}_i}^2)(s + t - M_{\widetilde{N}_j}^2) \right], \tag{6.204}$$

$$|\mathcal{M}_3|^2 = \frac{2 g^4 |U_{i1} X_{\tilde{N}jd}|^2}{(u - m_{\tilde{d}_L}^2)^2} (s + t - M_{\widetilde{C}_i}^2)(s + t - M_{\widetilde{N}_j}^2) \tag{6.205}$$

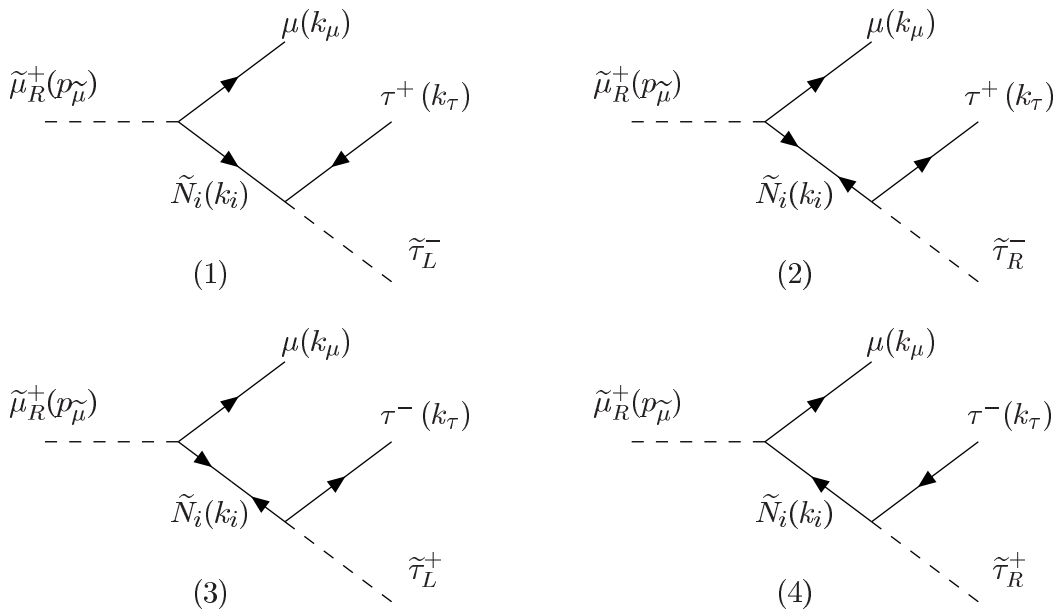

Figure 43: Four Feynman diagrams for the decay $\tilde{\mu}_R^+ \to \mu^+\tau^\pm\tilde{\tau}_1^\mp$ in the MSSM via neutralino exchange. We have shown in each diagram which component of the lightest stau couples.

$$|\mathcal{M}_4|^2 = \frac{2g^4|V_{i1}X_{\tilde{N}ju}|^2}{(t-m_{\tilde{u}_L}^2)^2}(M_{\widetilde{C}_i}^2 - t)(M_{\widetilde{N}_j}^2 - t) \tag{6.206}$$

Finally we compute the interference terms

6.18 $\tilde{\mu}_R^+ \to \mu^+\tau^\pm\tilde{\tau}_1^\mp$

The lightest stau mass eigenstate, $\tilde{\tau}_1^\pm$, is a mixture of the weak eigenstates $\tilde{\tau}_L^\pm$ and $\tilde{\tau}_R^\pm$. We denote the mixing angle by $\theta_{\tilde{\tau}}$

$$\tilde{\tau}_1^\pm = \cos\theta_{\tilde{\tau}}\,\tilde{\tau}_L^\pm + \sin\theta_{\tilde{\tau}}\,\tau_R^\pm \tag{6.207}$$

In gauge mediated supersymmetry breaking models the decay of the right-handed smuon to the lightest stau, is of interest because [...]. We shall employ the Mandelstam variables

$$s = (p_{\tilde{\mu}} - k_{\tilde{\tau}})^2 = (k_\mu + k_{\tau^\pm})^2 \tag{6.208}$$

$$t = (p_{\tilde{\mu}} - k_\mu)^2 = (k_{\tilde{\tau}} + k_{\tau^\pm})^2 \tag{6.209}$$

$$u = (p_{\tilde{\mu}} - k_{\tau^\pm})^2 = (k_\mu + k_{\tilde{\tau}})^2 \tag{6.210}$$

Neglecting the final state muon and tau masses we then obtain

$$p_{\tilde{\mu}}\cdot k_{\tilde{\tau}} = \tfrac{1}{2}(M_{\tilde{\mu}}^2 + M_{\tilde{\tau}}^2 - s)\,, \qquad k_\mu\cdot k_{\tau^\pm} = \tfrac{1}{2}s\,, \tag{6.211}$$

$$p_{\widetilde{\mu}}\cdot k_\mu \;=\; \tfrac{1}{2}(M^2_{\widetilde{\mu}}-t)\,, \qquad\qquad k_{\tau\pm}\cdot k_{\widetilde{\tau}} \;=\; \tfrac{1}{2}(M^2_{\widetilde{\tau}}-t)\,, \tag{6.212}$$

$$p_{\widetilde{\mu}}\cdot k_{\tau\pm} \;=\; \tfrac{1}{2}(M^2_{\widetilde{\mu}}-u)\,, \qquad\qquad k_{\mu}\cdot k_{\widetilde{\tau}} \;=\; \tfrac{1}{2}(M^2_{\widetilde{\tau}}-u)\,, \tag{6.213}$$

$$\tag{6.214}$$

The four amplitudes are given by

$$\mathcal{M}_1 = \frac{-i2g^2 s_W Q_\mu A_f^* N_{i1}}{c_W(t-M^2_{\widetilde{N}_i})}\,(\bar{x}_\mu k_i\cdot\overline{\sigma} y_{\tau^+})\,, \tag{6.215}$$

$$\mathcal{M}_2 = \frac{-i2g^2 s_W^2 Q_\mu Q_\tau N_{i1}^2 M_{\widetilde{N}_i}}{c_W^2(t-M^2_{\widetilde{N}_i})}\,(\bar{x}_\mu \bar{x}_{\tau^+})\,, \tag{6.216}$$

$$\mathcal{M}_3 = \frac{i2g^2 s_W Q_\mu A_f N_{i1} M_{\widetilde{N}_i}}{c_W(t-M^2_{\widetilde{N}_i})}\,(\bar{x}_\mu \bar{x}_{\tau^-})\,, \tag{6.217}$$

$$\mathcal{M}_4 = \frac{i2g^2 s_W^2 Q_\mu Q_\tau |N_{i1}|^2}{c_W^2(t-M^2_{\widetilde{N}_i})}\,(\bar{x}_\mu k_i\cdot\overline{\sigma} y_{\tau^-})\,. \tag{6.218}$$

$A_{fi} = T_3^f N_{i2} + \frac{s_W}{c_W}(Q_f - T_3^f)N_{i1}$, $k_i = p(\widetilde{\mu}_R^+) - k_\mu$

The interference between the amplitudes $\mathcal{M}_{1,2}$ is proportional to m_τ, which we neglect; similarly for the amplitudes $\mathcal{M}_{3,4}$. There is no interference between the first two diagrams and the last two since they involve different final states, $\tau^\pm$. The total amplitude squared is thus given in this approximation as

$$|\mathcal{M}_{\rm tot}|^2 = |\mathcal{M}_1|^2 + |\mathcal{M}_2|^2 + |\mathcal{M}_3|^2 + |\mathcal{M}_4|^2\,, \tag{6.219}$$

note however, that the individual terms contain interference terms from the different neutralinos contributing.

$$|\mathcal{M}_1|^2 = \frac{4g^4 s_W^2 Q_\mu^2}{c_W^2}(ut - M^2_{\widetilde{\mu}}M^2_{\widetilde{\tau}})\sum_{i,j}\frac{A_{fi}^* A_{fj} N_{i1} N_{j1}^*}{(t-M^2_{\widetilde{N}_i})(t-M^2_{\widetilde{N}_j})}\,, \tag{6.220}$$

$$|\mathcal{M}_2|^2 = \frac{4g^4 s_W^4 Q_\mu^2 Q_\tau^2}{c_W^4(k_i^2-M^2_{\widetilde{N}_i})^2}\,s\sum_{i,j}\frac{(N_{i1})^2(N_{j1})^2 M_{\widetilde{N}_i}M_{\widetilde{N}_j}}{(t-M^2_{\widetilde{N}_i})(t-M^2_{\widetilde{N}_j})}\,, \tag{6.221}$$

$$|\mathcal{M}_3|^2 = \frac{4g^4 s_W^2 Q_\mu^2}{c_W^2}\,s\sum_{i,j}\frac{A_{fi}A_{fj}^* N_{i1}N_{j1}^* M_{\widetilde{N}_i}M_{\widetilde{N}_j}}{(t-M^2_{\widetilde{N}_i})(t-M^2_{\widetilde{N}_j})}\,, \tag{6.222}$$

$$|\mathcal{M}_4|^2 = \frac{4g^4 s_W^4 Q_\mu^2 Q_\tau^2}{c_W^4(t-M^2_{\widetilde{N}_i})^2}(ut - M^2_{\widetilde{\mu}}M^2_{\widetilde{\tau}})\sum_{i,j}\frac{|N_{i1}N_{j1}|^2}{(t-M^2_{\widetilde{N}_i})(t-M^2_{\widetilde{N}_j})}\,. \tag{6.223}$$

In order to get differential decay rates and the total decay rate must integrate over the phase space of the final state particles.

In four-component notation this has some tricky minus signs because of the virtual neutralino. (Compare with answer given in paper with Sandro and Graham.)

6.19 $\widetilde{\gamma} \to \gamma \widetilde{G}$ (done)

The Goldstino $\widetilde{G}$ is a Weyl fermion which couples to the photino $\widetilde{\gamma}$ and photon field A^μ according to the Lagrangian:

$$\mathcal{L} = -\frac{1}{2\sqrt{2}\langle F\rangle}\partial_\mu \widetilde{G}\sigma^\nu\overline{\sigma}^\rho\sigma^\mu\widetilde{\gamma}\left[\partial_\nu A_\rho - \partial_\rho A_\nu\right] + \text{c.c.} \tag{6.224}$$

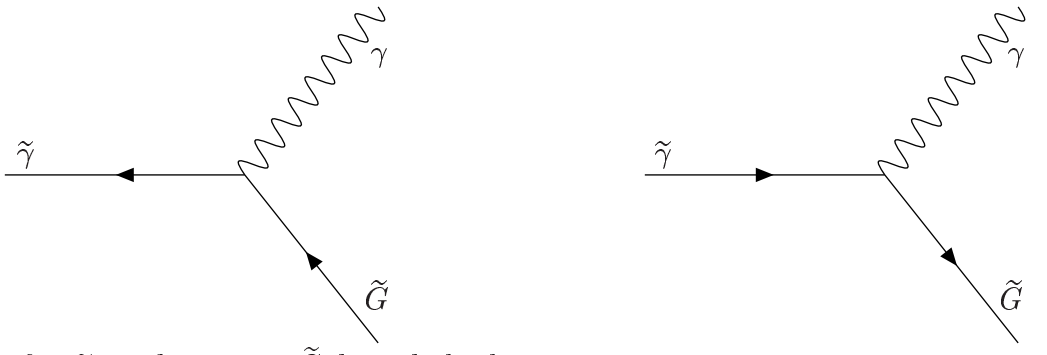

Therefore $\widetilde{\gamma}$ can decay to γ+$\widetilde{G}$ through the diagrams:
with amplitudes:

$$\mathcal{M}_1 = \frac{i}{2\sqrt{2}\langle F\rangle}\, y(\widetilde{G})\left[k_\gamma\cdot\sigma\epsilon\cdot\overline{\sigma} - \epsilon\cdot\sigma k_\gamma\cdot\overline{\sigma}\right] k_{\widetilde{G}}\cdot\sigma y^\dagger(\widetilde{\gamma})\,, \tag{6.225}$$

$$\mathcal{M}_2 = -\frac{i}{2\sqrt{2}\langle F\rangle}\, x^\dagger(\widetilde{G})\left[k_\gamma\cdot\overline{\sigma}\epsilon\cdot\sigma - \epsilon\cdot\overline{\sigma}k_\gamma\cdot\sigma\right] k_{\widetilde{G}}\cdot\overline{\sigma}x(\widetilde{\gamma})\,. \tag{6.226}$$

Using the on-shell condition $k_\gamma\cdot\epsilon = 0$, we have $-\epsilon\cdot\sigma k_\gamma\cdot\overline{\sigma} = k_\gamma\cdot\sigma\epsilon\cdot\overline{\sigma}$ and $-\epsilon\cdot\overline{\sigma}k_\gamma\cdot\sigma = k_\gamma\cdot\overline{\sigma}\epsilon\cdot\sigma$ from eqs. (A.1) and (A.2). So we can rewrite the total amplitude as

$$\mathcal{M} = \mathcal{M}_1 + \mathcal{M}_2 = i\left[y(\widetilde{G})Ay^\dagger(\widetilde{\gamma}) - x^\dagger(\widetilde{G})Bx(\widetilde{\gamma})\right], \tag{6.227}$$

where

$$A = \frac{1}{\sqrt{2}\langle F\rangle}k_\gamma\cdot\sigma\epsilon\cdot\overline{\sigma}k_{\widetilde{G}}\cdot\sigma; \tag{6.228}$$

$$B = \frac{1}{\sqrt{2}\langle F\rangle}k_\gamma\cdot\overline{\sigma}\epsilon\cdot\sigma k_{\widetilde{G}}\cdot\overline{\sigma}\,. \tag{6.229}$$

The squared matrix element is therefore (taking $\langle F\rangle$ to be real):

$$\begin{aligned}|\mathcal{M}|^2 = {}& y(\widetilde{G})Ay^\dagger(\widetilde{\gamma})y(\widetilde{\gamma})\overleftarrow{A}y^\dagger(\widetilde{G}) + x^\dagger(\widetilde{G})Bx(\widetilde{\gamma})x^\dagger(\widetilde{\gamma})\overleftarrow{B}x(\widetilde{G}) \\ & -y(\widetilde{G})Ay^\dagger(\widetilde{\gamma})x^\dagger(\widetilde{\gamma})\overleftarrow{B}x(\widetilde{G}) - x^\dagger(\widetilde{G})Bx(\widetilde{\gamma})y(\widetilde{\gamma})\overleftarrow{A}y^\dagger(\widetilde{G})\,.\end{aligned} \tag{6.230}$$

Summing over Goldstino spins and averaging over photino spins gives:

$$\frac{1}{2}\sum_{s_{\widetilde{G}},s_{\widetilde{\gamma}}}|\mathcal{M}|^2 = \frac{1}{2}\mathrm{Tr}(Ap_{\widetilde{\gamma}}\cdot\overline{\sigma}\overleftarrow{A}k_{\widetilde{G}}\cdot\overline{\sigma}) + \frac{1}{2}\mathrm{Tr}(Bp_{\widetilde{\gamma}}\cdot\sigma\overleftarrow{B}k_{\widetilde{G}}\cdot\sigma)\,. \tag{6.231}$$

(The A, B cross terms die because of $m_{\widetilde{G}} = 0$.) Therefore:

$$\frac{1}{2}\sum_{s_{\widetilde{G}},s_{\widetilde{\gamma}}} |\mathcal{M}|^2 = \frac{1}{4\langle F\rangle^2}\mathrm{Tr}(k_\gamma\cdot\sigma\epsilon\cdot\overline{\sigma}k_{\widetilde{G}}\cdot\sigma p_{\widetilde{\gamma}}\cdot\overline{\sigma}k_{\widetilde{G}}\cdot\sigma\epsilon^*\cdot\overline{\sigma}k_\gamma\cdot\sigma p_{\widetilde{G}}\cdot\overline{\sigma}) + (\sigma\leftrightarrow\overline{\sigma})\,. \tag{6.232}$$

Now use

$$k_{\widetilde{G}}\cdot\sigma p_{\widetilde{\gamma}}\cdot\overline{\sigma}k_{\widetilde{G}}\cdot\sigma = -2k_{\widetilde{G}}\cdot p_{\widetilde{\gamma}}k_{\widetilde{G}}\cdot\sigma \tag{6.233}$$

$$k_\gamma\cdot\sigma k_{\widetilde{G}}\cdot\overline{\sigma}k_\gamma\cdot\sigma = -2k_\gamma\cdot k_{\widetilde{G}}k_\gamma\cdot\sigma \tag{6.234}$$

and the corresponding identities with $\sigma\leftrightarrow\overline{\sigma}$ to rewrite this as:

$$\frac{1}{2}\sum_{s_{\widetilde{G}},s_{\widetilde{\gamma}}} |\mathcal{M}|^2 = \frac{1}{\langle F\rangle^2}(k_\gamma\cdot k_{\widetilde{G}})(p_{\widetilde{\gamma}}\cdot k_{\widetilde{G}})\mathrm{Tr}(\epsilon\cdot\overline{\sigma}k_\gamma\cdot\sigma\epsilon^*\cdot\overline{\sigma}k_{\widetilde{G}}\cdot\sigma) + (\sigma\leftrightarrow\overline{\sigma})\,. \tag{6.235}$$

Now, using the photon spin sum identity

$$\sum_{\gamma\,\mathrm{spin}} \epsilon^\mu\epsilon^{\nu *} = g^{\mu\nu} \tag{6.236}$$

we get

$$\frac{1}{2}\sum_{\mathrm{spins}} |\mathcal{M}|^2 = -\frac{8}{\langle F\rangle^2}(k_\gamma\cdot k_{\widetilde{G}})^2 k_{\widetilde{G}}\cdot p_{\widetilde{\gamma}} = \frac{m_{\widetilde{\gamma}}^6}{\langle F\rangle^2} \tag{6.237}$$

So,

$$\Gamma(\widetilde{\gamma}\to\gamma\widetilde{G}) = \frac{1}{16\pi m_{\widetilde{\gamma}}}\left(\frac{1}{2}\sum_{\mathrm{spins}}|\mathcal{M}|^2\right) = \frac{m_{\widetilde{\gamma}}^5}{16\pi\langle F\rangle^2} \tag{6.238}$$

Can also redo this in GMSB directly using loop amplitudes!

6.20 SUSY QCD Feynman Rules

In two component formalism the gluon-quark-quark Lagrangian is given by [2]

$$\mathcal{L} = -g_s T^a_{jk}\left(\bar{q}^j\overline{\sigma}_\mu q^k - \overline{q^{ck}}\overline{\sigma}_\mu q^{cj}\right)A^\mu_a\,. \tag{6.239}$$

In two component formalism the gluon-gluino-gluino Lagrangian is given by [2]

$$\mathcal{L} = ig_s f_{abc}\,(\bar{\widetilde{g}}^a\,\overline{\sigma}^\mu\,\widetilde{g}^b)A^c_\mu\,, \tag{6.240}$$

where g_s is the strong coupling constant, a, b, c are $SU(3)$ colour indices and f_{abc} are the $SU(3)$ structure constants. We have denoted the (2-component) gluino field by $\widetilde{g}^a$ as in Table 1 and the gluon field by A^a_μ. The gluino-squark-quark Lagrangian for each squark flavour f is given by

$$\mathcal{L} = -\sqrt{2}g_s T^a_{jk}\sum_f\left[(\widetilde{g}_a q^k_f)\widetilde{q}^{j*}_{fL} + (\bar{q}^j_f\bar{\widetilde{g}}_a)\widetilde{q}^k_{fL} - (\bar{\widetilde{g}}_a\overline{(q^c)}^k_f)\widetilde{q}^{j*}_{fR} - (q^c)^j_f\widetilde{g}_a\widetilde{q}^k_{fR}\right] \tag{6.241}$$

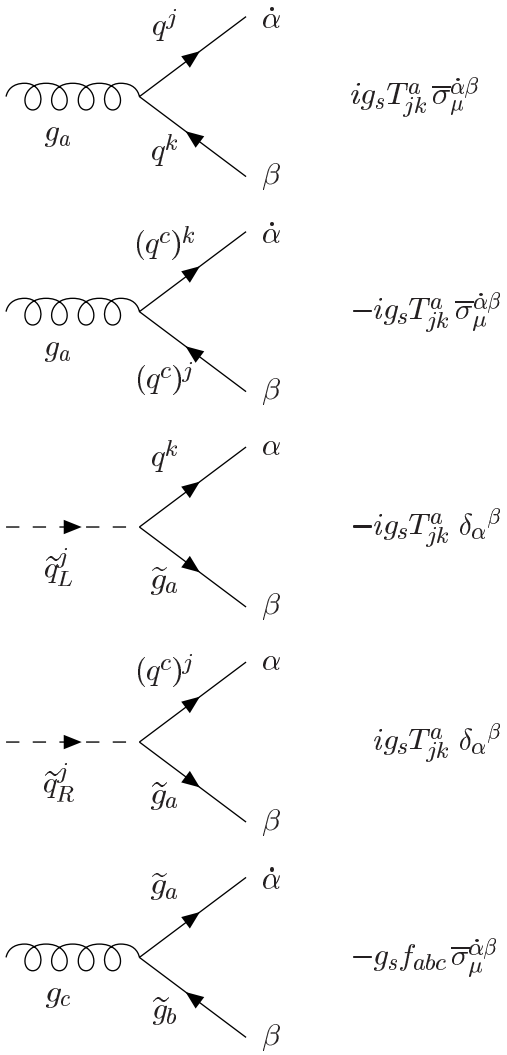

Figure 44: Fermionic Feynman rules for SUSY QCD

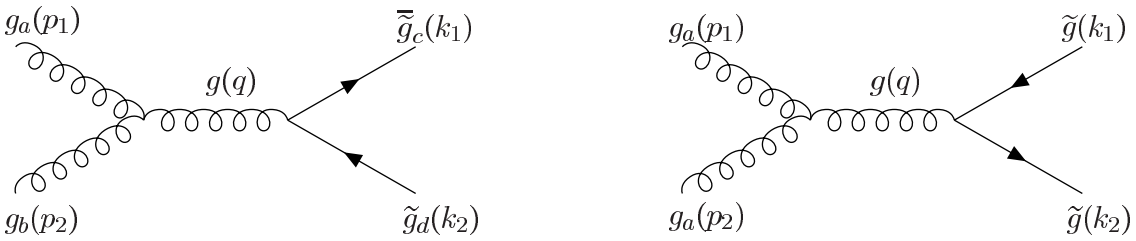

Figure 45: The four tree-level Feynman diagrams for $gg \to \widetilde{g}\widetilde{g}$ via s-channel gluon exchange.

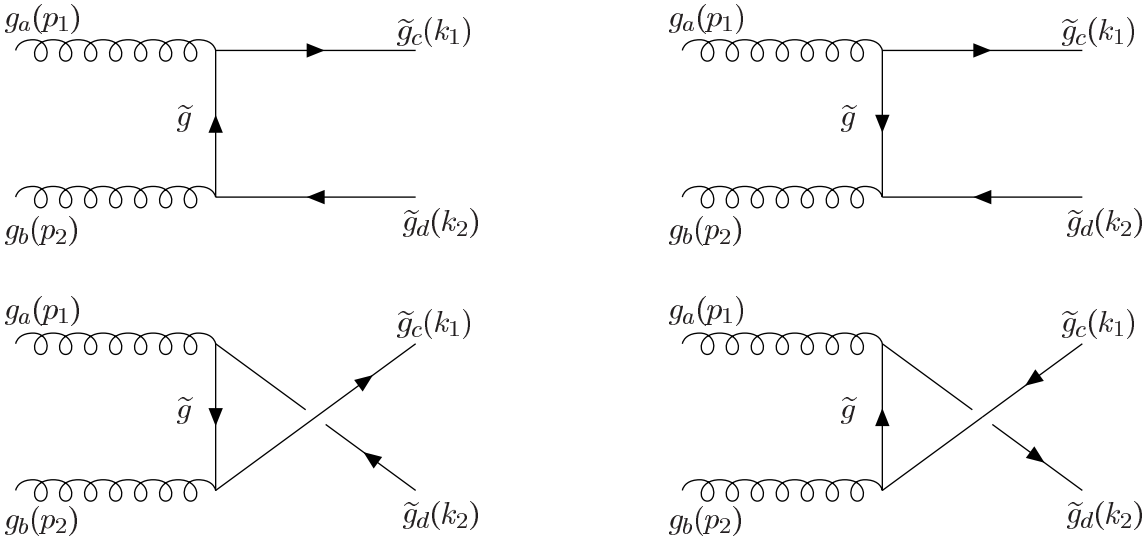

Figure 46: Four Feynman diagrams for $gg \to \widetilde{g}\widetilde{g}$ via t-channel gluino exchange.

6.21 $gg \to \widetilde{g}\widetilde{g}$

Using the Feynman rules of the previous section we can now compute the process $gg \to \widetilde{g}\widetilde{g}$. The Feynman diagrams are shown in Figs. 45,46, and 47. In writing down the amplitudes we shall associate with the final state gluinos $\widetilde{g}^c(k_1)$, $\widetilde{g}^d(k_2)$, by the spinors x_1^c, y_1^c and x_2^d, y_2^d, respectively. We have included the colour indices. With the initial state gluons $g_a(p_1)$, $g_b(p_2)$ we associate the polarisation vectors ϵ_1 and ϵ_2, respectively. Numbering the amplitudes in the order of the displayed Feynman diagrams we obtain

$$\mathcal{M}_1 = \frac{-ig_s^2 f_{cdx} f_{abx}}{s}(\bar{x}_1^c \overline{\sigma}^\mu y_2^d)\left[(p_1-p_2)_\mu \epsilon_1\cdot\epsilon_2 + (p_2+q)\cdot\epsilon_1\,\epsilon_{2\mu} - (q+p_1)\cdot\epsilon_2\,\epsilon_{1\mu}\right], \quad (6.242)$$

$$\mathcal{M}_2 = \frac{ig_s^2 f_{dcx} f_{abx}}{s}(\bar{x}_2^d \overline{\sigma}^\mu y_1^c)\left[(p_1-p_2)_\mu \epsilon_1\cdot\epsilon_2 + (p_2+q)\cdot\epsilon_1\,\epsilon_{2\mu} - (q+p_1)\cdot\epsilon_2\,\epsilon_{1\mu}\right], \quad (6.243)$$

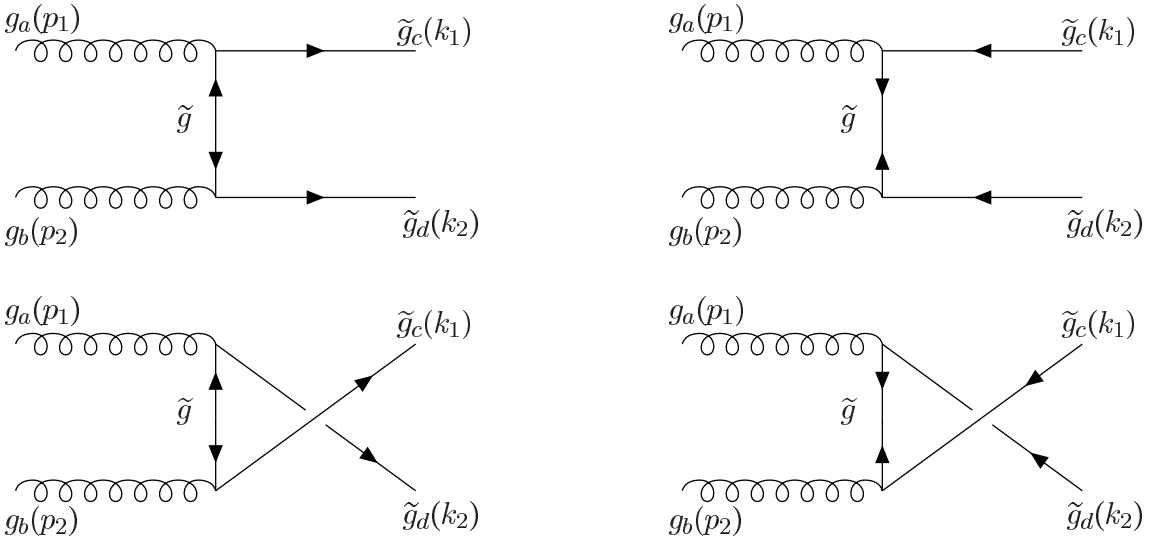

Figure 47: Four Feynman diagrams for $gg \to \widetilde{g}\widetilde{g}$ via t-channel gluino exchange and where the arrowson the gluino propagator clash.

$$\mathcal{M}_3 = \frac{ig_s^2 f_{cxa} f_{xdb}}{t - m_{\widetilde{g}}^2}[\bar{x}_1^c \overline{\sigma}^\mu (k_1 - p_1)\cdot\sigma\, \overline{\sigma}^\nu y_2^d]\epsilon_{1\mu}\epsilon_{2\nu}\,, \tag{6.244}$$

$$\mathcal{M}_4 = \frac{-ig_s^2 f_{xca} f_{dxb}}{t - m_{\widetilde{g}}^2}[\bar{x}_2^d \overline{\sigma}^\mu (k_2 - p_2)\cdot\sigma\, \overline{\sigma}^\nu y_1^c]\epsilon_{1\mu}\epsilon_{2\nu}\,, \tag{6.245}$$

$$\mathcal{M}_5 = \frac{ig_s^2 f_{cxb} f_{xda}}{u - m_{\widetilde{g}}^2}[\bar{x}_1^c \overline{\sigma}^\mu (k_1 - p_2)\cdot\sigma\, \overline{\sigma}^\nu y_2^d]\epsilon_{1\nu}\epsilon_{2\mu}\,, \tag{6.246}$$

$$\mathcal{M}_6 = \frac{-ig_s^2 f_{dxa} f_{xcb}}{u - m_{\widetilde{g}}^2}[\bar{x}_2^d \overline{\sigma}^\mu (k_2 - p_1)\cdot\sigma\, \overline{\sigma}^\nu y_1^c]\epsilon_{1\mu}\epsilon_{2\nu}\,, \tag{6.247}$$

$$\mathcal{M}_7 = \frac{ig_s^2 f_{cxa} f_{dxb} m_{\widetilde{g}}}{t - m_{\widetilde{g}}^2}[\bar{x}_1^c \overline{\sigma}^\mu \sigma^\nu \bar{x}_2^d]\epsilon_{1\mu}\epsilon_{2\nu}\,, \tag{6.248}$$

$$\mathcal{M}_8 = \frac{ig_s^2 f_{xca} f_{xdb} m_{\widetilde{g}}}{t - m_{\widetilde{g}}^2}[y_1^c \sigma^\mu \overline{\sigma}^\nu y_2^d]\epsilon_{1\mu}\epsilon_{2\nu}\,, \tag{6.249}$$

$$\mathcal{M}_9 = \frac{-ig_s^2 f_{dxa} f_{cxb} m_{\widetilde{g}}}{u - m_{\widetilde{g}}^2}[\bar{x}_2^d \overline{\sigma}^\mu \sigma^\nu \bar{x}_1^c]\epsilon_{1\mu}\epsilon_{2\nu}\,, \tag{6.250}$$

$$\mathcal{M}_{10} = \frac{-ig_s^2 f_{xda} f_{xcb} m_{\widetilde{g}}}{u - m_{\widetilde{g}}^2}[y_2^d \sigma^\mu \overline{\sigma}^\nu y_1^c]\epsilon_{1\mu}\epsilon_{2\nu}\,. \tag{6.251}$$

x is an intermediate colour index. Mandelstam variables are given by

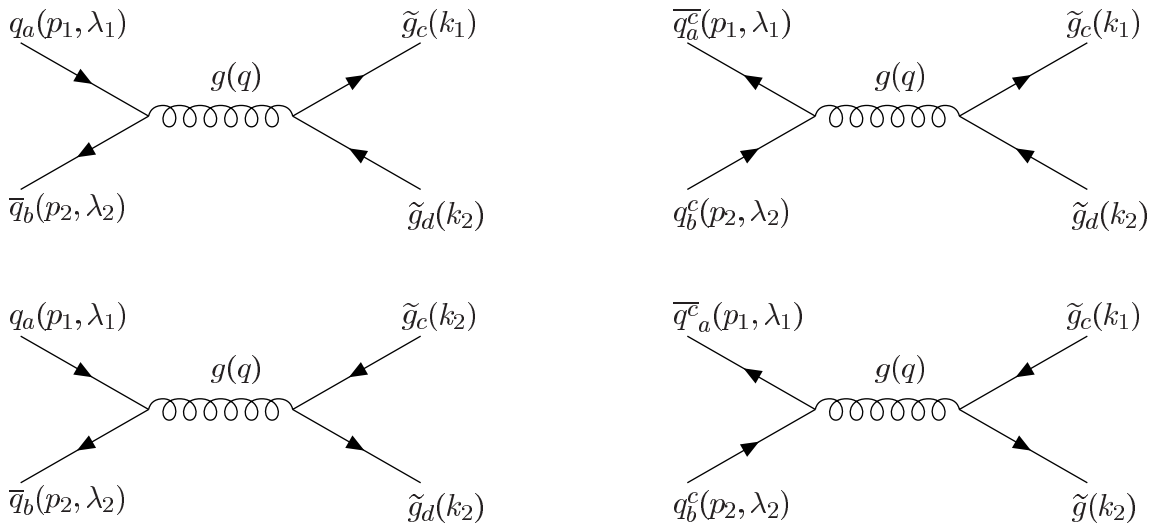

Figure 48: Four Feynman diagrams for $q\bar{q} \to \widetilde{g}\widetilde{g}$ via s-channel gluon exchange.

These amplitudes can also be combined as

$$\mathcal{M}_1 + \mathcal{M}_2 = \frac{-ig_s^2 f_{cdx} f_{abx}}{s} \epsilon_{1\mu}\epsilon_{2\nu} \left[\bar{x}_1^c \overline{\sigma}_\tau y_2^d + \bar{x}_2^d \overline{\sigma}_\tau y_1^c\right] \\ [(p_1 - p_2)^\tau g^{\mu\nu} + (p_2 + q)^\mu g^{\nu\tau} - (p_1 + q)^\nu g^{\mu\tau}] \,, \tag{6.252}$$

$$\mathcal{M}_3 + \mathcal{M}_4 + \mathcal{M}_7 + \mathcal{M}_8 = \frac{ig_s^2 f_{cxa} f_{xdb}}{t - m_{\widetilde{g}}^2} \epsilon_{1\mu}\epsilon_{2\nu} \left[\bar{x}_1^c \overline{\sigma}^\mu (k_1 - p_1)\cdot\sigma\, \overline{\sigma}^\nu y_2^d \right. \\ \left. - \bar{x}_2^d \overline{\sigma}^\mu (k_2 - p_2)\cdot\sigma\, \overline{\sigma}^\nu y_1^c - m_{\widetilde{g}} \bar{x}_1^c \overline{\sigma}^\mu \sigma^\nu \bar{x}_2^d - m_{\widetilde{g}} y_1^c \sigma^\mu \overline{\sigma}^\nu y_2^d\right] \,, \tag{6.253}$$

$$\mathcal{M}_5 + \mathcal{M}_6 + \mathcal{M}_9 + \mathcal{M}_{10} = \frac{ig_s^2 f_{cxb} f_{xda}}{u - m_{\widetilde{g}}^2} \epsilon_{1\mu}\epsilon_{2\nu} \left[\bar{x}_1^c \overline{\sigma}^\nu (k_1 - p_2)\cdot\sigma\, \overline{\sigma}^\mu y_2^d \right. \\ \left. - \bar{x}_2^d \overline{\sigma}^\mu (k_2 - p_1)\cdot\sigma\, \overline{\sigma}^\nu y_1^c + m_{\widetilde{g}} \bar{x}_2^d \overline{\sigma}^\mu \sigma^\nu \bar{x}_1^c + m_{\widetilde{g}} y_2^d \sigma^\mu \overline{\sigma}^\nu y_1^c\right] . \tag{6.254}$$

45 interference terms. Shall we do that?? I find this puts some doubt on our formalism, no? This calculation is much easier with 4-component fermions.

6.22 $q\overline{q} \to \widetilde{g}\widetilde{g}$

This computation is very similar to $f\overline{f} \to \widetilde{N}_i \widetilde{N}_j$

6.23 $\widetilde{N}_i \widetilde{N}_j \to f\overline{f}$

Do this as a dark matter problem, perhaps in the slow approximation.

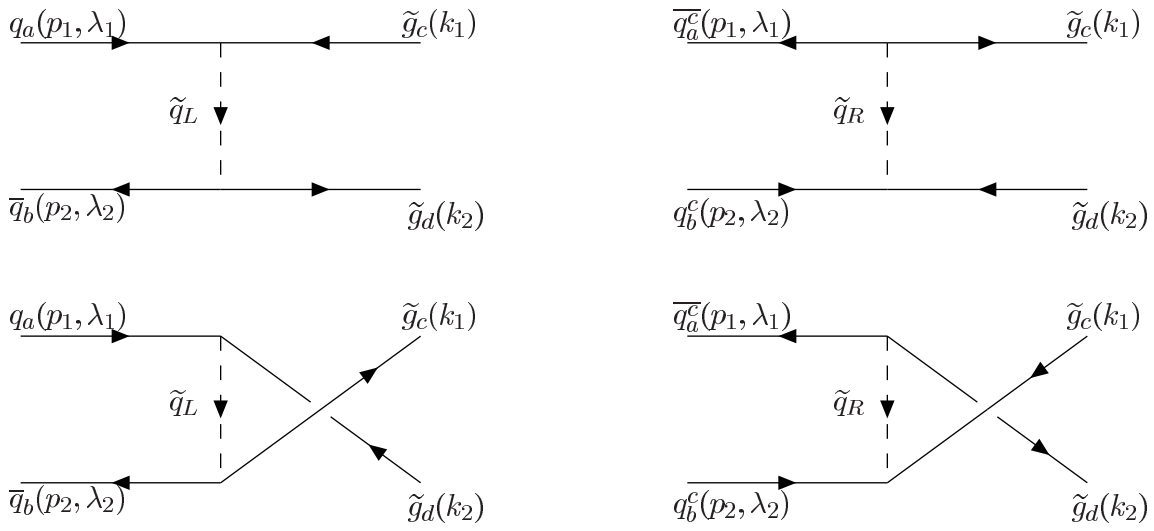

Figure 49: Four Feynman diagrams for $q\bar{q} \to \widetilde{g}\widetilde{g}$ via t-channel squark exchange.

6.24 Gauge boson wave function renormalization due to chiral fermion loops

6.25 Chiral fermion wave function renormalization due to gauge boson loops

6.26 Triangle anomaly from chiral fermion loops

6.27 Pole mass of the top quark.

6.28 Pole mass of the gluino.

6.29 Nambu-Jona-Lasinio model gap equation (e.g. top-quark condensation from 4-fermion interaction)

6.30 Neutrino mixing (??)

6.31 Polarized Muon Decay

6.32 R-parity violating decay $\widetilde{N}_i \to \mu^- ud$

Appendix A: Two-component spinor notation and identities

In this Appendix, we list various identities involving the σ and $\overline{\sigma}$ matrices. When considering a theory regularized by dimensional-continuation, one must be careful in treating cases with contracted spacetime vector indices $\mu, \nu, \rho, \ldots$. Instead of taking on 4 possible values, these vector indices formally run over d values, where d is infinitesimally larger than 4 in dimensional regularization, and infinitesimally less than 4 in dimensional reduction. This means that some identities that would hold in unregularized 4-dimensional theories are inconsistent and must not be used; other identities remain valid if d replaces 4 in the appropriate spots; and still other identities hold without modification.

Two important identities that do hold in $d \neq 4$ dimensions are:

$$[\sigma^\mu \overline{\sigma}^\nu + \sigma^\nu \overline{\sigma}^\mu]_\alpha{}^\beta = 2g^{\mu\nu}\delta_\alpha^\beta\,, \tag{A.1}$$

$$[\overline{\sigma}^\mu \sigma^\nu + \overline{\sigma}^\nu \sigma^\mu]^{\dot\alpha}{}_{\dot\beta} = 2g^{\mu\nu}\delta_{\dot\beta}^{\dot\alpha}\,. \tag{A.2}$$

The trace identities:

$$\mathrm{Tr}[\sigma^\mu \overline{\sigma}^\nu] = \mathrm{Tr}[\overline{\sigma}^\mu \sigma^\nu] = 2g^{\mu\nu} \tag{A.3}$$

then follow.

In contrast, the Fierz identity (written here in three equivalent forms):

$$\sigma^\mu_{\alpha\dot\alpha}\overline{\sigma}_\mu^{\dot\beta\beta} = 2\delta_\alpha{}^\beta \delta^{\dot\beta}{}_{\dot\alpha} \tag{A.4}$$

$$\sigma^\mu_{\alpha\dot\alpha}\sigma_{\mu\beta\dot\beta} = 2\epsilon_{\alpha\beta}\epsilon_{\dot\alpha\dot\beta} \tag{A.5}$$

$$\overline{\sigma}^{\mu\dot\alpha\alpha}\overline{\sigma}_\mu^{\dot\beta\beta} = 2\epsilon^{\alpha\beta}\epsilon^{\dot\alpha\dot\beta} \tag{A.6}$$

does not have a consistent, unambiguous meaning outside of 4 dimensions. More discussion here about this problem, and references, would be helpful. However, the following identities that are implied by the Fierz identity do consistently generalize to $d \neq 4$ spacetime dimensions:

$$[\sigma^\mu \overline{\sigma}_\mu]_\alpha{}^\beta = d\delta_\alpha^\beta \tag{A.7}$$

$$[\overline{\sigma}^\mu \sigma_\mu]^{\dot\alpha}{}_{\dot\beta} = d\delta_{\dot\beta}^{\dot\alpha} \tag{A.8}$$

$$[\sigma^\mu \overline{\sigma}^\nu \sigma_\mu]_{\alpha\dot\beta} = (2-d)\sigma^\nu_{\alpha\dot\beta} \tag{A.9}$$

$$[\overline{\sigma}^\mu \sigma_\nu \overline{\sigma}_\mu]^{\dot\alpha\beta} = (2-d)\overline{\sigma}_\nu^{\dot\alpha\beta} \tag{A.10}$$

$$[\sigma^\mu \overline{\sigma}^\nu \sigma^\rho \overline{\sigma}_\mu]_\alpha{}^\beta = 4g^{\nu\rho}\delta_\alpha^\beta - (4-d)[\sigma^\nu \overline{\sigma}^\rho]_\alpha{}^\beta \tag{A.11}$$

$$[\overline{\sigma}^\mu \sigma^\nu \overline{\sigma}^\rho \sigma_\mu]^{\dot\alpha}{}_{\dot\beta} = 4g^{\nu\rho}\delta_{\dot\beta}^{\dot\alpha} - (4-d)[\overline{\sigma}^\nu \sigma^\rho]^{\dot\alpha}{}_{\dot\beta}, \tag{A.12}$$

$$[\sigma^\mu \overline{\sigma}^\nu \sigma^\rho \overline{\sigma}^\kappa \sigma_\mu]_{\alpha\dot\beta} = -2[\sigma^\kappa \overline{\sigma}^\rho \sigma^\nu]_{\alpha\dot\beta} + (4-d)[\sigma^\nu \overline{\sigma}^\rho \sigma^\kappa]_{\alpha\dot\beta} \tag{A.13}$$

$$[\overline{\sigma}^\mu \sigma^\nu \overline{\sigma}^\rho \sigma^\kappa \overline{\sigma}_\mu]^{\dot\alpha\beta} = -2[\overline{\sigma}^\kappa \sigma^\rho \overline{\sigma}^\nu]^{\dot\alpha\beta} + (4-d)[\overline{\sigma}^\nu \sigma^\rho \overline{\sigma}^\kappa]^{\dot\alpha\beta}\,. \tag{A.14}$$

Eq. (A.4) is the basis for other Fierz identities that hold in 4 dimensions, which are given in detail in Appendix A of ref. [6].

Identities that involve the (explicitly and inextricably 4-dimensional) $\epsilon^{\mu\nu\rho\kappa}$ symbol,

$$\overline{\sigma}^\mu\sigma^\nu\overline{\sigma}^\rho = g^{\mu\nu}\overline{\sigma}^\rho - g^{\mu\rho}\overline{\sigma}^\nu + g^{\nu\rho}\overline{\sigma}^\mu - i\epsilon^{\mu\nu\rho\kappa}\overline{\sigma}_\kappa, \tag{A.15}$$

$$\sigma^\mu\overline{\sigma}^\nu\sigma^\rho = g^{\mu\nu}\sigma^\rho - g^{\mu\rho}\sigma^\nu + g^{\nu\rho}\sigma^\mu + i\epsilon^{\mu\nu\rho\kappa}\sigma_\kappa \tag{A.16}$$

are also only meaningful in exactly four dimensions. This applies as well to the trace identities which follow from them:[16]

$$\mathrm{Tr}[\sigma^\mu\overline{\sigma}^\nu\sigma^\rho\overline{\sigma}^\kappa] = 2\left(g^{\mu\nu}g^{\rho\kappa} - g^{\mu\rho}g^{\nu\kappa} + g^{\mu\kappa}g^{\nu\rho} + i\epsilon^{\mu\nu\rho\kappa}\right), \tag{A.17}$$

$$\mathrm{Tr}[\overline{\sigma}^\mu\sigma^\nu\overline{\sigma}^\rho\sigma^\kappa] = 2\left(g^{\mu\nu}g^{\rho\kappa} - g^{\mu\rho}g^{\nu\kappa} + g^{\mu\kappa}g^{\nu\rho} - i\epsilon^{\mu\nu\rho\kappa}\right). \tag{A.18}$$

This could lead to ambiguities in loop computations where it is necessary to perform the computation in $d \neq 4$ dimensions (until the end of the calculation where the limit $d \to 4$ is taken). However, in practice one typically finds that the above expressions appear multiplied by the metric and/or other external tensors (such as four-momenta appropriate to the problem at hand). In almost all such cases, two of the indices appearing in eqs. (A.17) and (A.18) are symmetrized which eliminates the $\epsilon^{\mu\nu\rho\kappa}$ term, rendering the resulting expressions unambiguous. Similarly, the sum of the above trace identities can be assigned an unambiguous meaning in $d \neq 4$ dimensions:

$$\mathrm{Tr}[\sigma^\mu\overline{\sigma}^\nu\sigma^\rho\overline{\sigma}^\kappa + \overline{\sigma}^\mu\sigma^\nu\overline{\sigma}^\rho\sigma^\kappa] = 4\left(g^{\mu\nu}g^{\rho\kappa} - g^{\mu\rho}g^{\nu\kappa} + g^{\mu\kappa}g^{\nu\rho}\right). \tag{A.19}$$

By repeatedly applying the identities given in eqs. (A.1)–(A.3) to eqs. (A.17) and (A.18) in 4 dimensions and eq. (A.19) in d dimensions, and using the cyclic property of the trace, one can recursively derive trace formulas for products of 6 or more σ and $\overline{\sigma}$ matrices.

¿From the sigma matrices, one can construct the antisymmetrized products:

$$(\sigma^{\mu\nu})_\alpha{}^\beta \equiv \tfrac{i}{4}(\sigma^\mu_{\alpha\dot\gamma}\overline{\sigma}^{\nu\dot\gamma\beta} - \sigma^\nu_{\alpha\dot\gamma}\overline{\sigma}^{\mu\dot\gamma\beta}), \tag{A.20}$$

$$(\overline{\sigma}^{\mu\nu})^{\dot\alpha}{}_{\dot\beta} \equiv \tfrac{i}{4}(\overline{\sigma}^{\mu\dot\alpha\gamma}\sigma^\nu_{\gamma\dot\beta} - \overline{\sigma}^{\nu\dot\alpha\gamma}\sigma^\mu_{\gamma\dot\beta}). \tag{A.21}$$

The $\sigma^{\mu\nu}$ and $\overline{\sigma}^{\mu\nu}$ are mainly useful because of their role in the Lorentz transformation matrices of eq. (2.6). For the $(\frac{1}{2},0)$ representation, $s^{\mu\nu} = \sigma^{\mu\nu}$, while for the $(0,\frac{1}{2})$ representation,

[16] This is analogous to the statement that Tr $(\gamma^5\gamma^\mu\gamma^\nu\gamma^\rho\gamma^\kappa) = -4i\epsilon^{\mu\nu\rho\kappa}$ [in our convention where $\epsilon^{0123} = +1$] is only meaningful in $d = 4$ dimensions. In two-component notation, the equivalent result is $\mathrm{Tr}[\sigma^\mu\overline{\sigma}^\nu\sigma^\rho\overline{\sigma}^\kappa - \overline{\sigma}^\mu\sigma^\nu\overline{\sigma}^\rho\sigma^\kappa] = 4i\epsilon^{\mu\nu\rho\kappa}$. In the literature various schemes have been proposed for defining the properties of γ^5 in $d \neq 4$ dimensions [5]. In two-component notation, this would translate into a procedure for dealing with general traces involving four or more σ and $\overline{\sigma}$ matrices.

$s^{\mu\nu} = \overline{\sigma}^{\mu\nu}$, where the angles $\vec{\boldsymbol{\theta}}$ and $\vec{\boldsymbol{\zeta}}$ in eq. (2.6) are related to the antisymmetric $\theta_{\mu\nu}$ by: $\theta^i \equiv \frac{1}{2}\epsilon^{ijk}\theta_{jk}$ and $\zeta^i = \theta^{i0} = -\theta^{0i}$.

The matrices $\sigma^{\mu\nu}$ and $\overline{\sigma}^{\mu\nu}$ satisfy self-duality relations in exactly 4 spacetime dimensions:

$$\sigma^{\mu\nu} = -\tfrac{1}{2}i\epsilon^{\mu\nu\rho\kappa}\sigma_{\rho\kappa}\,, \qquad\qquad \overline{\sigma}^{\mu\nu} = \tfrac{1}{2}i\epsilon^{\mu\nu\rho\kappa}\overline{\sigma}_{\rho\kappa}\,. \tag{A.22}$$

Appendix B: Correspondence to four-component spinor notation

It useful to note the correspondence between the two-component notation of Appendix A and the usual four-component Dirac spinor notation. This is most easily exhibited in the basis in which γ_5 is diagonal (this is called the *chiral* representation). In 2×2 blocks, the gamma matrices are given by:

$$\gamma^\mu = \begin{pmatrix} 0 & \sigma^\mu_{\alpha\dot\beta} \\ \overline{\sigma}^{\mu\dot\alpha\beta} & 0 \end{pmatrix}, \qquad\qquad \gamma_5 \equiv i\gamma^0\gamma^1\gamma^2\gamma^3 = \begin{pmatrix} -\delta_\alpha{}^\beta & 0 \\ 0 & \delta^{\dot\alpha}{}_{\dot\beta} \end{pmatrix}. \tag{B.1}$$

In addition, we introduce:[17]

$$\tfrac{1}{2}\Sigma^{\mu\nu} \equiv \frac{i}{4}[\gamma^\mu,\gamma^\nu] = \begin{pmatrix} \sigma^{\mu\nu}{}_\alpha{}^\beta & 0 \\ 0 & \overline{\sigma}^{\mu\nu\dot\alpha}{}_{\dot\beta} \end{pmatrix}. \tag{B.2}$$

A four component Dirac spinor field, $\Psi(x)$, is made up of two mass-degenerate two-component spinor fields, $\chi_\alpha(x)$ and $\eta_\alpha(x)$ as follows:

$$\Psi(x) \equiv \begin{pmatrix} \chi_\alpha(x) \\ \bar\eta^{\dot\alpha}(x) \end{pmatrix}. \tag{B.3}$$

We define chiral projections operators $P_L \equiv \frac{1}{2}(1-\gamma_5)$ and $P_R \equiv \frac{1}{2}(1+\gamma_5)$ so that

$$\Psi_L(x) \equiv P_L\Psi(x) = \begin{pmatrix} \chi_\alpha(x) \\ 0 \end{pmatrix}, \qquad\qquad \Psi_R(x) \equiv P_R\Psi(x) = \begin{pmatrix} 0 \\ \bar\eta^{\dot\alpha}(x) \end{pmatrix}. \tag{B.4}$$

The free fields can be expanded in a Fourier series; each mode is multiplied by a *commuting* spinor wave function as in eq. (3.61). The field $\overline{\Psi}$ and the charge conjugate field are respectively given by

$$\overline{\Psi}(x) \equiv \Psi^\dagger A = (\eta^\alpha(x), \bar\chi_{\dot\alpha})\,, \tag{B.5}$$

$$\Psi^c(x) \equiv C\overline{\Psi}^T(x) = \begin{pmatrix} \eta_\alpha(x) \\ \bar\chi^{\dot\alpha}(x) \end{pmatrix}, \tag{B.6}$$

[17] In most textbooks, $\Sigma^{\mu\nu}$ is called $\sigma^{\mu\nu}$. Here, we use the former symbol so that there is no confusion with the two-component definition of $\sigma^{\mu\nu}$ given in eq. (A.20).

where the Dirac conjugation matrix A and the charge conjugation matrix C satisfy [9]:

$$A\gamma^\mu A^{-1} = \gamma^{\mu\dagger}\,, \qquad\qquad C^{-1}\gamma^\mu C = -\gamma^{\mu T}\,. \tag{B.7}$$

For completeness, we also introduce a matrix B that satisfies [9]:

$$B\gamma^\mu B^{-1} = \gamma^{\mu T}\,. \tag{B.8}$$

The matrix B arises in the study of time reversal invariance of the Dirac equation. In the chiral representation, A, B and C are explicitly given by

$$A = \begin{pmatrix} 0 & \delta^{\dot\alpha}{}_{\dot\beta} \\ \delta_\alpha{}^\beta & 0 \end{pmatrix}, \qquad B = \begin{pmatrix} \epsilon^{\alpha\beta} & 0 \\ 0 & -\epsilon_{\dot\alpha\dot\beta} \end{pmatrix}, \qquad C = -\gamma_5 B^{-1} = \begin{pmatrix} \epsilon_{\alpha\beta} & 0 \\ 0 & \epsilon^{\dot\alpha\dot\beta} \end{pmatrix}. \tag{B.9}$$

Note the numerical equalities, $A = \gamma^0$, $B = \gamma^1\gamma^3$ and $C = i\gamma^0\gamma^2$, although these identifications do not respect the structure of the undotted and dotted indices specified in eq. (B.9). In calculations that involve translations between two-component and four-component notation, the expressions given in eq. (B.9) should be used. In calculations involving only four-component notation, there is no harm in using the numerical values for the matrices noted above.

The external two-component spinor momentum space wave functions are related to the traditional four-component spinors according to:

$$u(\vec{\boldsymbol{p}},s) = \begin{pmatrix} x_\alpha(\vec p,s) \\ \\ \bar y^{\dot\alpha}(\vec{\boldsymbol{p}},s) \end{pmatrix}, \qquad \bar u(\vec{\boldsymbol{p}},s) = (y^\alpha(\vec{\boldsymbol{p}},s),\, \bar x_{\dot\alpha}(\vec{\boldsymbol{p}},s))\,, \tag{B.10}$$

$$v(\vec{\boldsymbol{p}},s) = \begin{pmatrix} y_\alpha(\vec{\boldsymbol{p}},s) \\ \\ \bar x^{\dot\alpha}(\vec{\boldsymbol{p}},s) \end{pmatrix}, \qquad \bar v(\vec{\boldsymbol{p}},s) = (x^\alpha(\vec{\boldsymbol{p}},s),\, \bar y_{\dot\alpha}(\vec{\boldsymbol{p}},s))\,, \tag{B.11}$$

where $v(\vec{\boldsymbol{p}},s) = C\bar u(\vec{\boldsymbol{p}},s)^T$. One can check that u and v satisfy the Dirac equations[18]

$$(\not p - m)\,u(\vec{\boldsymbol{p}},s) = (\not p + m)\,v(\vec{\boldsymbol{p}},s) = 0\,, \qquad \bar u(\vec{\boldsymbol{p}},s)\,(\not p - m) = \bar v(\vec{\boldsymbol{p}},s)\,(\not p + m) = 0\,, \tag{B.12}$$

corresponding to eqs. (3.9)–(3.12), and

$$(\gamma_5\not s - 1)\,u(\vec{\boldsymbol{p}},s) = (\gamma_5\not s - 1)\,v(\vec{\boldsymbol{p}},s) = 0\,, \qquad \bar u(\vec{\boldsymbol{p}},s)\,(\gamma_5\not s - 1) = \bar v(\vec{\boldsymbol{p}},s)\,(\gamma_5\not s - 1) = 0\,, \tag{B.13}$$

corresponding to eqs. (3.24)–(3.27). For massive fermions, eqs. (3.38)–(3.41) correspond to

$$u(\vec{\boldsymbol{p}},s)\bar u(\vec{\boldsymbol{p}},s) = \tfrac{1}{2}(1 + \gamma_5\not s)\,(\not p + m)\,, \tag{B.14}$$

$$v(\vec{\boldsymbol{p}},s)\bar v(\vec{\boldsymbol{p}},s) = \tfrac{1}{2}(1 + \gamma_5\not s)\,(\not p - m)\,. \tag{B.15}$$

[18] We use the standard Feynman slash notation: $\not p \equiv \gamma_\mu p^\mu$.

To apply the above formulas to the massless case, recall that in the $m \to 0$ limit, $s = 2\lambda p/m + \mathcal{O}(m/E)$. Inserting this result in eqs. (B.12) and (B.13), it follows that the massless helicity spinors are eigenstates of γ_5

$$\gamma_5 u(\vec{\boldsymbol{p}}, s) = 2\lambda u(\vec{\boldsymbol{p}}, s)\,, \tag{B.16}$$

$$\gamma_5 v(\vec{\boldsymbol{p}}, s) = -2\lambda v(\vec{\boldsymbol{p}}, s)\,. \tag{B.17}$$

Applying the same limiting procedure to eq. (B.15) and using the mass-shell condition ($\not{p}\not{p} = p^2 = m^2$), one obtains the helicity projection operators for a massless spin-1/2 particle

$$u(\vec{\boldsymbol{p}}, s)\bar{u}(\vec{\boldsymbol{p}}, s) = \tfrac{1}{2}(1 + 2\lambda\gamma_5)\not{p}\,, \tag{B.18}$$

$$v(\vec{\boldsymbol{p}}, s)\bar{v}(\vec{\boldsymbol{p}}, s) = \tfrac{1}{2}(1 - 2\lambda\gamma_5)\not{p}\,, \tag{B.19}$$

which correspond to eqs. (3.47)–(3.50). Finally, the spin-sum identities

$$\sum_\lambda u(\vec{\boldsymbol{p}}, s)\bar{u}(\vec{\boldsymbol{p}}, s) = \not{p} + m\,, \tag{B.20}$$

$$\sum_\lambda v(\vec{\boldsymbol{p}}, s)\bar{v}(\vec{\boldsymbol{p}}, s) = \not{p} - m\,, \tag{B.21}$$

$$\sum_\lambda u(\vec{\boldsymbol{p}}, s)v^T(\vec{\boldsymbol{p}}, s) = (\not{p} + m)C^T\,, \tag{B.22}$$

$$\sum_\lambda \bar{u}^T(\vec{\boldsymbol{p}}, s)\bar{v}(\vec{\boldsymbol{p}}, s) = C^{-1}(\not{p} - m)\,, \tag{B.23}$$

$$\sum_\lambda \bar{v}^T(\vec{\boldsymbol{p}}, s)\bar{u}(\vec{\boldsymbol{p}}, s) = C^{-1}(\not{p} + m)\,, \tag{B.24}$$

$$\sum_\lambda v(\vec{\boldsymbol{p}}, s)u^T(\vec{\boldsymbol{p}}, s) = (\not{p} - m)C^T\,, \tag{B.25}$$

correspond to eqs. (3.51)–(3.54).

Bilinear covariants are quantities that are quadratic in the Dirac spinor field which transform irreducibly as Lorentz tensors. These are easily constructed from corresponding quantities that are quadratic in the two-component fermion fields. To construct a translation table between the two-component form and the four-component forms for the bilinear covariants, we first introduce two Dirac spinor fields [*cf.* eq. (B.3)]:

$$\Psi_1(x) \equiv \begin{pmatrix} \chi_1(x) \\ \\ \bar{\eta}_1(x) \end{pmatrix}\,, \qquad \Psi_2(x) \equiv \begin{pmatrix} \chi_2(x) \\ \\ \bar{\eta}_2(x) \end{pmatrix}\,, \tag{B.26}$$

where spinor indices have been suppressed on the two-component fields $\chi_i(x)$ and $\bar{\eta}_i(x)$.[19] The following results are then obtained:

$$\overline{\Psi}_1 P_L \Psi_2 = \eta_1 \chi_2 \,, \tag{B.27}$$

$$\overline{\Psi}_1 P_R \Psi_2 = \bar{\chi}_1 \bar{\eta}_2 \,, \tag{B.28}$$

$$\overline{\Psi}_1 \gamma^\mu P_L \Psi_2 = \bar{\chi}_1 \bar{\sigma}^\mu \chi_2 \,, \tag{B.29}$$

$$\overline{\Psi}_1 \gamma^\mu P_R \Psi_2 = \eta_1 \sigma^\mu \bar{\eta}_2 \,, \tag{B.30}$$

$$\overline{\Psi}_1 \Sigma^{\mu\nu} P_L \Psi_2 = 2\, \eta_1 \sigma^{\mu\nu} \chi_2 \,, \tag{B.31}$$

$$\overline{\Psi}_1 \Sigma^{\mu\nu} P_R \Psi_2 = 2\, \bar{\chi}_1 \bar{\sigma}^{\mu\nu} \bar{\eta}_2 \,. \tag{B.32}$$

Note that eqs. (B.27)–(B.32) apply to both commuting and anti-commuting fermion fields. If other combinations of the two-component spinors appear in the bilinear covariant, the corresponding four-component expression will necessarily involve a charge-conjugated four-component spinor. For example, $\overline{\Psi}_1^c P_L \Psi_2 = \chi_1 \chi_2$, *etc.* In general, if one replaces Ψ_j with Ψ_j^c ($j = 1$ and/or 2) in any of the above results, then in the corresponding two-component expression one simply interchanges $\chi_j \leftrightarrow \eta_j$ and $\bar{\chi}_j \leftrightarrow \bar{\eta}_j$.

Using eqs. (B.27)–(B.32), it then follows that:

$$\overline{\Psi}_1 \Psi_2 = \eta_1 \chi_2 + \bar{\chi}_1 \bar{\eta}_2 \tag{B.33}$$

$$\overline{\Psi}_1 \gamma_5 \Psi_2 = -\eta_1 \chi_2 + \bar{\chi}_1 \bar{\eta}_2 \tag{B.34}$$

$$\overline{\Psi}_1 \gamma^\mu \Psi_2 = \bar{\chi}_1 \bar{\sigma}^\mu \chi_2 + \eta_1 \sigma^\mu \bar{\eta}_2 \tag{B.35}$$

$$\overline{\Psi}_1 \gamma^\mu \gamma_5 \Psi_2 = -\bar{\chi}_1 \bar{\sigma}^\mu \chi_2 + \eta_1 \sigma^\mu \bar{\eta}_2 \tag{B.36}$$

$$\overline{\Psi}_1 \Sigma^{\mu\nu} \Psi_2 = 2(\eta_1 \sigma^{\mu\nu} \chi_2 + \bar{\chi}_1 \bar{\sigma}^{\mu\nu} \bar{\eta}_2) \tag{B.37}$$

$$\overline{\Psi}_1 \Sigma^{\mu\nu} \gamma_5 \Psi_2 = 2(-\eta_1 \sigma^{\mu\nu} \chi_2 + \bar{\chi}_1 \bar{\sigma}^{\mu\nu} \bar{\eta}_2) \,. \tag{B.38}$$

Note that eqs. (B.35) and (B.36) contain both σ^μ and $\overline{\sigma}^\mu$.[20] One useful consequence of the

[19] Here i is a flavor index. In the convention of Section 3.2, the flavor index of an unbarred two-component field appears as a lowered index and the flavor index of a barred two-component fermion field appears as a raised index. If one wanted to introduce both raised and lowered indices for four-component fermion fields, one would demand that the flavor indices of $\Psi_L \equiv P_L \Psi$ and $\overline{\Psi}_R \equiv \overline{\Psi} P_L$ appear as lowered indices, whereas the flavor indices of $\Psi_R \equiv P_R \Psi$ and $\overline{\Psi}_L \equiv \overline{\Psi} P_R$ appear as raised indices. However, such a convention appears unwieldy for vector-like interactions. Hence in this section we shall depart from our flavor index convention, and employ only lowered flavor indices for all fermion fields.

[20] It is sometimes more convenient to apply eq. (2.34) to eqs. (B.35) and (B.36) and rewrite $\eta_1 \sigma^\mu \bar{\eta}^2 = \pm \bar{\eta}_2 \overline{\sigma}^\mu \eta^1$, where the plus [minus] sign is employed for commuting [anticommuting] spinors.

above results are the following relations satisfied by the (commuting) u and v spinors:

$$\bar{u}(\vec{\boldsymbol{p}}_1,s_1)P_Lv(\vec{\boldsymbol{p}}_2,s_2)=-\bar{u}(\vec{\boldsymbol{p}}_2,s_2)P_Lv(\vec{\boldsymbol{p}}_1,s_1)\,, \tag{B.39}$$

$$\bar{u}(\vec{\boldsymbol{p}}_1,s_1)P_Rv(\vec{\boldsymbol{p}}_2,s_2)=-\bar{u}(\vec{\boldsymbol{p}}_2,s_2)P_Rv(\vec{\boldsymbol{p}}_1,s_1)\,, \tag{B.40}$$

$$\bar{u}(\vec{\boldsymbol{p}}_1,s_1)\gamma^\mu P_Lv(\vec{\boldsymbol{p}}_2,s_2)=\bar{u}(\vec{\boldsymbol{p}}_2,s_2)\gamma^\mu P_Rv(\vec{\boldsymbol{p}}_1,s_1)\,, \tag{B.41}$$

$$\bar{u}(\vec{\boldsymbol{p}}_1,s_1)\gamma^\mu P_Rv(\vec{\boldsymbol{p}}_2,s_2)=\bar{u}(\vec{\boldsymbol{p}}_2,s_2)\gamma^\mu P_Lv(\vec{\boldsymbol{p}}_1,s_1)\,. \tag{B.42}$$

The results derived above also apply to four-component Majorana fermions, Ψ_{Mi}, by setting $\eta_i=\chi_i$. However, the extra condition imposed by $\Psi_{Mi}^c=\Psi_{Mi}$ can yield further restrictions. For example, eqs. (B.35)–(B.38) imply [after employing eqs. (2.34)–(2.36)] that *anticommuting* Majorana four-component fermions satisfy:

$$\overline{\Psi}_{Mi}\gamma^\mu P_L\Psi_{Mj}=-\overline{\Psi}_{Mj}\gamma^\mu P_R\Psi_{Mi}\,, \tag{B.43}$$

$$\overline{\Psi}_{Mi}\Sigma^{\mu\nu}\Psi_{Mj}=-\overline{\Psi}_{Mj}\Sigma^{\mu\nu}\Psi_{Mi}\,, \tag{B.44}$$

$$\overline{\Psi}_{Mi}\Sigma^{\mu\nu}\gamma_5\Psi_{Mj}=-\overline{\Psi}_{Mj}\Sigma^{\mu\nu}\gamma_5\Psi_{Mi}\,. \tag{B.45}$$

If we set $i=j$, we learn that $\overline{\Psi}_M\gamma^\mu\Psi_M=\overline{\Psi}_M\Sigma^{\mu\nu}\gamma\Psi_M=\overline{\Psi}_M\Sigma^{\mu\nu}\gamma_5\Psi_M=0$.

We now illustrate some basic applications of the the above analysis by considering a set of neutral and charged fermions interacting with a neutral scalar or vector boson. To convert to four-component notation, we first identify the neutral two-component fields ξ_i and the mass-degenerate charged pairs χ_j and η_j that combine to form the Dirac fermions. We may then rewrite the interaction Lagrangian given in eq. (4.10) in the following form:

$$\begin{aligned}\mathcal{L}_{\rm int}=&-\tfrac{1}{2}(\lambda^{ij}\xi_i\xi_j+\lambda_{ij}\bar{\xi}^i\bar{\xi}^j)\phi-(\kappa^{ij}\chi_i\eta_j+\kappa_{ij}\bar{\chi}^i\bar{\eta}^j)\phi\\&-(G_\xi)_i{}^j\,\bar{\xi}^i\overline{\sigma}^\mu\xi_jA_\mu-[(G_\chi)_i{}^j\bar{\chi}^i\overline{\sigma}^\mu\chi_j+(G_\eta)_i{}^j\bar{\eta}^i\overline{\sigma}^\mu\eta_j]A_\mu\,,\end{aligned} \tag{B.46}$$

where λ is a complex symmetric matrix, κ is an arbitrary complex matrix and G_ξ, G_χ and G_η are hermitian matrices. By assumption, χ and η have the opposite U(1) charges, while all other fields in eq. (B.46) are neutral. It is now simple to convert this result into four-component notation:[21]

$$\begin{aligned}\mathcal{L}_{\rm int}=&-\tfrac{1}{2}(\lambda^{ij}\overline{\Psi}_{Mi}P_L\Psi_{Mj}+\lambda_{ij}\overline{\Psi}_{Mi}P_R\Psi_{Mj})\phi-(\kappa^{ji}\overline{\Psi}_iP_L\Psi_j+\kappa_{ij}\overline{\Psi}_iP_R\Psi_j)\phi\\&-\Big[(G_\xi)_i{}^j\overline{\Psi}_{Mi}\gamma^\mu P_L\Psi_{Mj}+(G_\chi)_i{}^j\overline{\Psi}_i\gamma^\mu P_L\Psi_j-(G_\eta)_j{}^i\overline{\Psi}_i\gamma^\mu P_R\Psi_j\Big]A_\mu\,,\end{aligned} \tag{B.47}$$

[21] As noted in footnote 19, all flavor indices attached to four-component fermion fields appear as lowered indices. Nevertheless, we continue to distinguish λ_{ij} and $\lambda^{ij}\equiv\lambda^*_{ij}$, *etc.*

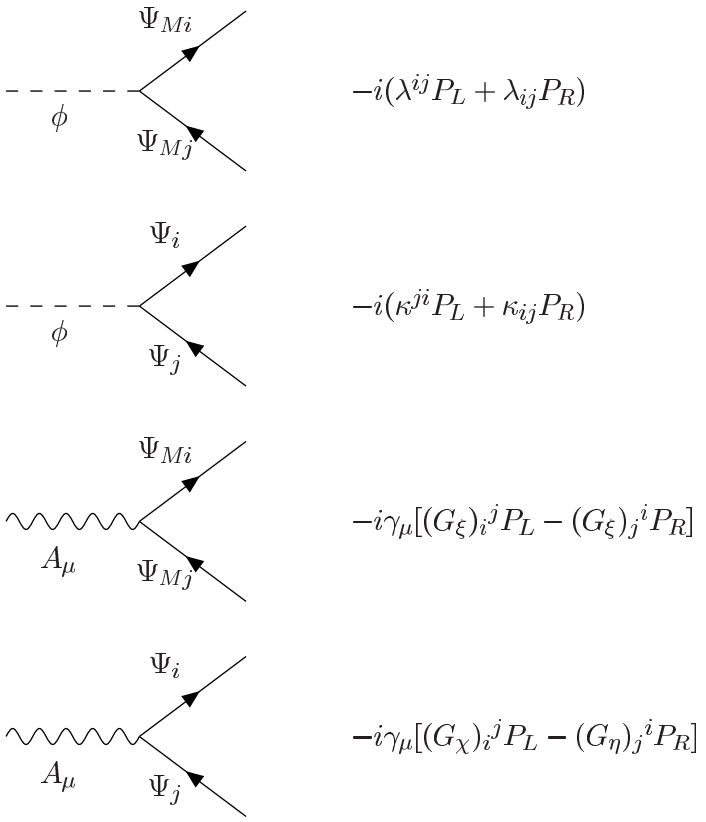

Figure 50: Feynman rules for four-component fermion interactions with neutral bosons

where Ψ_{Mj} [Ψ_j] are a set of Majorana [Dirac] four-component fermions. It is convenient to use eq. (B.44) to rewrite the term proportional to $(G_\xi)_i{}^j$ in eq. (B.47) as follows

$$(G_\xi)_i{}^j\overline{\Psi}_{Mi}\gamma^\mu P_L\Psi_{Mj} = \tfrac{1}{2}\overline{\Psi}_{Mi}\gamma^\mu\left[(G_\xi)_i{}^j P_L - (G_\xi)_j{}^i P_R\right]\Psi_{Mj}\,. \tag{B.48}$$

Using standard four-component methods, the Feynman rules for the vertices are easily obtained and displayed in Fig. 50. Note that the arrows on the Dirac fermion lines depict the flow of the conserved charge. A Majorana fermion is neutral under all conserved charges (and thus equal to its own anti-particle). Thus an arrow on a Majorana fermion line simply reflects the structure of the interaction Lagrangian; *i.e.*, $\overline{\Psi}_M$ [Ψ_M] is represented by an arrow pointing out of [into] the vertex. The arrows are then used for determining the placement of the u and v spinors in an invariant amplitude.

We can also treat the interaction of fermions with charged bosons. We may then rewrite the interaction Lagrangian given in eq. (4.12) in four-component notation:

$$\mathcal{L}_{\rm int} = -\tfrac{1}{2}\left[(\kappa_2)^{ij}\overline{\Psi}_i P_L\Psi_{Mj} + (\kappa_1)_{ij}\overline{\Psi}_i P_R\Psi_{Mj}\right]\phi$$

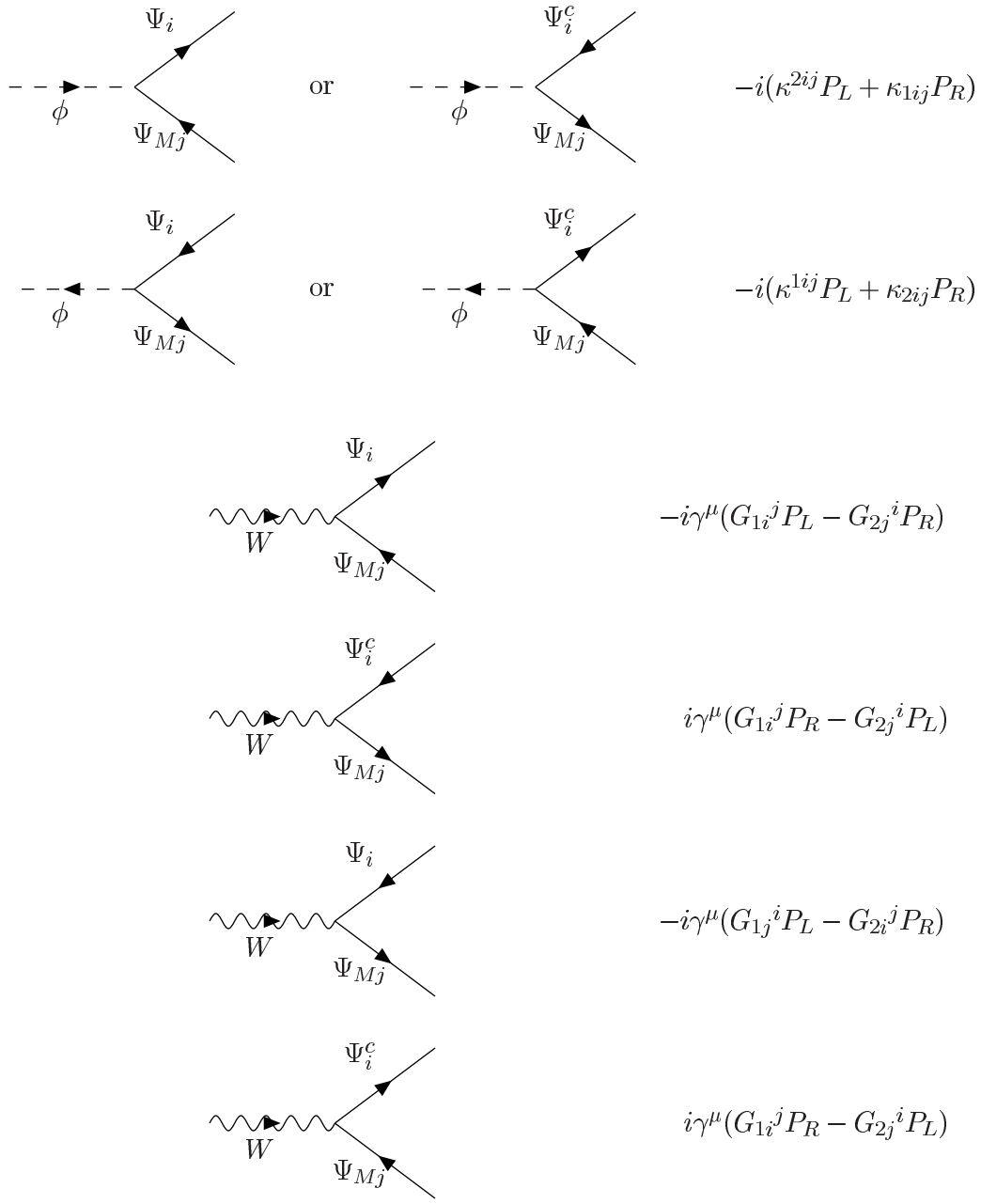

Figure 51: Feynman rules for four-component fermion interactions with charged bosons. The arrows on the boson and Dirac fermion lines indicate the direction of charge flow.

$$-\left[(G_1)_i{}^j\overline{\Psi}_i\gamma^\mu P_L\Psi_{Mj} - (G_2)_j{}^i\overline{\Psi}_i\gamma^\mu P_R\Psi_{Mj}\right]W_\mu + \text{h.c.} \tag{B.49}$$

There is an equivalent form of the interaction given in eq. (B.49) where $\mathcal{L}$ is written in

terms of charge-conjugated fields. In general,[22]

$$\overline{\Psi}_i^c \Gamma \Psi_j^c = \overline{\Psi}_j C \Gamma^T C^{-1} \Psi_i = \eta_\Gamma \overline{\Psi}_j \Gamma \Psi_i \,, \tag{B.50}$$

where the sign $\eta_\Gamma = +1$ for $\Gamma = 1, \gamma_5, \gamma^\mu\gamma_5$ and $\eta_\Gamma = -1$ for $\Gamma = \gamma^\mu, \Sigma^{\mu\nu}$, $\Sigma^{\mu\nu}\gamma_5$. Noting that Majorana fermions are self-conjugate, the Feynman rules for the interactions of neutral and charged fermions with charged bosons can take two possible forms, as shown in Fig. 51. Here, the direction of an arrow on a Dirac fermion line is meaningful and indicates the direction of charge flow. However, we are free to choose either a Ψ or Ψ^c line to represent a Dirac fermion at any place in a given Feynman graph.[23] Moreover, the structure of the interactions above imply that the arrow directions on fermion lines flow continuously through the diagram. This requirement then determines the direction of the arrows on Majorana fermion lines. Virtual Dirac fermion lines can either correspond to Ψ or Ψ^c. Here, there is no ambiguity in the propagator Feynman rule, since for free Dirac fermion fields,

$$\Big\langle 0|T(\Psi_\alpha(x)\overline{\Psi}_\beta(y))|0\Big\rangle = \Big\langle 0|T(\Psi^c_\alpha(x)\overline{\Psi}^c_\beta(y))|0\Big\rangle \,, \tag{B.51}$$

so that the Feynman rules for the propagator of a Ψ and Ψ^c line are identical.

For a given process, there may be a number of distinct choices for the arrow directions on the Majorana fermion lines, which may depend on whether one represents a given Dirac fermion by Ψ or Ψ^c. However, different choices do *not* lead to independent Feynman diagrams.[24] When computing an invariant amplitude, one first writes down the relevant Feynman diagrams with no arrows on any Majorana fermion line. The number of distinct graphs contributing to the process is then determined. Finally, one makes some choice for how to distribute the arrows on the Majorana fermion lines and how to label Dirac fermion lines (either as the field or its conjugate) in a manner consistent with the rules of Figs. 50 and 51. The end result for the invariant amplitude (apart from an overall unobservable phase) does not depend on the choices made for the direction of the fermion arrows.

Using the above procedure, the Feynman rules for the external fermion wave functions are the same for Dirac and Majorana fermions:

- $u(\vec{\boldsymbol{p}}, s)$: incoming Ψ [or Ψ^c] with momentum $\vec{\boldsymbol{p}}$ parallel to the arrow direction,
- $\bar{u}(\vec{\boldsymbol{p}}, s)$: outgoing Ψ [or Ψ^c] with momentum $\vec{\boldsymbol{p}}$ parallel to the arrow direction,

[22] In deriving eq. (B.50), we noted that $C^T = -C$ and used the fact that the fermion fields anticommute.

[23] Since the charge of Ψ^c is opposite to that of Ψ, the corresponding arrow direction of the two lines are also point in opposite directions.

[24] In contrast, the two-component Feynman rules developed in Section 3 require that two vertices differing by the direction of the arrows on the two-component fermion lines must both be included in the calculation of the matrix element.

- $v(\vec{\boldsymbol{p}},s)$: outgoing Ψ [or Ψ^c] with momentum $\vec{\boldsymbol{p}}$ anti-parallel to the arrow direction,
- $\bar{v}(\vec{\boldsymbol{p}},s)$: incoming Ψ [or Ψ^c] with momentum $\vec{\boldsymbol{p}}$ anti-parallel to the arrow direction.

The proof that the above rules for external wave functions apply unambiguously to Majorana fermions is straightforward. Simply insert the plane wave expansion of the Majorana field:

$$\Psi_M(x) = \sum_s \int \frac{d^3p}{(2\pi)^{3/2}(2E_{\boldsymbol{p}})^{1/2}} \left[u(\vec{\boldsymbol{p}},s)a(\vec{\boldsymbol{p}},s)e^{-ip\cdot x} + v(\vec{\boldsymbol{p}},s)a^\dagger(\vec{\boldsymbol{p}},s)e^{+ip\cdot x}\right] \tag{B.52}$$

into eq. (B.47), and evaluate matrix elements for, *e.g.*, the decay of a scalar or vector particle into a pair of Majorana fermions.

We now reconsider the matrix elements for scalar and vector particle decays into fermion pairs and $2 \to 2$ elastic scattering of a fermion off a scalar and vector boson, respectively. We shall compute the matrix elements using the Feynman rules of fig. 50, and check that the results agree with the ones obtained by two-component methods in Section 3.

The matrix element for the decay $\phi \to \Psi_M(\vec{\boldsymbol{p}}_1,s_1)\Psi_M(\vec{\boldsymbol{p}}_2,s_2)$ is given by

$$i\mathcal{M} = -i\bar{u}(\vec{\boldsymbol{p}}_1,s_1)(\lambda P_L + \lambda^* P_R)v(\vec{\boldsymbol{p}}_2,s_2)\,. \tag{B.53}$$

One can easily check that this result matches with eq. (4.19), which was derived using two-component techniques. Note that if one had chosen to switch the two final states (equivalent to switching the directions of the Majorana fermion arrows), then the resulting matrix element would simply exhibit an overall sign change [due to the results of eqs. (B.39) and (B.40)].[25] Similarly, for $\phi \to \Psi_{Mi}\Psi_{Mj}$ $(i \neq j)$ or for the decay into a pair of Dirac fermions, $\phi \to \overline{\Psi}\Psi$, one again obtains the invariant matrix element given in eq. (B.53).

For the decay $A_\mu \to \Psi_M(\vec{\boldsymbol{p}}_1,s_1)\Psi_M(\vec{\boldsymbol{p}}_2,s_2)$, one obtains:

$$i\mathcal{M} = iG_\xi \bar{u}(\vec{\boldsymbol{p}}_1,s_1)\gamma^\mu\gamma_5 v(\vec{\boldsymbol{p}}_2,s_2)\varepsilon_\mu\,. \tag{B.54}$$

One can easily check that this result matches with eq. (4.22). For the decay into non-identical Majorana fermions, $A_\mu \to \Psi_{Mi}\Psi_{Mj}$ $(i \neq j)$, we can use the Feynman rules of Fig. 50 to obtain:

$$i\mathcal{M} = -i\bar{u}(\vec{\boldsymbol{p}}_i,s_i)\gamma^\mu \left[(G_\xi)_i{}^j P_L - (G_\xi)_j{}^i P_R\right] v(\vec{\boldsymbol{p}}_j,s_j)\varepsilon_\mu\,, \tag{B.55}$$

Again, we note that if one had chosen to switch the two final states (equivalent to switching the directions of the Majorana fermion arrows), then the resulting matrix element would simply exhibit an overall sign change [due to the results of eqs. (B.41) and (B.42)]. Finally, for the

[25] The overall sign change is a consequence of the Fermi-Dirac statistics, and corresponds to changing which order one uses to construct the two particle final state.

decay of the vector particle into a Dirac fermion-antifermion pair, $A_\mu \to \overline{\Psi}\Psi$, the matrix element is given by:

$$i\mathcal{M} = -i\bar{u}(\vec{\boldsymbol{p}}_1, s_1)\gamma^\mu(G_\chi P_L - G_\eta P_R)v(\vec{\boldsymbol{p}}_2, s_2)\varepsilon_\mu\,, \tag{B.56}$$

which matches the result of eq. (4.26).

Turning to the elastic scattering of a neutral Majorana fermion and a neutral scalar, we shall examine two equivalent ways for computing the amplitude. Following the rules previously stated, there are two possible choices for the direction of arrows on the Majorana fermion lines. Thus, may evaluate either one of the following two diagrams:

plus a second diagram in each case (not shown) where the initial and final state scalars are crossed. Evaluating the first diagram above, the matrix element for $\phi\Psi_M \to \phi\Psi_M$ is given by:

$$\begin{aligned} i\mathcal{M} &= \frac{-i}{s-m^2}\,\bar{u}(\vec{\boldsymbol{p}}_2, s_2)(\lambda P_L + \lambda^* P_R)(\not{p} + m)(\lambda P_L + \lambda^* P_R)u(\vec{\boldsymbol{p}}_1, s_1) + (\text{crossed}) \\ &= \frac{-i}{s-m^2}\,\bar{u}(\vec{\boldsymbol{p}}_2, s_2)\left[|\lambda|^2\not{p} + \left(\lambda^2 P_L + (\lambda^*)^2 P_R\right)m\right]u(\vec{\boldsymbol{p}}_1, s_1) + (\text{crossed})\,, \end{aligned} \tag{B.57}$$

where m is the Majorana fermion mass, s is the center-of-mass energy squared. Using eqs. (B.1) and (B.10), one recovers the results of eq. (4.27). Had we chose to evaluate the second diagram instead, the resulting amplitude would have been given by:

$$i\mathcal{M} = \frac{-i}{s-m^2}\,\bar{v}(\vec{\boldsymbol{p}}_1, s_1)\left[-|\lambda|^2\not{p} + \left(\lambda^2 P_L + (\lambda^*)^2 P_R\right)m\right]v(\vec{\boldsymbol{p}}_2, s_2) + (\text{crossed})\,. \tag{B.58}$$

Using eqs. (B.10) and (B.11) and the results of eqs. (2.32)–(2.34) one can derive the following results:

$$\bar{v}(\vec{\boldsymbol{p}}_1, s_1)v(\vec{\boldsymbol{p}}_2, s_2) = -\bar{u}(\vec{\boldsymbol{p}}_2, s_2)u(\vec{\boldsymbol{p}}_1, s_1)\,, \qquad \bar{v}(\vec{\boldsymbol{p}}_1, s_1)\gamma^\mu v(\vec{\boldsymbol{p}}_2, s_2) = \bar{u}(\vec{\boldsymbol{p}}_2, s_2)\gamma^\mu u(\vec{\boldsymbol{p}}_1, s_1)\,. \tag{B.59}$$

Consequently, the amplitude computed in eq. (B.58) is just the negative of eq. (B.57). This is expected, since the order of spinor wave functions (12) in eq. (B.58) is an odd permutation (21) of the order of spinor wave functions in eq. (B.57). As in the two-component Feynman rules, the overall sign of the amplitude is arbitrary, but the relative signs of any pair of diagrams is not ambiguous. This relative sign is positive [negative] if the permutation of the order of spinor wave functions of one diagram relative to the other diagram is even [odd].

Next, we consider the elastic scattering of a charged fermion and a neutral scalar. Again, we examine two equivalent ways for computing the amplitude. Following the rules previously stated, there are two possible choices for the direction of arrows on the fermion lines, depending on whether we represent the fermion by Ψ or Ψ^c. Thus, we may evaluate either one of the following two diagrams:

plus a second diagram in each case (not shown) where the initial and final state scalars are crossed. Evaluating the first diagram above, the matrix element for $\phi\Psi \to \phi\Psi$ is given by eq. (B.57), with λ replaced by κ. Had we chose to evaluate the second diagram instead, the resulting amplitude would have been given by eq. (B.58), with λ replaced by κ. Thus, the discussion above in the case of neutral fermion scattering processes also applies to charged fermion scattering processes.

In processes that only involve vertices with two Dirac fields, it is never necessary to use charge-conjugated Dirac fermion lines. In contrast, consider the following process that involves a vertex with one Dirac and one Majorana fermion. Specifically, we examine the scattering of a charged Dirac fermion and a charged scalar via the exchange of a neutral Majorana fermion, in which the charge of the outgoing fermion is opposite to that of the incoming fermion. If one attempts to draw the relevant Feynman diagram employing Dirac fermion lines but with no charge-conjugated Dirac fermion lines, one finds that there is no possible choice of arrow direction for the Majorana fermion that is consistent with the the vertex rules of Fig. 51. The resolution is simple: one can choose the incoming line to be Ψ and the outgoing line to be Ψ^c or vice versa. Thus, the two possible choices are given by:

plus a second diagram in each case (not shown) in which the initial and final scalars are crossed. If we evaluate the first diagram, the resulting amplitude is given by:

$$
\begin{aligned}
i\mathcal{M} &= \frac{-i}{s-m^2}\,\bar{u}(\vec{\boldsymbol{p}}_2,s_2)(\kappa_1 P_L+\kappa_2^* P_R)(\not{p}+m)(\kappa_1 P_L+\kappa_2^* P_R)u(\vec{\boldsymbol{p}}_1,s_1)+(\text{crossed})\\
&= \frac{-i}{s-m^2}\,\bar{u}(\vec{\boldsymbol{p}}_2,s_2)\left[\kappa_1\kappa_2^*\not{p}+\left(\kappa_1^2 P_L+(\kappa_2^*)^2 P_R\right)m\right]u(\vec{\boldsymbol{p}}_1,s_1)+(\text{crossed})\,, \qquad \text{(B.60)}
\end{aligned}
$$

where m is the Majorana fermion mass. One can check that this is equivalent to eq. (4.31) obtained via the two-component methods. Had we evaluated the second diagram, then after using the relations given in eq. (B.59), one finds that the resulting amplitude is just the negative of eq. (B.60), as expected. As before, the relative sign between diagrams for the same process is not ambiguous.

In the literature, there are a number of alternative methods for dealing with scattering processes involving Majorana particles. For example, one can define a fermion-number violating propagator for four-component fermions (see, *e.g.*, [2]). These methods involve subtle choices of signs which often require first-principles computations to verify. The advantage of the method described above is that there is never any ambiguity in the choice of relative signs.

In the case of elastic scattering of a fermion and a neutral vector boson, the two contributing diagrams are

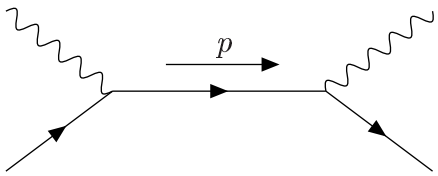

plus a second diagram (not shown) where the initial and final state vector bosons are crossed. Consider first the scattering of a neutral Majorana fermion of mass m. Using the Feynman rules of Fig. 50, we see that the Feynman rule for the $A_\mu \overline{\Psi}_M \Psi_M$ vertex is given by $iG_\xi \gamma^\mu \gamma_5$. Hence, the corresponding matrix element is given by

$$i\mathcal{M} = \frac{-iG_\xi^2}{s-m^2}\bar{u}(\vec{\boldsymbol{p}}_2, s_2)\,\gamma\cdot\varepsilon_2^*\,(\not{p}-m)\,\gamma\cdot\varepsilon_1 u(\vec{\boldsymbol{p}}_1, s_1) + (\text{crossed})\,, \tag{B.61}$$

where we have used $\gamma^\nu\gamma_5(\not{p}+m)\gamma^\mu\gamma_5 = \gamma^\nu(\not{p}-m)\gamma^\mu$. Using eqs. (B.1) and (B.10), one easily recovers the results of eq. (4.28).

Next, consider the scattering of a Dirac fermion. The corresponding matrix element is given by

$$\begin{aligned} i\mathcal{M} &= \frac{-i}{s-m^2}\bar{u}(\vec{\boldsymbol{p}}_2, s_2)\,\gamma\cdot\varepsilon_2^*\,(G_\chi P_L - G_\eta P_R)(\not{p}+m)\,\gamma\cdot\varepsilon_1\,(G_\chi P_L - G_\eta P_R)u(\vec{\boldsymbol{p}}_1, s_1) + (\text{crossed}) \\ &= \frac{-i}{s-m^2}\bar{u}(\vec{\boldsymbol{p}}_2, s_2)\,\gamma\cdot\varepsilon_2^*\left[(G_\chi^2 P_L + G_\eta^2 P_R)\not{p} - G_\chi G_\eta m\right]\,\gamma\cdot\varepsilon_1 u(\vec{\boldsymbol{p}}_1, s_1) + (\text{crossed})\,. \end{aligned} \tag{B.62}$$

One can easily check that this result coincides with that of eq. (4.32).

Finally, we examine the elastic scattering of two identical Majorana fermions via scalar exchange. The three contributing diagrams are:
and the corresponding matrix element is given by

$$i\mathcal{M} = \frac{-i}{s-m_\phi^2}\left[\bar{v}_1(\lambda P_L + \lambda^* P_R)u_2\,\bar{u}_3(\lambda P_L + \lambda^* P_R)v_4\right]$$

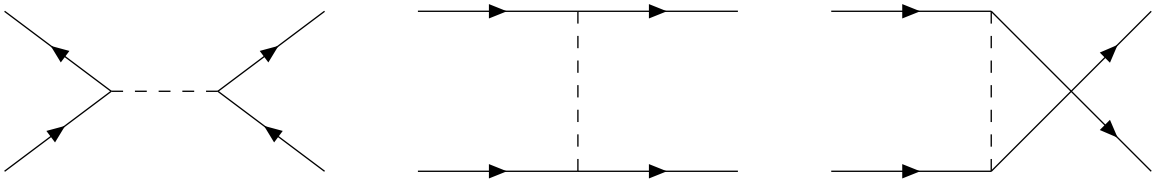

$$+ (-1)\frac{-i}{t-m_\phi^2}\,[\bar{u}_3(\lambda P_L + \lambda^* P_R)u_1\,\bar{u}_4(\lambda P_L + \lambda^* P_R)u_2]$$

$$+ \frac{-i}{u-m_\phi^2}\,[\bar{u}_4(\lambda P_L + \lambda^* P_R)u_1\,\bar{u}_3(\lambda P_L + \lambda^* P_R)u_2]\ , \qquad \text{(B.63)}$$

where $u_i \equiv u(\vec{\boldsymbol{p}}_i, s_i)$, $v_j \equiv u(\vec{\boldsymbol{p}}_j, s_j)$ and m_ϕ is the exchanged scalar mass. The relative minus sign of the t-channel graph relative to the other two is obtained by noting that 3142 [4132] is an odd [even] permutation of 1234. Using eqs. (B.1) and (B.10), one easily recovers the results of eq. (4.33).

Appendix C: Standard Model Fermion Interaction Vertices

In the Standard Model, one generation of quarks and leptons is described by the two-component fermion fields listed in Table 2, where Y is the weak hypercharge, T_3 is the third component of the weak isospin and Q is the electric charge. After $\mathrm{SU}(2)_L\times\mathrm{U}(1)_Y$ breaking, the quark and lepton fields gain mass in such a way that the above two-component fields combine to make up four-component Dirac fermions:

$$U = \begin{pmatrix} u \\ \overline{u^c} \end{pmatrix}\ , \qquad D = \begin{pmatrix} d \\ \overline{d^c} \end{pmatrix}\ , \qquad E = \begin{pmatrix} e \\ \overline{e^c} \end{pmatrix}\ . \qquad \text{(C.1)}$$

while the neutrino remains massless. (The extension of the Standard Model to include neutrino mass will be treated elsewhere.)

Here, we follow the convention for particle symbols established in Table 1. Although there is some potential for confusion, note that u and d are two-component fields, whereas the usual four-component quark and charged lepton fields are denoted by capital letters U, D and E. Consider a generic four-component field expressed in terms of the corresponding two-component fields:

$$F = \begin{pmatrix} f \\ \overline{f^c} \end{pmatrix}\ . \qquad \text{(C.2)}$$

The electroweak quantum numbers of f are denoted by T_3^f, Y_f and Q_f, whereas the corresponding quantum numbers for f^c are $T_3^{f^c} = 0$ and $Q_{f^c} = \frac{1}{2}Y_{f^c} = -Q_f$. Thus we have the

Two-component fermion fields	$\mathrm{SU}(2)_L$	Y	T_3	$Q = T_3 + \frac{1}{2}Y$
$\begin{pmatrix} u \\ d \end{pmatrix}$	doublet	$\frac{1}{3}$ $\frac{1}{3}$	$\frac{1}{2}$ $-\frac{1}{2}$	$\frac{2}{3}$ $-\frac{1}{3}$
u^c	singlet	$-\frac{4}{3}$	0	$-\frac{2}{3}$
d^c	singlet	$\frac{2}{3}$	0	$\frac{1}{3}$
$\begin{pmatrix} \nu \\ e \end{pmatrix}$	doublet	-1 -1	$\frac{1}{2}$ $-\frac{1}{2}$	0 -1
e^c	singlet	2	0	1

Table 2: Fermions of the Standard Model and their quantum numbers.

correspondence to our general notation [eq. (B.3)]

$$f \longleftrightarrow \chi, \qquad f^c \longleftrightarrow \eta\,. \tag{C.3}$$

We can then immediately translate the couplings given in the general case [Fig. 9] to the Standard Model.

We now write out the Feynman rules for the electroweak interactions of quarks and leptons. As an example, consider the charged current interactions of the fermions:

$$\mathcal{L}_{\rm int} = -\frac{g}{\sqrt{2}}\left[\bar{\hat{u}}^i\overline{\sigma}^\mu\hat{d}_i W_\mu^+ + \overline{\hat{d}}^i\overline{\sigma}^\mu\hat{u}_i W_\mu^-\right], \tag{C.4}$$

where the hatted symbols indicate interaction-eigenstates and i labels the generations. Following the discussion of Appendix B, we convert to mass-eigenstates. That is, we introduce four unitary matrices, L_u, L_d, R_u and R_d, [*cf.* eq. (3.75)] such that

$$\hat{u} = L_u u\,, \qquad \hat{d} = L_d d\,, \qquad \hat{u}^c = R_u u^c\,, \quad \text{and} \quad \hat{d}^c = R_d d^c\,, \tag{C.5}$$

where u, d, u^c and d^c are the corresponding mass-eigenstates. It then follows that $\bar{\hat{u}}^i\overline{\sigma}^\mu\hat{d}_i = \boldsymbol{K}_i{}^j\bar{u}^i\overline{\sigma}^\mu d_j$, where

$$\boldsymbol{K} = L_u^\dagger L_d \tag{C.6}$$

is the Cabibbo-Kobayashi-Maskawa (CKM) matrix. (Note that $\boldsymbol{K}$ is a unitary matrix.) Thus, the charged current interactions now take the form

$$\mathcal{L}_{\rm int} = -\frac{g}{\sqrt{2}}\left[\boldsymbol{K}_i{}^j \bar{u}^i \overline{\sigma}^\mu d_j W_\mu^+ + \boldsymbol{K}^j{}_i \bar{d}^i \overline{\sigma}^\mu u_j W_\mu^-\right], \tag{C.7}$$

where $\boldsymbol{K}^j{}_i \equiv (\boldsymbol{K}^\dagger)_i{}^j$ [see eq. (4.11)]. Note that Standard Model does not possess $W^\pm$ interactions with u^c and d^c. The corresponding Feynman rules are given in Fig. 52. It is convenient to introduce the following notation: $[\boldsymbol{K}]_{ij} \equiv \boldsymbol{K}_i{}^j$ and $[\boldsymbol{K}^\dagger]_{ij} \equiv \boldsymbol{K}^j{}_i$, which is employed in Fig. 52.

The corresponding interaction of the fermions with the neutral gauge bosons are also given in Fig. 52. As expected, the neutral current interactions are flavor-conserving. We use the notation $s_W = \sin\theta_W$, $c_W = \cos\theta_W$. For each of the rules of Fig. 52, we have chosen to employ $\overline{\sigma}_\mu^{\dot\alpha\beta}$. If the indices are lowered one should take $\overline{\sigma}_\mu^{\dot\alpha\beta} \to -\sigma_{\mu\beta\dot\alpha}$. There is a corresponding set of Feynman rules for leptons, by replacing $u \to \nu$, $d \to e$ and $\boldsymbol{K} \to 1$.

The Yukawa interactions of the fermions with the Higgs boson ($h_{\rm SM}$) are given by:

$$-\mathcal{L}_{\rm Y} = (\boldsymbol{Y}_u^{\rm SM})^{ij}\left[\Phi^0 \hat{u}_i \hat{u}_j^c - \Phi^+ \hat{d}_i \hat{u}_j^c\right] + (\boldsymbol{Y}_d^{\rm SM})^{ij}\left[\Phi^- \hat{u}_i \hat{d}_j^c + \Phi^{0*} \hat{d}_i \hat{d}_j^c\right] + \text{h.c.} \tag{C.8}$$

In the unitary gauge, $\Phi^\pm = \text{Im}\ \Phi^0 = 0$ and $\text{Re}\ \Phi^0 = (v + h_{\rm SM})/\sqrt{2}$, where $v = 2m_W/g = 246$ GeV. After diagonalization of the quark mass matrices, $M_U^{ij} = v(\boldsymbol{Y}_u^{\rm SM})^{ij}/\sqrt{2}$ and $M_D^{ij} = v(\boldsymbol{Y}_d^{\rm SM})^{ij}/\sqrt{2}$, one obtains $L_u^T M_U R_u = \text{diag}(m_u, m_c, m_t)$ and $L_d^T M_D R_d = \text{diag}(m_d, m_s, m_b)$. The resulting Higgs-fermion interactions are diagonal as shown in Fig. 53. Here, the *diagonal* Higgs-fermion Yukawa coupling matrices appear

$$\boldsymbol{y}_u^{\rm SM} = L_u^T \boldsymbol{Y}_u^{\rm SM} R_u\,, \qquad\qquad \boldsymbol{y}_d^{\rm SM} = L_d^T \boldsymbol{Y}_d^{\rm SM} R_d\,. \tag{C.9}$$

The diagonal entries of $\boldsymbol{y}_f$ ($f = u$ or d) are related to the corresponding quark masses via $y_{fi}^{\rm SM} = \sqrt{2} m_{fi}/v$, where i labels the fermion generation.

In the Landau gauge, the Goldstone bosons, $G^0 \equiv \sqrt{2}\,\text{Im}\ \Phi^0$ and $G^\pm \equiv \Phi^\pm$ appear explicitly in internal lines of Feynman diagrams. The Feynman rules for G^0-fermion interactions are flavor diagonal, whereas the corresponding rules for $G^\pm$ possess a flavor-changing component that depends on the CKM matrix elements. The relevant interaction Lagrangian follows easily from eqs. (C.8) and (C.9):

$$\mathcal{L}_{\rm int} = \frac{i}{\sqrt{2}}\left[y_{di}^{\rm SM} d_i d_i^c - y_{ui}^{\rm SM} u_i u_i^c\right] G^0 + y_{u_i}^{\rm SM} [\boldsymbol{K}]_{ij} d_j u_i^c G^+ - y_{d_i}^{\rm SM} [\boldsymbol{K}^\dagger]_{ij} u_j d_i^c G^- + \text{h.c.}\,, \tag{C.10}$$

where as before $[\boldsymbol{K}]_{ij} \equiv \boldsymbol{K}_i{}^j$ and $[\boldsymbol{K}^\dagger]_{ij} \equiv \boldsymbol{K}^j{}_i$, and a sum over the repeated generation index i is implicit. The corresponding diagrammatic Feynman rules are straightforward and will not be presented explicitly here.

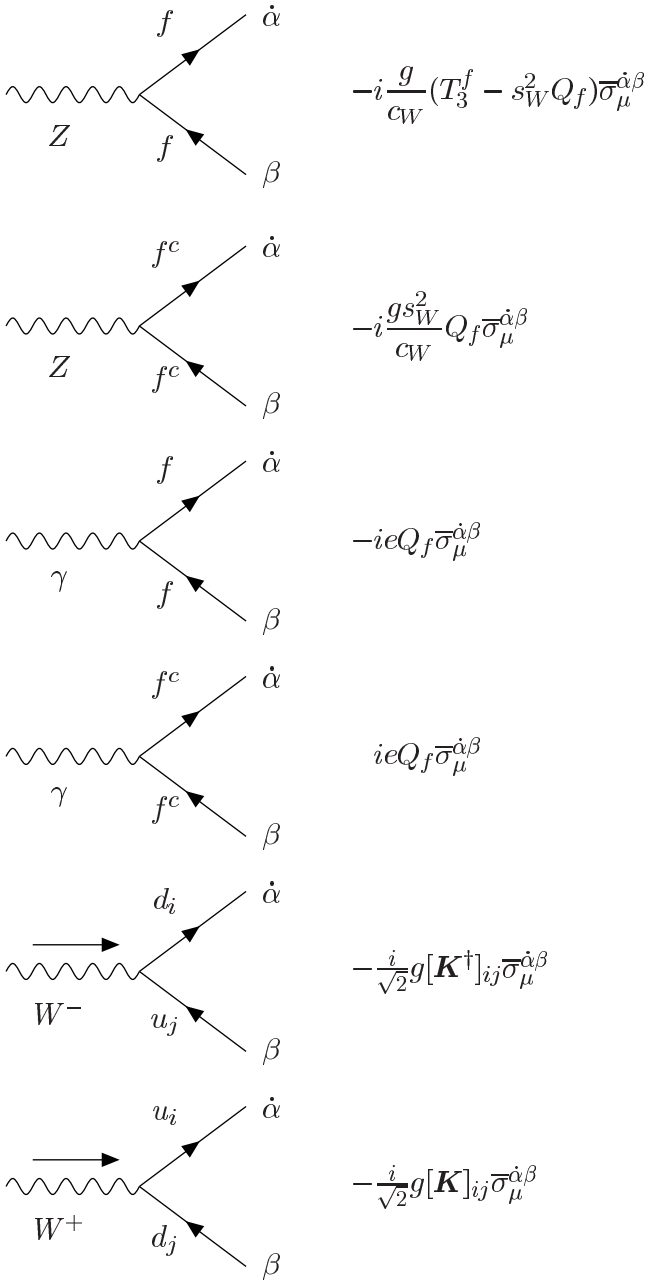

Figure 52: Feynman rules for the two-component fermion interactions with gauge bosons in the Standard Model. Note that $s_W \equiv \sin\theta_W$, $c_W \equiv \cos\theta_W$ and $e \equiv g\sin\theta_W$. For the $W^\pm$ interactions, the W boson is directed into the vertex, as indicated. The charge operator is normalized so that $Q_f = -1$ for the electron ($f = e$).

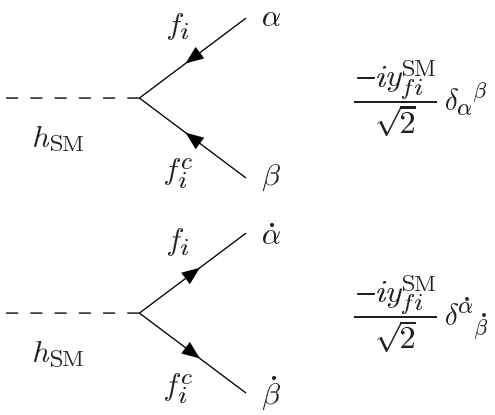

Figure 53: Feynman rules for the SM Higgs-fermion interactions.

Appendix D: MSSM Fermion Interaction Vertices

D.1 Gauge interaction vertices for neutralinos and charginos

First, we introduce some notation. Following ref. [2], we define: (Have changed some *'s below.)

$$O_{ij}^L = -\tfrac{1}{\sqrt{2}} N_{i4} V_{j2}^* + N_{i2} V_{j1}^* \,, \tag{D.1}$$

$$O_{ij}^R = \tfrac{1}{\sqrt{2}} N_{i3}^* U_{j2} + N_{i2}^* U_{j1} \,, \tag{D.2}$$

$$O_{ij}'^L = -V_{i1} V_{j1}^* - \tfrac{1}{2} V_{i2} V_{j2}^* + \delta_{ij} s_W^2 \,, \tag{D.3}$$

$$O_{ij}'^R = -U_{i1}^* U_{j1} - \tfrac{1}{2} U_{i2}^* U_{j2} + \delta_{ij} s_W^2 \,, \tag{D.4}$$

$$O_{ij}''^L = -O_{ij}''^{R*} = \tfrac{1}{2}(N_{i4} N_{j4}^* - N_{i3} N_{j3}^*) \,. \tag{D.5}$$

where U and V are unitary matrices that diagonalize the chargino mass matrix,

$$U^* X V^{-1} = \mathrm{diag}(M_{\widetilde{C}_1}, M_{\widetilde{C}_2}) \,, \tag{D.6}$$

with

$$X = \begin{pmatrix} M_2 & \sqrt{2} m_W s_\beta \\ \sqrt{2} m_W c_\beta & \mu \end{pmatrix} . \tag{D.7}$$

N is a unitary matrix that diagonalizes the neutralino mass matrix,

$$N^* Y N^{-1} = \mathrm{diag}(M_{\widetilde{N}_1}, M_{\widetilde{N}_2}, M_{\widetilde{N}_3}, M_{\widetilde{N}_4}) \,, \tag{D.8}$$

with

$$Y = \begin{pmatrix} M_1 & 0 & -m_Z s_W c_\beta & m_Z s_W s_\beta \\ 0 & M_2 & m_Z c_W c_\beta & -m_Z c_W s_\beta \\ -m_Z s_W c_\beta & m_Z c_W c_\beta & 0 & -\mu \\ m_Z s_W s_\beta & -m_Z c_W s_\beta & -\mu & 0 \end{pmatrix} . \tag{D.9}$$

Above we use the shorthand notation $s_\beta \equiv \sin\beta$, $c_\beta \equiv \cos\beta$, *etc.*, where $\tan\beta \equiv v_u/v_d$ is the ratio of the two neutral Higgs vacuum expectation values.

We now list the gauge boson interactions with the neutralinos and charginos. For each of these rules, one has a version with lowered spinor indices by replacing $\overline{\sigma}^{\dot\alpha\beta} \to -\sigma_{\beta\dot\alpha}$. We label fermion lines with the symbols of the two-component fermion fields as given in Table 1. The Feynman rules for Z and γ interactions with charginos and neutralinos are given in Fig. 54 and the corresponding rules for $W^\pm$ interactions are given in Fig. 55.

Note that the $Z\widetilde{N}_i\widetilde{N}_j$ interaction vertex also subsumes the O''^R_{ij} interaction found in four-component Majorana Feynman rules as in ref. [2], due to the result of eq. (B.44) and the relation $O''^R_{ij} = -O''^L_{ji}$ in eq. (D.5).

D.2 Higgs-fermion interaction vertices in the MSSM

The MSSM Higgs sector is a two-Higgs-doublet model containing eight real scalar degrees of freedom: one complex $Y = -1$ doublet, $\boldsymbol{\Phi_d} = (\Phi^0_d, \Phi^-_d)$ and one complex $Y = +1$ doublet, $\boldsymbol{\Phi_u} = (\Phi^+_u, \Phi^0_u)$. The notation reflects the form of the MSSM Higgs sector coupling to fermions: Φ^0_d [Φ^0_u] couples exclusively to down-type [up-type] fermion pairs. In the supersymmetric model, both hypercharge $Y = -1$ and $Y = +1$ complex Higgs doublets are required in order that the theory (which now contains the corresponding Higgsino superpartners) remain anomaly-free. The supersymmetric structure of the theory also requires (at least) two Higgs doublets to generate mass for both "up"-type and "down"-type quarks (and charged leptons).

When the Higgs potential is minimized, the neutral components of the Higgs fields acquire vacuum expectation values:

$$\langle \boldsymbol{\Phi_d} \rangle = \frac{1}{\sqrt{2}} \begin{pmatrix} v_d \\ 0 \end{pmatrix}, \qquad \langle \boldsymbol{\Phi_u} \rangle = \frac{1}{\sqrt{2}} \begin{pmatrix} 0 \\ v_u \end{pmatrix}, \tag{D.10}$$

where the normalization has been chosen such that $v^2 \equiv v_d^2 + v_u^2 = 4m_W^2/g^2 = (246\ \text{GeV})^2$. The phases of the Higgs fields can be chosen such that the vacuum expectation values are real and positive. That is, the tree-level MSSM Higgs sector conserves CP, which implies that the neutral Higgs mass eigenstates possess definite CP quantum numbers. Spontaneous electroweak symmetry breaking results in three Goldstone bosons, which are absorbed and become the longitudinal components of the $W^\pm$ and Z. The remaining five physical Higgs particles consist of a charged Higgs pair

$$H^\pm = \Phi^\pm_d \sin\beta + \Phi^\pm_u \cos\beta\,, \tag{D.11}$$

one CP-odd scalar

$$A^0 = \sqrt{2}\left(\text{Im}\,\Phi^0_d \sin\beta + \text{Im}\,\Phi^0_u \cos\beta\right), \tag{D.12}$$

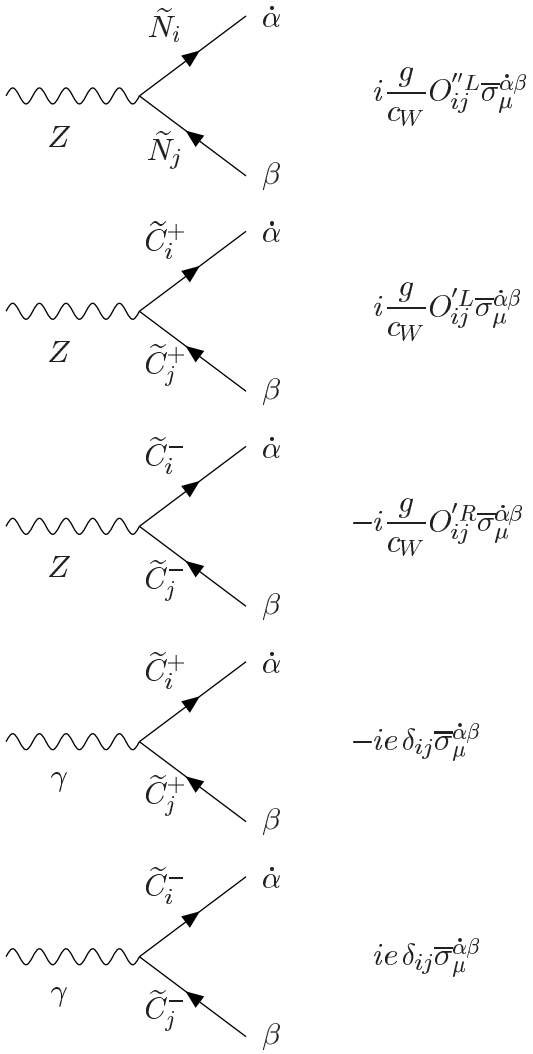

Figure 54: Feynman rules for the 2-component chargino/neutralino-neutral gauge boson interactions. I have changed the chargino and neutralino symbols.

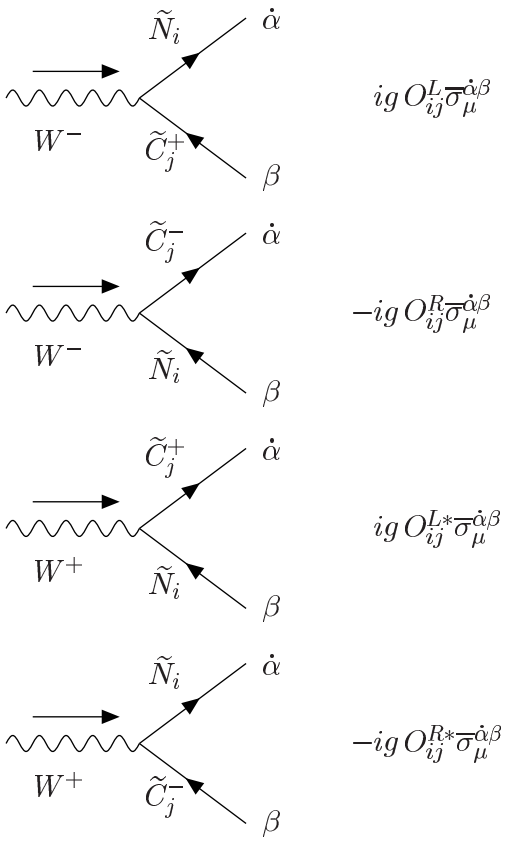

Figure 55: Feynman rules for the chargino-neutralino-$W^\pm$ gauge boson interactions. I have changed the chargino and neutralino symbols.

and two CP-even scalars:

$$\begin{aligned} h^0 &= -(\sqrt{2}\,\mathrm{Re}\,\Phi_d^0 - v_d)\sin\alpha + (\sqrt{2}\,\mathrm{Re}\,\Phi_u^0 - v_u)\cos\alpha\,, \\ H^0 &= (\sqrt{2}\,\mathrm{Re}\,\Phi_d^0 - v_d)\cos\alpha + (\sqrt{2}\,\mathrm{Re}\,\Phi_u^0 - v_u)\sin\alpha\,, \end{aligned} \tag{D.13}$$

with $m_{h^0} \leq m_{H^0}$. The angle α arises when the tree-level CP-even Higgs squared-mass matrix (in the Φ_d^0—Φ_u^0 basis) is diagonalized to obtain the physical CP-even Higgs states.

It is sometimes useful to keep track of the Goldstone scalars, $G^\pm$ and G^0, which have been absorbed by the $W^\pm$ and Z in the generation of gauge boson masses. In the Landau gauge, these states appear explicitly in internal lines in Feynman diagrams. They are orthogonal to $H^\pm$ and A^0, respectively:

$$G^\pm = \Phi_u^\pm \sin\beta - \Phi_d^\pm \cos\beta\,, \tag{D.14}$$

$$G^0 = \sqrt{2}\left(\mathrm{Im}\,\Phi_u^0 \sin\beta - \mathrm{Im}\,\Phi_d^0 \cos\beta\right). \tag{D.15}$$

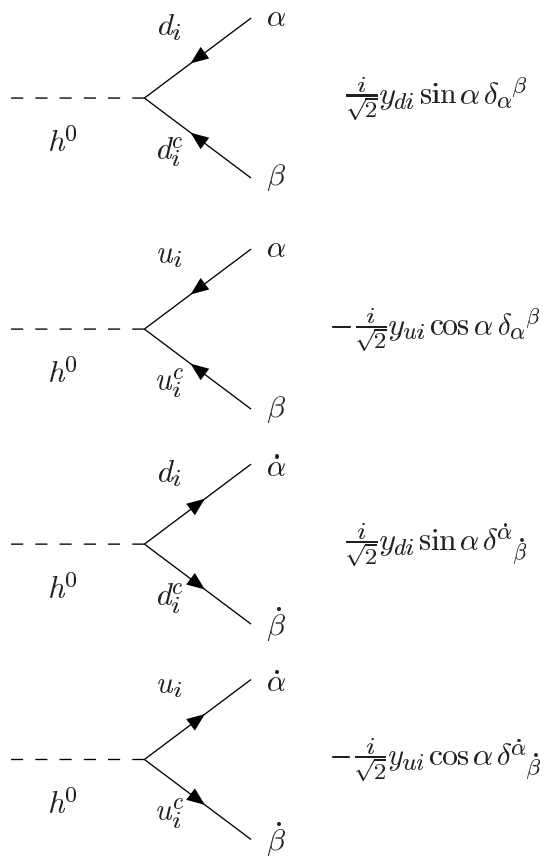

Figure 56: Feynman rules for the interactions of neutral CP-even Higgs bosons with quark-antiquark pairs in the MSSM. For the H^0 interactions, replace $\sin\alpha \to -\cos\alpha$ and $\cos\alpha \to \sin\alpha$ in the h^0 interactions.

Note that G^0 is a CP-odd scalar.

The Higgs-fermion Yukawa couplings in the interaction-basis are given by:

$$-\mathcal{L}_{\rm Y} = \boldsymbol{Y}_u^{ij}\left[\hat{u}_i\hat{u}_j^c\Phi_u^0 - \hat{d}_i\hat{u}_j^c\Phi_u^+\right] + \boldsymbol{Y}_d^{ij}\left[\hat{d}_i\hat{d}_j^c\Phi_d^0 - \hat{u}_i\hat{d}_j^c\Phi_d^-\right] + \text{h.c.} \tag{D.16}$$

Let us change to the mass-eigenstate basis by using eq. (C.5). After diagonalization of the fermion mass matrices, $M_U^{ij} = v_u\boldsymbol{Y}_u^{ij}/\sqrt{2}$ and $M_D^{ij} = v_d\boldsymbol{Y}_d^{ij}/\sqrt{2}$, one obtains $L_u^T M_U R_u = \text{diag}(m_u, m_c, m_t)$ and $L_d^T M_D R_d = \text{diag}(m_d, m_s, m_b)$. The resulting neutral Higgs-fermion interactions are diagonal. Here, the *diagonal* Higgs-fermion Yukawa coupling matrices appear:[26]

$$\boldsymbol{y}_u = L_u^T\boldsymbol{Y}_u R_u\,, \qquad\qquad \boldsymbol{y}_d = L_d^T\boldsymbol{Y}_d R_d\,. \tag{D.17}$$

[26]Note that $\boldsymbol{y}_u = \boldsymbol{y}_u^{\rm SM}/\sin\beta$ and $\boldsymbol{y}_d = \boldsymbol{y}_d^{\rm SM}/\cos\beta$, where the Standard Model diagonal Higgs-fermion coupling matrices are defined in eq. (C.9).

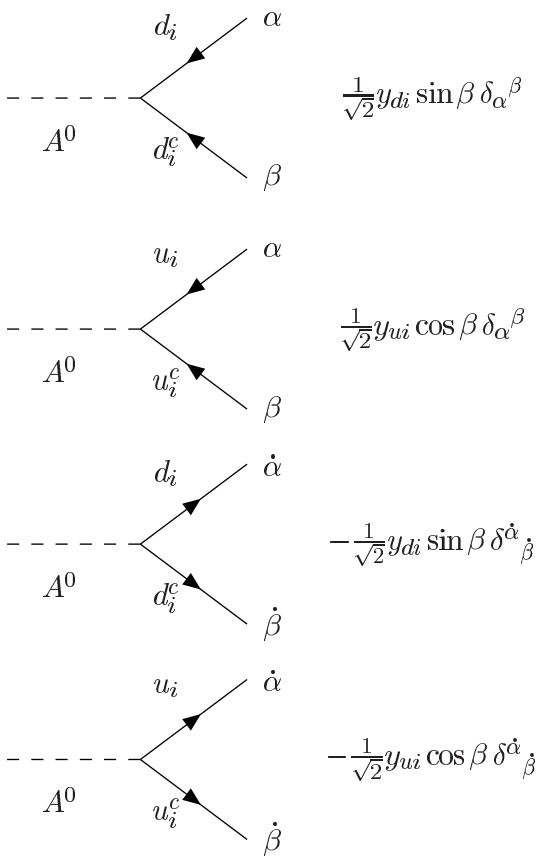

Figure 57: Feynman rules for the interactions of neutral CP-odd Higgs bosons with quark-antiquark pairs in the MSSM. For the G^0 interactions, replace $\sin\beta \to -\cos\beta$ and $\cos\beta \to \sin\beta$ in the A^0 interactions.

The diagonal entries of $\boldsymbol{y}_u$ and $\boldsymbol{y}_d$ are related to the corresponding up-type and down-type quark masses via

$$y_{u_i} = \frac{\sqrt{2} m_{u_i}}{v_u}\,, \qquad\qquad y_{d_i} = \frac{\sqrt{2} m_{d_i}}{v_d}\,. \tag{D.18}$$

The interactions of h^0 with fermion-antifermion pairs are given in Fig. 56. One obtains Feynman rules for the H^0 interactions by taking $\sin\alpha \to -\cos\alpha$ and $\cos\alpha \to \sin\alpha$. Note that starting with the rule with undotted fermion indices, one obtains the corresponding rule with dotted indices (with the direction of the arrows reversed) by taking $\delta_\alpha{}^\beta \to \delta^{\dot\alpha}{}_{\dot\beta}$. The interactions of A^0 with fermion-antifermion pairs are given in Fig. 57. One obtains Feynman rules for the Goldstone boson (G^0) interactions by taking $\sin\beta \to -\cos\beta$ and $\cos\beta \to \sin\beta$. The resulting neutral Goldstone boson rules match precisely those of the Standard Model [eq. (C.10)]. Note that starting with the rule with undotted fermion indices, one obtains the corresponding rule with dotted indices (with the direction of the arrows reversed) by taking $\delta_\alpha{}^\beta \to -\delta^{\dot\alpha}{}_{\dot\beta}$. The

minus sign in the last operation is a signal that A^0 and G^0 are CP-odd scalars.[27].

The couplings of the charged Higgs boson to quark anti-quark pairs are not flavor diagonal and involve the CKM matrix $\boldsymbol{K}$. Starting with eq. (D.16), and changing to the mass-eigenstate basis as before, one obtains

$$\mathcal{L}_{\rm int} = (L_d^T \boldsymbol{Y}_u R_u)_{ij} d_i u_j^c H^+ \cos\beta + (L_u^T \boldsymbol{Y}_d R_d)_{ij} u_i d_j^c H^- \sin\beta + \text{h.c.}, \tag{D.19}$$

and the corresponding $G^\pm$ interactions by taking $\sin\beta \to -\cos\beta$ and $\cos\beta \to \sin\beta$. Using eqs. (C.6) and (D.17), one easily obtains $L_d^T \boldsymbol{Y}_u R_u = \boldsymbol{K}^T \boldsymbol{y}_u$ and $L_u^T \boldsymbol{Y}_d R_d = \boldsymbol{K}^* \boldsymbol{y}_d$. Employing the notation for $[K]_{ij}$ and $[K^\dagger]_{ij}$ introduced below eq. (C.7), the resulting charged-scalar Feynman rules are given in Fig. 58. One can check that the corresponding charged Goldstone boson rules match precisely those of the Standard Model [eq. (C.10)].

D.3 Higgs interaction vertices for charginos and neutralinos

First, we introduce some notation. Following refs. [3] and [8], we define:

$$Q_{ij} = \frac{1}{\sqrt{2}} V_{i1} U_{j2}\,, \tag{D.20}$$

$$S_{ij} = \frac{1}{\sqrt{2}} V_{i2} U_{j1}\,, \tag{D.21}$$

$$Q'^L_{ij} = V_{j1} N_{i4} + \frac{1}{\sqrt{2}} V_{j2} \left(N_{i2} + N_{i1} \tan\theta_W\right)\,, \tag{D.22}$$

$$Q'^R_{ij} = U_{j1} N_{i3} - \frac{1}{\sqrt{2}} U_{j2} \left(N_{i2} + N_{i1} \tan\theta_W\right)\,, \tag{D.23}$$

$$Q''_{ij} = \tfrac{1}{2}\left[N_{i3}(N_{j2} - N_{j1}\tan\theta_W) + N_{j3}(N_{i2} - N_{i1}\tan\theta_W)\right]\,, \tag{D.24}$$

$$S''_{ij} = \tfrac{1}{2}\left[N_{i4}(N_{j2} - N_{j1}\tan\theta_W) + N_{j4}(N_{i2} - N_{i1}\tan\theta_W)\right]\,. \tag{D.25}$$

We list the Higgs boson interactions with the neutralinos and charginos in Fig. 59. For each of the Feynman rules in Fig. 59, one can reverse all arrows by taking $\delta_\alpha{}^\beta \to \delta^{\dot\alpha}{}_{\dot\beta}$ and complex conjugating the corresponding rule (after removing the overall factor of i).

D.4 Chargino and neutralino interactions with quark-squark and lepton-slepton

In the MSSM, scalar partners of the two-component fields q and q^c are the squarks, denoted by $\widetilde{q}_L$ and $\widetilde{q}^c_R$, respectively. In our notation, $\widetilde{q}^c_L$ and $\widetilde{q}^c_R$ are the antiparticles of $\widetilde{q}_L$ and $\widetilde{q}_R$, respectively.[28] Likewise, the scalar partners of the two-component fields ℓ and ℓ^c are the

[27] Because the Feynman rules for A^0 and G^0 arise from a term in $\mathcal{L}_{\rm int}$ proportional to i Im Φ^0, the latter i flips sign when the rule is conjugated resulting in the extra minus sign noted above. As an additional consequence, noting that the Feynman rules are obtained from $i\mathcal{L}_{\rm int}$, the overall A^0 and G^0 rules contain no i

[28] For example, u, $\widetilde{u}_L$ and $\widetilde{u}_R$ all have an electric charge of $+2/3$, whereas u^c, $\widetilde{u}^c_L$ and $\widetilde{u}^c_R$ all have an electric charge of $-2/3$.

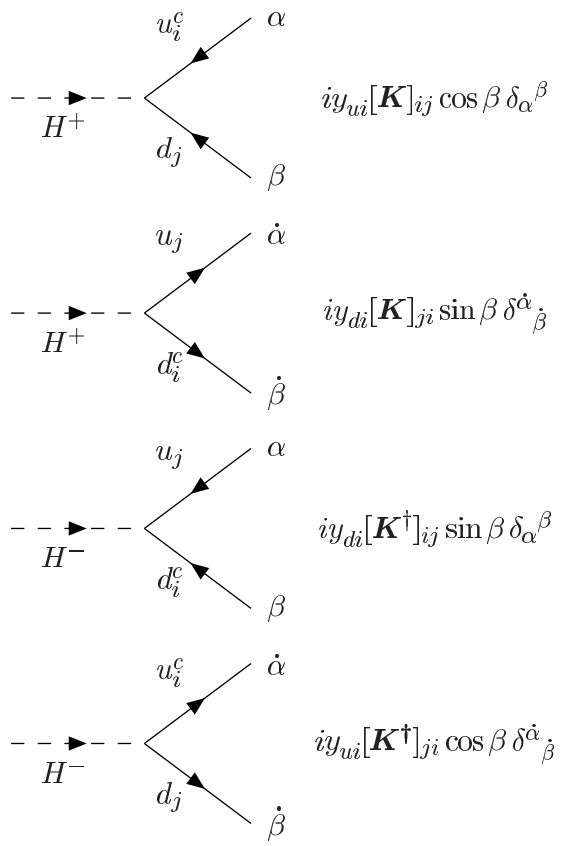

Figure 58: Feynman rules for the interactions of charged Higgs bosons with quark-antiquark pairs in the MSSM. For the $G^\pm$ interactions, replace $\sin\beta \to -\cos\beta$ and $\cos\beta \to \sin\beta$ in the $H^\pm$ interactions. In the above rules, there is *no* implicit sum over the repeated index i.

charged sleptons, denoted by $\widetilde{\ell}_L$ and $\widetilde{\ell}_R^c$, respectively. The sneutrino, $\widetilde{\nu}$ is the superpartner of the neutrino. There is no $\widetilde{\nu}_R$, since ν^c is absent from the Standard Model.[29]

For simplicity, we assume that the squark squared-mass matrices are diagonal in the same basis in which the quark mass matrix is diagonal. In this case, the super-CKM mixing matrix coincides with the CKM mixing matrix. We also ignore $\widetilde{q}_L$–$\widetilde{q}_R$ mixing. The Feynman rules for the chargino-quark-squark interactions are given in Fig. 60, and the rules for the neutralino-quark-squark interactions are given in Fig. 61. Note that chargino interaction vertices involving $u^c\widetilde{d}_R$ and $d^c\widetilde{u}_R$ are absent from the MSSM and thus do not appear in Fig. 60. For each of the Feynman rules in Figs. 60 and 61, one can reverse all arrows by taking $\delta_\alpha{}^\beta \to \delta^{\dot\alpha}{}_{\dot\beta}$ and complex conjugating the corresponding rule (after removing the overall factor of i).

In the more general case, unitary matrices that rotate from the squark interaction-basis to

[29]If the Standard Model is extended to include mass for neutrinos, then the MSSM must likewise be extended.

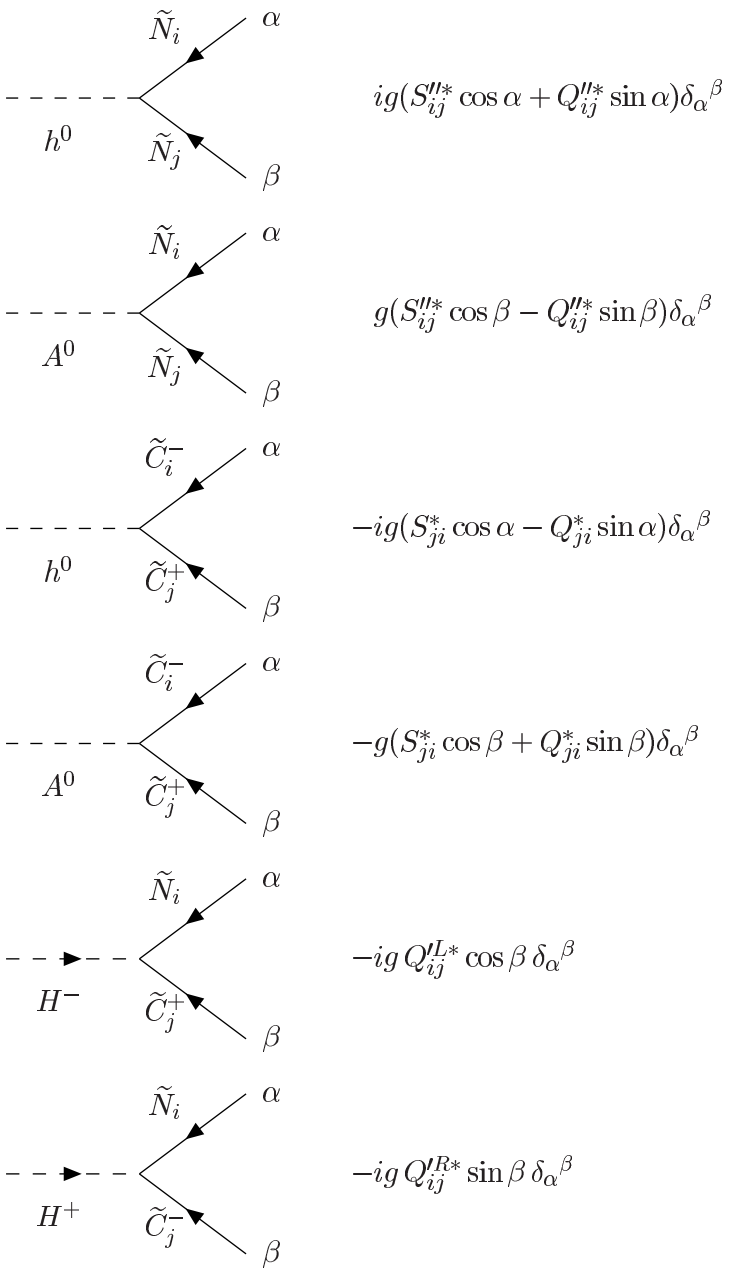

Figure 59: Feynman rules for the Higgs boson interactions with chargino/neutralino pairs. For the H^0 interactions, replace $\sin\alpha \to -\cos\alpha$ and $\cos\alpha \to \sin\alpha$ in the h^0 interactions. For the G^0 interactions, replace $\sin\beta \to -\cos\beta$ and $\cos\beta \to \sin\beta$ in the A^0 interactions. For the $G^\pm$ interactions, replace $\sin\beta \to -\cos\beta$ and $\cos\beta \to \sin\beta$ in the $H^\pm$ interactions. I have changed all the neutralino and chargino symbols to $\widetilde{N}_i$ and $\widetilde{C}_i^+, \widetilde{C}_i^-$, respectively.

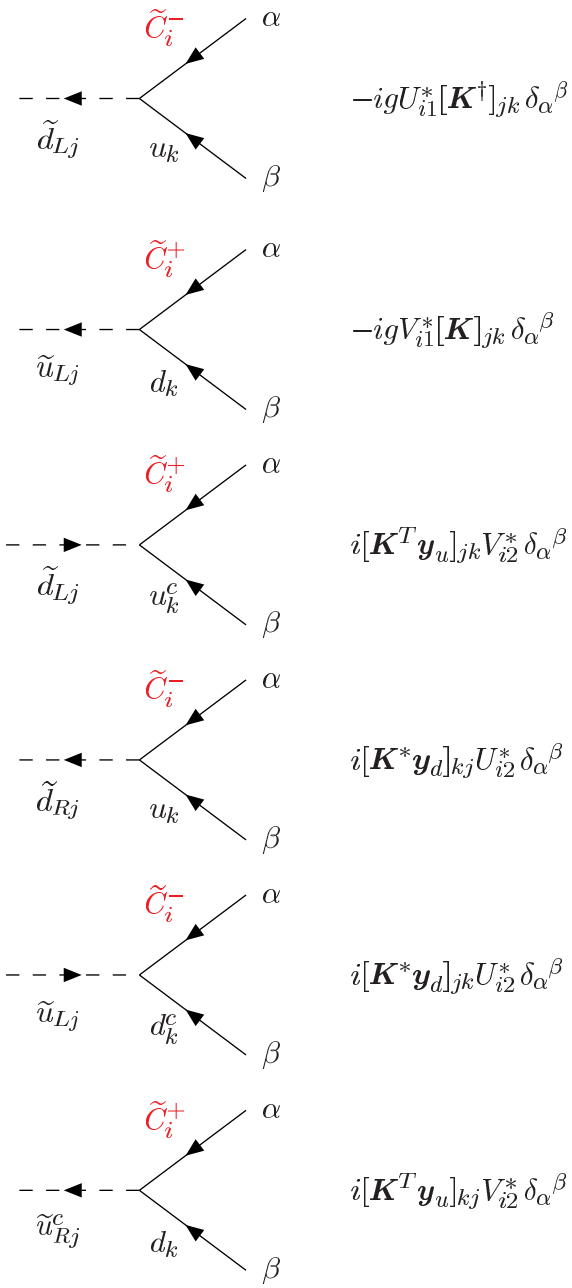

Figure 60: Feynman rules for the interactions of charginos with quark/squark pairs in the MSSM. We have neglected $\widetilde{q}_L$–$\widetilde{q}_R$ mixing and have assumed that the CKM and super-CKM mixing matrices coincide.

the squark mass-basis will appear in the corresponding Feynman rules.

To obtain the rules for chargino and neutralino couplings to lepton-slepton pairs, simply replace $d \to e$, $d^c \to e^c$, $u \to \nu$, $\boldsymbol{K} \to 1$ and $\mathbf{y}_d \to \mathbf{y}_e$, while discarding all rules containing u^c (since ν^c does not exist in the original version of the Standard Model).

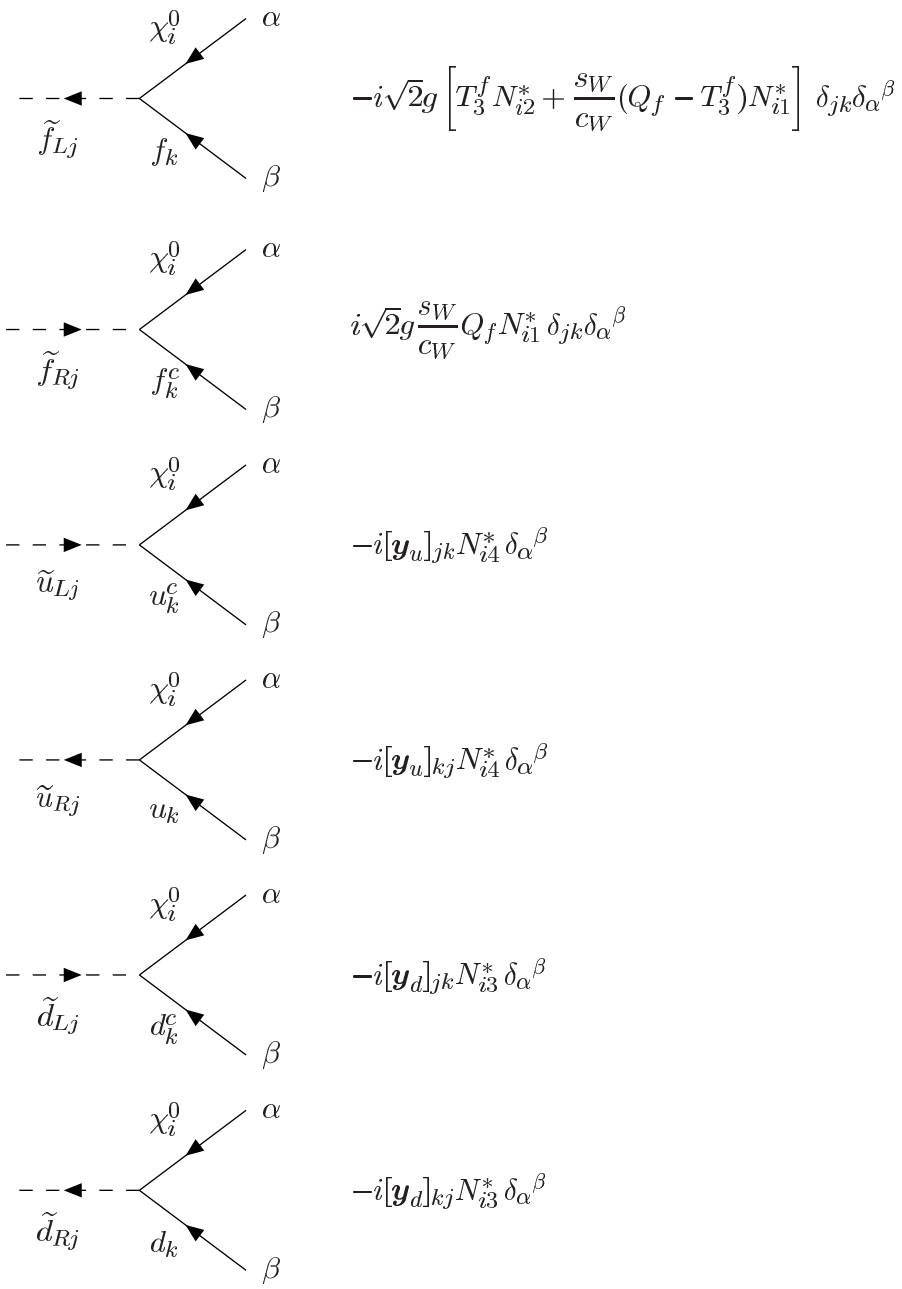

Figure 61: Feynman rules for the interactions of neutralinos with quark/squark pairs in the MSSM. We have neglected $\widetilde{q}_L$–$\widetilde{q}_R$ mixing and have assumed that the CKM and super-CKM mixing matrices coincide.

References

[1] Introduction to the Lorentz group.

[2] H.E. Haber and G.L. Kane, Phys. Rep. **117** (1985) 75.

[3] J.F. Gunion, H.E. Haber, G. Kane and S. Dawson, *The Higgs Hunter's Guide* (Perseus Publishing, Cambridge, MA, 2000).

[4] M. Peskin and D. Schroeder, *Introduction to Quantum Field Theory* (Addison Wesley, Reading, MA, 1995).

[5] How to define γ_5 in $d \neq 4$ dimensions.

[6] D. Bailin and A, Love, *Supersymmetric Gauge Field Theory and String Theory* (Institute of Physics Publishing, Bristol, England, 1994).

[7] R.A. Horn and C.R. Johnson, *Matrix Analysis* (Cambridge University Press, Cambridge, England, 1990); R.N. Mohapatra and P.B. Pal, *Massive Neutrinos in Physics and Astrophysics*, 2nd edition (World Scientific, Singapore, 1998).

[8] J.F. Gunion and H.E. Haber, *Nucl. Phys.* **B272** (1986) 1.

[9] J.M. Jauch and F. Rohrlich, *The Theory of Photons and Electrons*, second expanded edition (Springer-Verlag, New York, 1976), Appendix A2-2; D. Bailin, *Weak Interactions*, second edition (Adam Hilger Ltd., Bristol, England, 1982), chapter 2.